



UNIVERSITÀ
DEGLI STUDI
DI PADOVA

Sede Amministrativa: Università degli Studi di Padova

Dipartimento di Biologia

SCUOLA DI DOTTORATO DI RICERCA IN BIOSCIENZE E BIOTECNOLOGIE

INDIRIZZO: GENETICA E BIOLOGIA MOLECOLARE DELLO SVILUPPO

CICLO XXVIII

**SURFACE PLASMON RESONANCE BASED PLATFORMS
FOR CLINICAL AND ENVIRONMENTAL BIOSENSING APPLICATIONS**

Direttore della Scuola: Ch.mo Prof. Paolo Bernardi

Coordinatore d'indirizzo: Ch.mo Prof. Rodolfo Costa

Supervisore: Ch.mo Prof. Gerolamo Lanfranchi

Dottorando: Anna Meneghello

Abstract

My PhD Thesis work, developed in Veneto Nanotech Laboratories (Nanofab in Marghera, LaNN in Padova and ECSIN in Rovigo), was aimed at the exploitation of the Surface Plasmon Resonance (SPR) phenomenon for the set-up of biosensing platforms for clinical and environmental applications.

In particular, two types of SPR-based platforms were set-up and optimised: the first one was an oligonucleotide-based platform for the detection of Cystic Fibrosis (CF) causing mutations while the second one was an antibody-based platform for the detection of *Legionella pneumophila* whole cells.

Both sensors are based on the same detection strategy, exploiting the advantages of using a highly sensitive Grating Coupled - Surface Plasmon Resonance (GC-SPR) enhanced spectroscopy method, designed using a conical illumination configuration for label-free molecular detection.

Concerning DNA platform for Cystic Fibrosis, a strategy for the detection of some of the most frequent mutations responsible for CF among the Italian population is investigated. For the detection of the CF mutations, gold sinusoidal gratings are used as sensing surfaces, and the specific biodetection is achieved through the usage of allele specific oligonucleotide (ASO) DNA hairpin probes, designed for single nucleotide discrimination. Substrates were used to test unlabeled PCR amplified homozygous wild type (wt) and heterozygous samples (wt/mut) - deriving from clinical samples - for the screened mutations.

Hybridisation conditions were optimised to obtain the maximum discrimination ratio (DR) between the homozygous wild type and the heterozygous samples. SPR signals obtained from hybridising wild type and heterozygous samples showed DRs able to identify univocally the correct genotypes, as confirmed by fluorescence microarray experiments run in parallel. Furthermore, SPR genotyping was not impaired in samples containing unrelated DNA, allowing the platform to be used for the parallel discrimination of several alleles also scalable for a high throughput screening setting.

Concerning antibody platform for *Legionella pneumophila* bacteria detection, a strategy for the exploitation of the SPR phenomenon to develop a fully automated platform for fast optical detection of *Legionella pneumophila* pathogens was investigated. The legal limit of *L. pneumophila* in a high-risk hospital

environment in Italy is 10^2 CFU/L, and the gold standard for its identification is a time consuming microbiological culture method, that requires up to 7 days.

Starting from these considerations a sensitive GC-SPR system was applied to the detection of *L. pneumophila* to test the detection limit of the developed sensing device in term of detectable bacterium CFU. The detection was accurately set up and precisely optimised firstly through the usage of flat gold functionalised slides to be then translated to sinusoidal gold gratings for label-free GC-SPR detection using ellipsometer, in order to ensure a reproducible and precise identification of bacteria. Through azimuthally-controlled GC-SPR, 10 CFU were detected, while in the case of fluorescence analysis results, a negative readout is obtained if incubating less than 10^4 CFU. Successful results were obtained when incubating environmental derived samples. This detection platform could be implemented as a prototype in which water and air samples will be sequentially concentrated, injected into a microfluidic system, and delivered to the SPR sensor for analysis.

The peculiar Grating Coupled - Surface Plasmon Resonance method applied for this work has therefore revealed to be an accurate and highly sensitive strategy – with multiplexing possibility - for the sensing and detecting of different kind of biomolecules, from DNA fragments to whole bacteria cell.

Riassunto

Il mio lavoro di Tesi di Dottorato, sviluppato presso i laboratori Veneto Nanotech (Nanofab a Marghera, LaNN a Padova ed ECSIN a Rovigo), ha avuto come obiettivo l'utilizzo della tecnologia di risonanza plasmonica di superficie (SPR – *Surface Plasmon Resonance*) per lo sviluppo di piattaforme biosensoristiche per applicazioni clinica ed ambientali.

In particolare, durante il lavoro di Dottorato sono state messe a punto due piattaforme SPR: la prima piattaforma utilizza sonde oligonucleotidiche a DNA per l'individuazione di mutazioni causanti fibrosi cistica (CF) mentre la seconda utilizza anticorpi per il rilevamento di cellule di *Legionella pneumophila*.

Entrambi i sensori sono basati sulla stessa strategia di rilevamento, ovvero l'utilizzo di una metodologia *Grating Coupled – Surface Plasmon Resonance* (GC-SPR) progettata utilizzando una configurazione conica di illuminazione ad azimut rotato per la rilevazione diretta – senza passaggi di marcatura, *label-free* – dell'analita in esame.

Per quanto riguarda la piattaforma a DNA per la fibrosi cistica, si è sviluppata una strategia per l'individuazione di alcune delle mutazioni più frequenti responsabili CF tra la popolazione italiana. Per la rilevazione di tali mutazioni le superfici di analisi utilizzate sono grigliati sinusoidali, e la rilevazione specifica delle sequenze di interesse si ottiene attraverso l'utilizzo di oligonucleotidi allele-specifici (ASO – *allele specific oligonucleotide*) con struttura ad *hairpin*, disegnati per la discriminazione di un singolo nucleotide. I substrati plasmonici sono stati utilizzati per testare campioni *wild-type* ed eterozigoti (*wt/mut*) per le mutazioni in esame, amplificati tramite PCR a partire da campioni clinici.

Le condizioni di ibridazione sono state ottimizzate per ottenere il rapporto di discriminazione (DR – *discrimination ratio*) massimo tra campioni *wild-type* ed eterozigoti. I segnali SPR ottenuti ibridando campioni *wild-type* e campioni eterozigoti hanno mostrato DR in grado di identificare univocamente i genotipi corretti, come confermato da esperimenti di fluorescenza in *microarray* eseguiti in parallelo. Inoltre la genotipizzazione ottenuta tramite SPR non è stata inficiata in campioni contenenti DNA interferente, consentendo quindi di utilizzare la piattaforma per la discriminazione in parallelo dei diversi alleli, e la possibilità futura di scalare il sistema con un approccio di *high throughput screening*.

Per quanto riguarda la piattaforma ad anticorpi per la rilevazione di *Legionella pneumophila*, la medesima strategia basata su GC-SPR è stata messa a punto per ottenere una rilevazione rapida e sensibile di tale patogeno. Il limite legale di *L. pneumophila* in ambienti ospedalieri ad alto rischio in Italia è di 10^2 UFC/L (unità formanti colonia) e la metodologia di riferimento per la sua identificazione è una tecnica di coltura microbiologica che richiede tempi di attesa fino a 7 giorni.

Partendo da tali considerazioni un sistema GC-SPR altamente sensibile è stato sviluppato ed applicato per la rivelazione di *L. pneumophila*: la rivelazione è stata accuratamente impostata ed ottimizzata con un ceppo standard del battere, prima attraverso l'utilizzo di superfici d'oro non nanostrutturate (*flat*) opportunamente funzionalizzate ed analizzate tramite fluorescenza, e successivamente attraverso reticoli sinusoidali (*grating*) d'oro analizzati tramite ellissometria GC-SPR. Attraverso la metodologia GC-SPR ad azimut rotato è stato possibile rilevare fino a 10 UFC, mentre con l'analisi in fluorescenza non è stato possibile identificare quantitativi di battere inferiori a 10^4 UFC. Risultati positivi sono stati ottenuti anche incubando campioni di *L. pneumophila* isolati direttamente dall'ambiente ospedaliero.

Questa piattaforma di rilevazione potrà essere implementata come prototipo in cui campioni di acqua e aria potranno venir sequenzialmente concentrati, iniettati in un sistema di microfluidica, ed incubati sulla superficie del sensore SPR per l'analisi, obiettivi questi del progetto POSEIDON (Horizon2020) attualmente in corso.

La particolare metodologia GC-SPR ad azimut rotato applicata in questo lavoro di Tesi si è dimostrata essere una strategia accurata e altamente sensibile - con possibilità di *multiplexing* - per la rilevazione di diversi tipi di biomolecole, a partire da frammenti di DNA fino ad intere cellule batteriche.

Summary

Abbreviations	11
1. Introduction	15
1.1 Sensors: overview and focus on optic biosensors	15
1.2 Surface plasmon resonance (SPR).....	17
1.2.1 Definitions and basic principles.....	17
1.2.2 SPR interrogations	18
1.2.3 SP excitation: Prism Coupled-SPR versus Grating Coupled-SPR and symmetry breaking in GC-SPR.....	20
1.3 Microarrays and their applications in disease diagnostics.....	22
2. Fabrication and sensing platform	25
2.1 Reagents, solutions and instruments.....	25
2.1.1 Reagents and solutions for molecular biology.....	25
2.1.2 Reagents for SPR gold surfaces fabrication	25
2.1.3 Instruments.....	26
2.2 Fabrication	27
2.2.1 Commercial slides (e-Surf LifeLine).....	27
2.2.2 Gold surfaces	27
2.3 Substrates functionalisation.....	30
2.3.1 Gold substrates cleaning and SH-PEG-COOH functionalisation	30
2.3.2 Evaluation of the -COOH functionalisation	31
2.3.3 Biomolecules coupling to activates surfaces trough microarray printing.....	33
2.3.3.1 EDC-mediated activation of -COOH functionalised gold surfaces.....	33
2.3.3.2 Coupling of biomolecules to e-Surf microarray glass slides or gold activated slides	35
2.3.4 Samples labelling and incubation	38
2.3.5 Microarray fluorescent measurements.....	38

2.3.6	Surface plasmon resonance measurements.....	38
2.3.6.1	SPR interrogation parameters for DNA platform – angular interrogation.....	39
2.3.6.2	SPR interrogation parameters for antibody platform – wavelenght interrogation.....	40
3.	DNA platform for Cystic Fibrosis causing mutations detection	41
3.1	Introduction.....	41
3.1.1	Cystic fibrosis disease.....	41
3.1.2	Cystic fibrosis genotyping	45
3.1.3	Aim of the study.....	45
3.2	Materials and Methods	47
3.2.1	Primers and Allele Specific Oligonucleotide DNA probes design	47
3.2.2	Surface functionalisation.....	47
3.2.3	Samples preparation and hybridisation	49
3.2.4	SPR and fluorescence measurements	51
3.3	Results and Discussion	53
3.3.1	Primers and Allele Specific Oligonucleotide DNA probes design	53
3.3.2	Hybridisation conditions setup and optimization through fluorescent analysis	56
3.3.3	SPR response to PCR amplified clinical samples	59
3.3.4	SPR response in presence of interferent DNA.....	62
3.3.5	System cut-off evaluation and test with blind samples	63
3.4	Conclusions.....	65
4.	Antibody platform for <i>Legionella pneumophila</i> bacteria detection	67
4.1	Introduction.....	67
4.1.1	Pathogen biosensing: overview and focus on Legionella.....	67
4.1.2	<i>Legionella pneumophila</i> and legionellosis	73
4.1.3	Aim of the study.....	75
4.2	Materials and Methods	76
4.2.1	Marketing antibodies evaluation and deposition.....	76
4.2.2	Protocols for bacteria culture, processing and identification	77

4.2.2.1	Bacteria strains and culture.....	77
4.2.2.2	Colony forming unit (CFU) number evaluation	79
4.2.2.3	Labelling and binding protocol for bacteria cells	79
4.2.2.4	Antibody labelling for “sandwich” fluorescent detection	80
4.2.2.5	Bacteria cell fragmentation.....	80
4.2.3	Microfluidic cell for SPR measurements.....	81
4.3	Results and Discussion	84
4.3.1	POSEIDON Project (ICT-26 Horizon 2020).....	84
4.3.2	Antibody binding evaluation	85
4.3.3	Bacteria capturing demonstration through confocal and scanning electron microscopy	87
4.3.4	Direct vs indirect bacteria detection	88
4.3.5	Sensitivity evaluation of the fluorescent set-up	92
4.3.6	Evaluation of ethanol fixation effect on sensitivity.....	94
4.3.7	Evaluation of system performances with whole vs fragmented cells.....	94
4.3.8	Florescence system performances with antibody deposition in microwells.....	96
4.3.9	Grating functionalisation and SPR measurements setup with microfluidic cell	97
4.3.10	<i>Legionella pneumophila</i> SPR detection - sensitivity and specificity	98
4.4	Conclusions.....	102
5.	Conclusions	105
6.	Acknowledgements	107
7.	Side activities	109
8.	Bibliography	113

Abbreviations

AFM	atomic force microscope
ARMS	amplification refractory mutation system
ASO	allele-specific oligonucleotide
ATCC	American type culture collection
BCYE	buffered charcoal yeast extract
BIA	biospecific interaction analysis
BLAST	basic local alignment search tool
bp	base pair
BSA	bovine serum albumin
BSL	biosafety level
CCD	charge-coupled device
cDNA	complementary deoxyribonucleic acid
CF	cystic fibrosis
CFTR	cystic fibrosis transmembrane conductance regulator
CFU	colony forming unit
CGH	comparative genomic hybridization
DGGE	denaturing gradient gel electrophoresis
DMA	N,N-dimethylacrylamide
DNA	deoxyribonucleic acid
DR	discrimination ratio
ECDC	European centre for disease prevention and control
EDC	N-(3-(dimethylamino)propyl)-N'-ethylcarbodiimide hydrochloride
ELDSNet	European Legionnaires' disease surveillance network
ESCMID	European society of clinical microbiology and infectious diseases

ESGLI	ESCMID Study Group for Legionella Infections
EU	European union
EWGLI	European working group for Legionella infections
FBS	fetal bovine serum
GC-SPR	grating-coupled surface plasmon resonance
HPLC	high performance liquid chromatography
IFA	immunofluorescence assay
ISO	international organization for standardization
IUPAC	international union of pure and applied chemistry
LIL	laser interference lithography
MAPS	[3-(methacryloyl-oxy)propyl]trimethoxysilyl
mRNA	messenger ribonucleic acid
mut	Mutant
MW	molecular weight
NAS	N,N-acryloyloxysuccinimide
NIR	near-infrared
NOA	Norland optical adhesive
OD	optical density
OLA	oligoligation assay
PAGE	polyacrylamide gel electrophoresis
PBS	phosphate-buffered saline
PC-SPR	prism-coupled surface plasmon resonance
PCR	polymerase chain reaction
PDMS	Polydimethylsiloxane
PEG	polyethylene glycol
PGMEA	propylene glycol monomethyl ether acetate
PNA	peptide nucleic acid

QCM	quartz crystalline microbalance
RIU	refractive index unit
RNA	ribonucleic acid
RT	room temperature
S-NHS	N-hydroxysulfosuccinimide sodium salt
SDS	sodium dodecyl sulphate
SEM	scanning electron microscopy
SNPs	single nucleotide polymorphisms
SP	surface plasmon
SPP	surface plasmon polariton
SPR	surface plasmon resonance
SSC	saline-sodium citrate
SSCP	single stranded conformation polymorphism
TASC-IOM-CNR	tecnologie avanzate e nanoscienza - istituto officina dei materiali – consiglio nazionale delle ricerche
TBO	toluidine blue O
TBS	tris-buffered saline
TEM	transverse electro magnetic
TEM	transmission electron microscopy
TM	transverse magnetic
TSA	tryptic soy agar
UV	ultraviolet
wt	wild type

1. Introduction

1.1 Sensors: overview and focus on optic biosensors

In the last decades there has been an increasing interest in sensitive, specific and fast biosensors to address several societal and industrial needs. In particular, reliable and fast detection in the diagnosis field application as well as in the microbiological one is a key challenge in biosensing due to the strong impact on health. Standard molecular biology and microbiology-based methods can be highly efficient for this purpose, but at the same time can be very time consuming. In addition, most of these conventional methods require a biological facility, with specific instrument and trained personnel, thus they are not suitable for on-site or point of care analysis and cannot be carried out by untrained personnel. Therefore, new biosensing devices, capable of detecting analytes in a faster and equally accurate manner, are needed to help contributing to solve significant sensing challenges.

According to IUPAC definition “A biosensor is a self-contained integrated device which is capable of providing specific quantitative or semi-quantitative analytical information using a biological recognition element (biochemical receptor) which is in direct spatial contact with a transducer element.”¹

A biosensor is a device composed of two elements (*Figure 1*):

1. a bioreceptor that is an immobilized sensitive biological element (e.g. enzyme, DNA, antibody, etc..) recognising the analyte (e.g. enzyme substrate, complementary DNA, antigen, etc..).
2. a transducer that is used to convert bio-chemical signal resulting from the interaction of the analyte with the bioreceptor into an electronic one.

Biosensors can be grouped and classified according to different parameters, but classifying them according to their signal transduction way and working principle can be helpful, also if continuous technological novelty can modify and implement this classification: according to that, biosensors can generally be divided into three main types (*Figure 2*), namely: (1) electrochemical biosensors; (2) mass-based biosensors; and (3) optical-based biosensors.

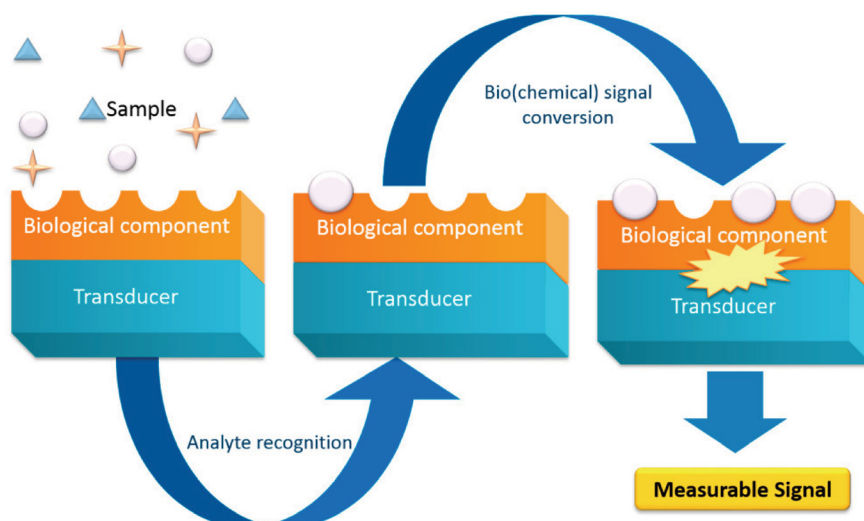


Figure 1. General scheme of a biosensor: the biological part is either integrated or closely associated with the physical transducer, and behave as a recognition element, capable to detect a specific analyte. Once the interaction takes place, the bio-chemical signal generated will be converted by a physical transducer in a measurable discrete or continuous signal, whose intensity could be correlated to the analyte concentration. Picture from².

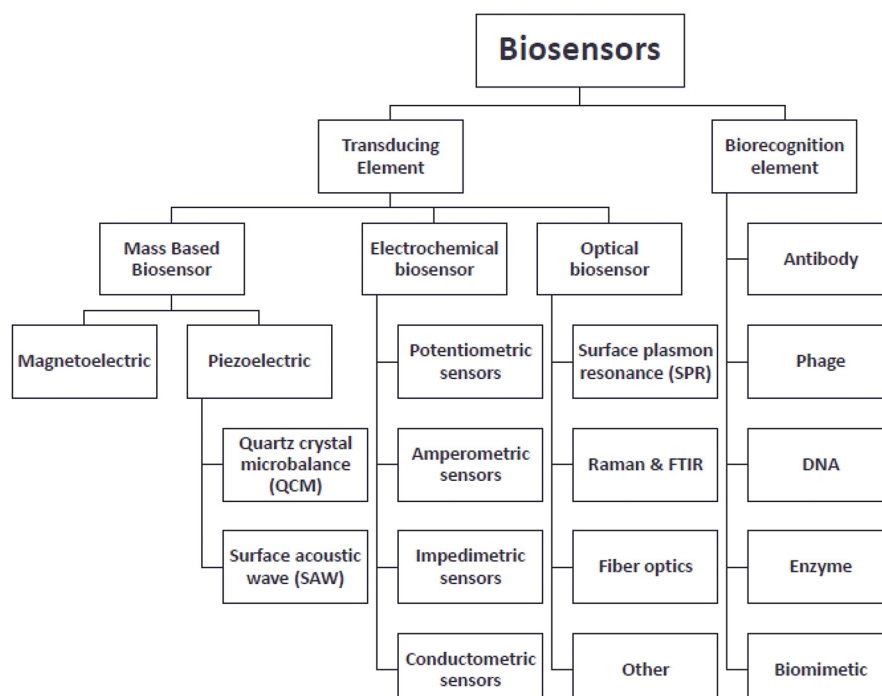


Figure 2. Biosensors classification according to the biorecognition element or to the transducing element: mass-based, electrochemical or optical biosensors. Picture from³.

Among these technologies, the optical one has reached a level of technological maturity that makes it a promising candidate for applications to specific sensing challenges.⁴

Optical biosensors are those which can sense phenomena related to the interaction of the biorecognition element with the analyte and correlate the observed optical signal to the presence and concentration of target compounds, based on the measurement of photons involved in the process. More specifically, optical detection is based on the measurement of luminescence, fluorescence, colour changes, by the measurement of absorbance, reflectance or fluorescence emissions that occur in the ultraviolet (UV), visible, or near-infrared (NIR) spectral regions.⁵

Optical biosensors can be further classified as labelled-fluorescent biosensor, or label-free biosensors: the most crucial distinction between these techniques is that in label-free biosensors target molecules are not labelled or altered, and are detected in their natural forms, while in the labelled ones target molecules or biorecognition molecules need to be labelled with fluorescent tags, such as dyes, to ensure the biodetection.

Both strategies are widely used in optical sensors construction⁶, with relative advantages and disadvantages: in this work the main optical label-free transduction strategy, i.e. surface plasmon resonance (SPR), will be exploited for biosensing application, using fluorescent microarray as reference technique.

1.2 Surface plasmon resonance (SPR)

1.2.1 Definitions and basic principles

Among the most advanced sensing technologies currently explored for bioanalytes detection, the one exploited in this work is the label-free surface plasmon resonance technique.

A surface plasmon (SP) is an electro-magnetic wave propagating along the surface of a metal-dielectric interface as charge density oscillations that may exist at the interface of two media with dielectric constants of opposite signs, for example air and a metal. Surface plasmons can couple with photons, creating the so-called polariton, called in this case, surface plasmon polaritons (SPP).⁷⁻¹⁰

SPPs are localized in the direction perpendicular to the interface and will propagate along this interface until its energy is lost, with an exponential intensity decays (*Figure 3*). These features make SPPs extremely sensitive to optical and geometrical properties of the supporting interface, such as shape, roughness and refractive indices of the facing media.¹¹

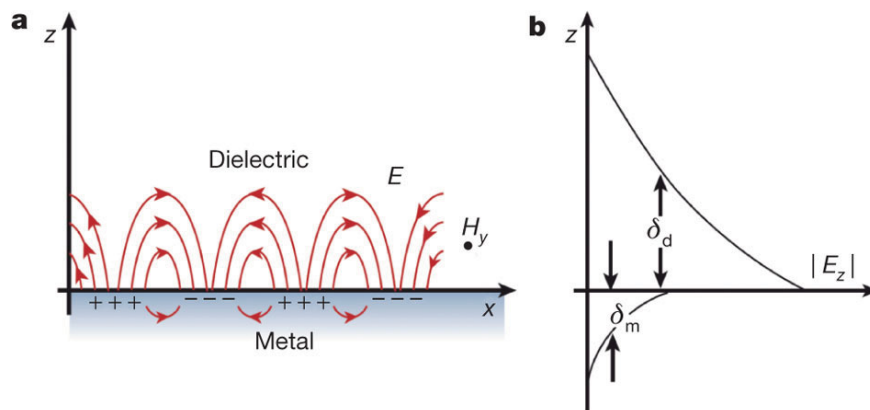


Figure 3. Basics of surface plasmon polaritons, from¹². a) SPP as a collective excitation at a metal–dielectric interface. The electromagnetic field (electric field, E , plotted in the z – x plane; magnetic field, H_y , sketched in the y direction) is drastically enhanced. b) Field intensity is enhanced near the surface and decays exponentially with distance (δ_d for the dielectric and δ_m for the metal).

SPPs can be excited by the photons of incident light at specific matching conditions, i.e. the momentum of incident photons must match the momentum of SPs, and the momentum matching results in resonance between SPs and incident photons. Thus, the energy carried by photons is transferred to SPs, which oscillate near the metal/dielectric interface. This resonance phenomenon is termed surface plasmon resonance.

1.2.2 SPR interrogations

A change in the refractive index of the dielectric – due for example to functionalisation, analyte binding, etc... – gives rise to a change in the propagation constant of the surface plasmon, which through the coupling condition alters the characteristics of the light wave coupled to the surface plasmon (e.g., coupling angle, coupling wavelength, intensity, phase).

On the basis of which characteristic of the light wave modulated by a surface plasmon is measured, SPR sensors are classified as sensors with angular (the most widely used), wavelength, intensity, or phase modulation.¹³

In SPR sensors with angular modulation, a monochromatic light wave is used to excite a surface plasmon. The strength of coupling between the incident wave and the surface plasmon is observed at multiple angles of incidence and the excitation of surface plasmons is observed as a dip in the angular spectrum of reflected light.

In SPR sensors with wavelength modulation, a surface plasmon is excited by a collimated light wave containing multiple wavelengths and the excitation of surface plasmons is observed as a dip in the wavelength spectrum of reflected light.

When a portion of the incident light energy is transferred to the SPP, as described before, with consequent absorption of light, it results in a reflectivity dip in the metal reflectivity spectrum at a certain resonance angle, θ_{res1} (Figure 4, in blue). If refractive index changes at the metal/dielectric interface, for example after surface functionalisation or upon analyte binding to the bioreceptor, this results in a shift of the reflectivity dip to a different resonance angles θ_{res2} (Figure 4, in yellow).

Thus the presence of a new material at the metal/dielectric interface is detected from the resonance angle shift $\Delta\theta_{res}$, without the need of labelling procedure, with all the advantages deriving from a label-free detection method.

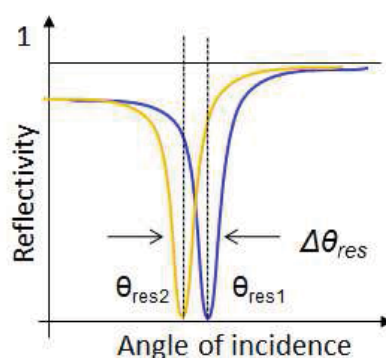


Figure 4. SPR causes an intensity dip in the reflected light at the sensor surface (θ_{res1}). The minimum of the dip can shift upon interaction occurring on the sensors surface (θ_{res2}), i.e. binding of the analyte.

1.2.3 SP excitation: Prism Coupled–SPR versus Grating Coupled–SPR and symmetry breaking in GC–SPR

SPPs cannot be excited directly by a freely propagating beam of light incident upon the metal surface (Figure 5 A): coupling of photons into SPPs have to be achieved using a coupling medium to match the photon and SPP wave vectors, and thus match their momenta. In a dielectric k_0 is increased and SPP can be excited since k_0 can equal k_{SPP} (Figure 5 B).

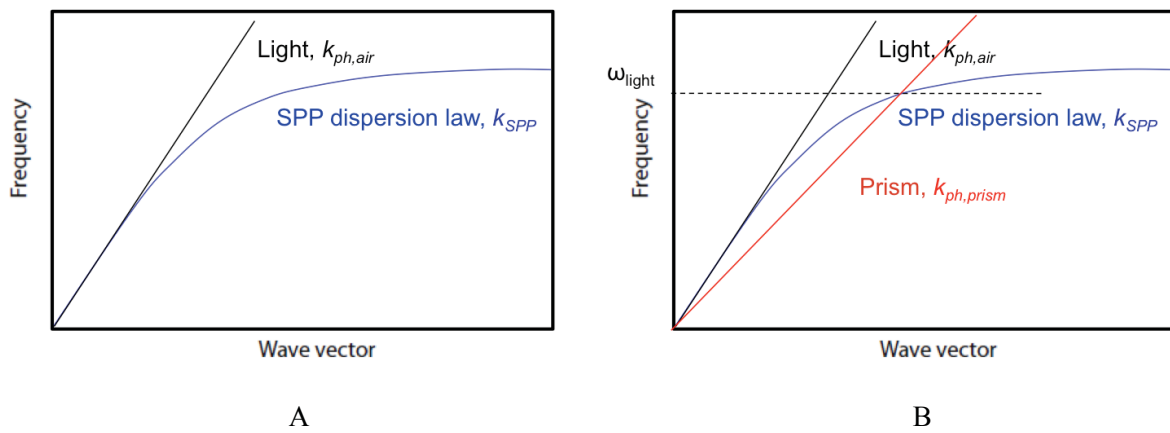


Figure 5. A) The dispersion curve for a SP mode on air-gold interface shows the momentum mismatch problem that must be overcome in order to couple photon and SP modes together, with the SP mode (blue line) always lying beyond the photon line (black line) ($k_{SPP} > k_{ph,air}$ of the same frequency ω). B) SPP excitation can occur when $k_{SP} \leq k_{ph,prism}$ (red line), through the usage of a coupling medium, like a prism.

The most common SPR based configuration is the one that adopts a prism to promote SPPs coupling with incident light (Kretschmann or prism coupling SPR – PC-SPR)^{8,15,16} like the one adopted by the well known Biacore® SPR instrument. Alternative configurations are available which are more suitable for instrumental miniaturization and multiplexing: unlike the most adopted Prism Coupled-SPR, that suffers from cumbersome optical alignment and bulky optics, GC-SPR configuration, where a metal layer is periodically patterned to couple incoming light with SPP modes, has shown indeed to be the most suitable solution for the miniaturization and integration of plasmonic platforms into nanodevices. PC-SPR and GC-SPR basic configurations are depicted in Figure 6.

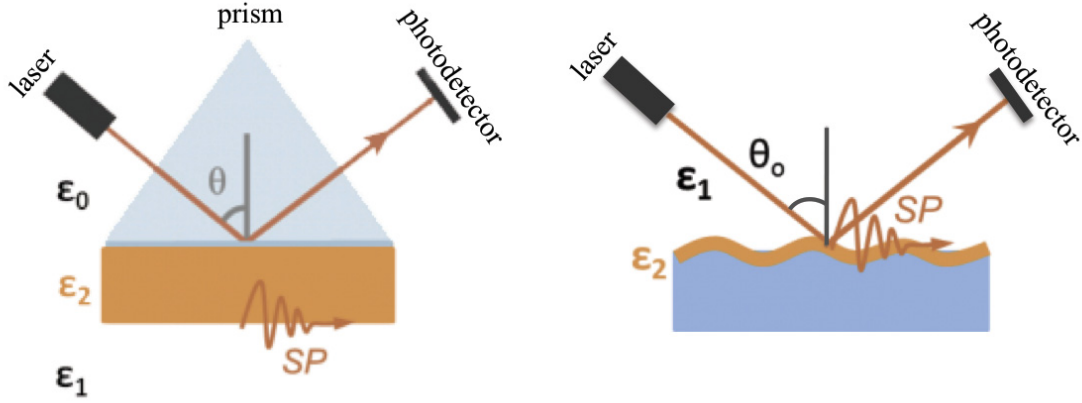


Figure 6. PC-SPR (left) and GC-SPR (right) basic configurations. SP: surface plasmon, θ : incident light angle, ϵ_0 : prism dielectric constant, ϵ_1 : air dielectric constant, ϵ_2 : gold dielectric constant.

GC-SPR configurations, however, are less sensitive in terms of RIU (refractive index unit)¹⁷, but, nevertheless, their sensing performances can be improved by almost one order of magnitude by modifying the traditional SPR configurations to an azimuthally rotated GC-SPR ($\phi \neq 0^\circ$ GC-SPR).¹⁸

As demonstrated recently^{19–22}, the symmetry breaking of the plasmonic platforms provides advantages in sensing analyses: the azimuthal rotation allows metallic gratings to support the excitation of sensitivity-enhanced surface plasmon polaritons with particular features, which are not present in the classical mounting. The sensitivity enhancement mechanism is attributed to the fact that the azimuthal orientation of the sinusoidal grating induces a double SPP excitation with a single incident wavelength.

Due to the resulting symmetry breaking, polarization plays a fundamental role in SPP excitation, and it must be appropriately tuned in order to optimize the coupling strength. Indeed, by exploiting the degree of freedom given by the azimuthal rotation of the grating, a novel SPR architecture based on polarization-modulation the incident light^{18,22–24} (Figure 7) will be used in the experiments illustrated in this Thesis.

Beside a resolution competitive with commercial products, down to 10^{-7} RIU, polarization-based SPR provides a sensing mechanic that is simplified in comparison with other common architectures based on angular or wavelength interrogation.

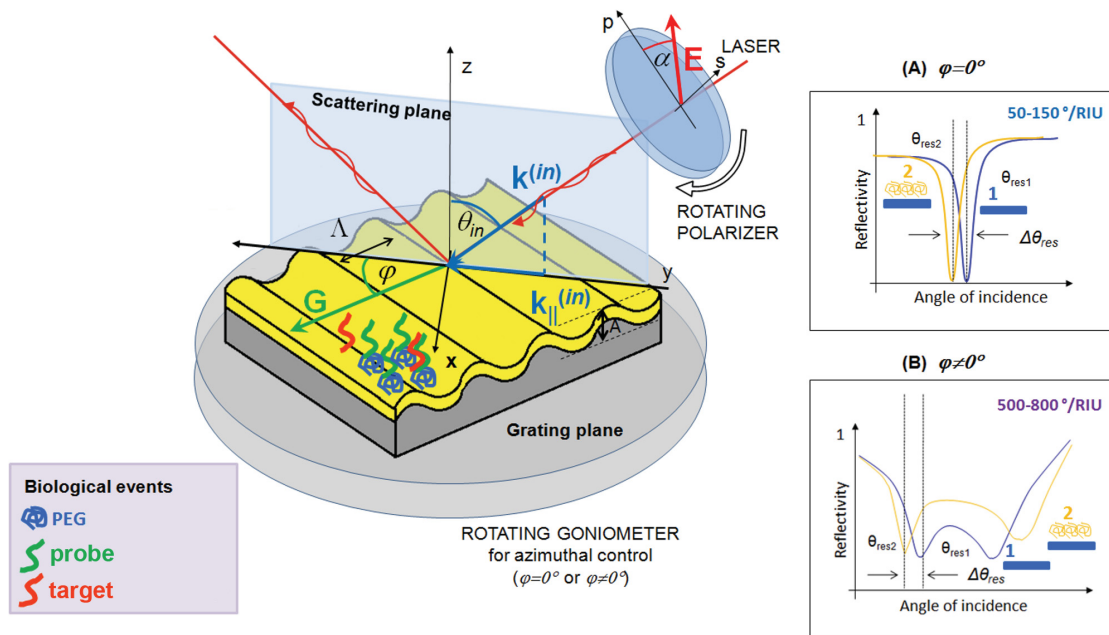


Figure 7. Scheme of the experimental configuration geometry used for GC-SPR, adapted from^{22,25}. The plasmonic substrate (period $\Lambda = 500$ nm and amplitude $A = 40$ nm) is mounted onto a rotating goniometer allowing the azimuthal control of the grating plane. In the azimuthal rotated configuration ($\phi \neq 0^\circ$), the photon scattering plane is rotated by an angle ϕ with respect to the grating vector G (in green), so that when the coupling between the incident photon momentum (k^{in}) and the surface plasmon polariton momentum occurs for a certain incident wavelength (λ_{in}) and angle (θ_{in}), a double reflectivity dip is registered, and sensitivities range from 500 to 800°/RIU (inset B). In the null azimuth configuration ($\phi = 0^\circ$), a single reflectivity dip is registered, and sensitivities range from 50 to 150°/RIU (inset A). Light polarization could be tuned through a rotating polarizer (α is the polarization angle). Biological events on a surface are detected by the resonance angle shift ($\Delta\theta_{res}$) derived from the reflectivity spectra.

1.3 Microarrays and their applications in disease diagnostics

The development of DNA microarray technology in mid 1990s allowed for the first time to simultaneously profile and study cell transcriptome and gene expression, exploiting the very same principle that makes nucleic acid so essential to information storage: hybridization to complementary sequences.

Simply defined, a microarray is a collection of microscopic features (most commonly DNA, but also antibodies, peptides, etc...), which can be probed with target molecules to produce either quantitative (i.e. gene expression) or qualitative (i.e. diagnostic) data. Microarrays can be distinguished based upon

characteristics such as the nature of the probe, the solid-surface support used, and the specific method used for probe addressing and/or target detection.

The “probe” refers to the DNA sequence bound to the solid-surface support in the microarray, whereas the “target” is the sequence of interest in the sample to be tested.

In general terms, probes are synthesised and immobilised as discrete features, or spots. Each feature contains millions of identical probes. The target is fluorescently labelled and then hybridised to the microarray probes. A successful hybridisation event between the labelled target and the immobilized probes will result in an increase of fluorescence intensity over a background level, which can be measured using a fluorescent scanner²⁶ (Figure 8).

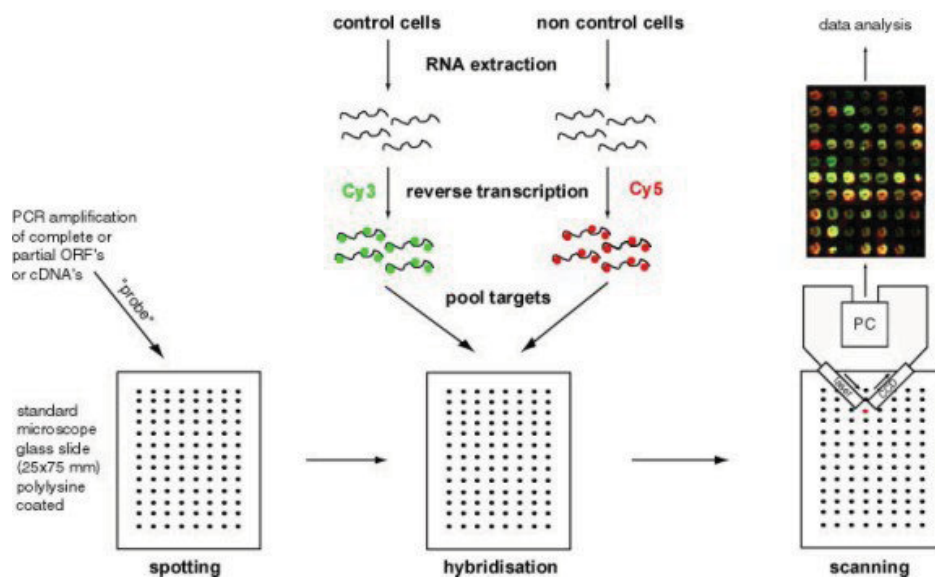


Figure 8. Classical steps for preparation and usage of a microarray for gene expression profiling. The targets for microarray analysis are two pools of fluorescently labelled cDNAs derived from mRNA of control (Cy3) and experiment (Cy5) cells.

Although, historically, microarrays have been used largely for gene expression studies, this technology has gradually been applied in other field, including diagnostics.

Several applications of DNA microarrays for diagnosing specific diseases have been reported and diagnostic microarrays have been used for genotyping and determination of disease-relevant genes or agents causing diseases, mutation analysis using relatively low-density DNA microarrays, screening of

single nucleotide polymorphisms (SNPs), detection of chromosome abnormalities like copy number changes at the level of chromosome using comparative genomic hybridization DNA microarrays (array CGH), global determination of post-translational modification, including methylation, acetylation, and alternative splicing²⁷ (Figure 9).

The performance of microarray-based diagnosis is continuously improving by the integration of other tools, and in this Thesis microarray technique has been used as reference when investigating SPR-based platforms performances for diagnostic application both in genetic disorder (oligo DNA-based platform) and infectious disease (antibody-based platform).

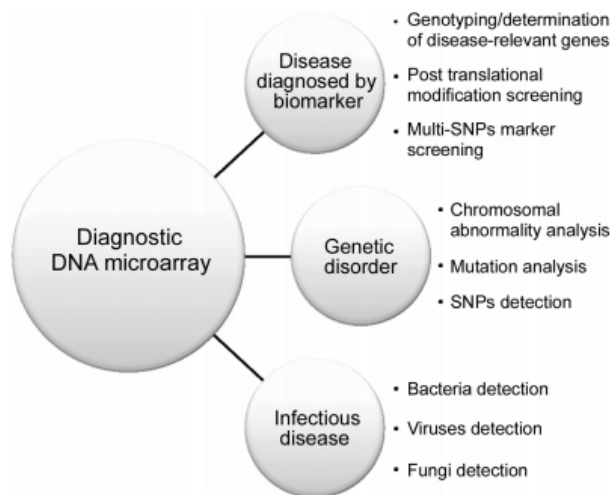


Figure 9. Use of DNA microarrays for diseases diagnosis. Picture from²⁷.

The ideal microarray platform for a diagnostic laboratory is a low- to medium-density array that offers limited, reliable, and straightforward results without the need for sophisticated equipment and data management.²⁸

2. Fabrication and sensing platform

2.1 Reagents, solutions and instruments

2.1.1 Reagents and solutions for molecular biology

All the reagents and solution components used were purchased from Sigma-Aldrich (St. Louis, MO, USA), if not otherwise specified. The water used was of bidistilled (dd-H₂O) or Milli-Q grade. Used solutions and buffers have the following composition:

- Basic piranha solution: 5:1:1 dd-H₂O, 30% H₂O₂ and 30% NH₄OH
- MES buffer for –COOH activation: 0.1 M 2-(N-morpholino) ethanesulfonic acid, 0.5 M NaCl, pH 6.0
- 20X SSC buffer: 3 M sodium chloride, 300 mM trisodium citrate, pH 7.0
- 2X Oligo microarray printing buffer: 300 mM sodium phosphate, 0.02% Triton, pH 8.5
- Oligo microarray blocking solution: 0.1 M Tris, 50 mM ethanolamine, pH 9
- Oligo microarray washing solution: 4X SSC, 0.1% SDS
- Protein microarray printing buffer: 0.1 M sodium phosphate, 0.3 M NaCl 0,01% Triton X100, pH 7.2
- Protein microarray blocking buffer: 50 mM sodium phosphate, 2.0% w/v Bovine Serum Albumin, pH 7.2
- 10X Protein microarray washing solution: 0.5 M Tris, 2.5 M NaCl, 0.5% w/v Tween 20, pH 9.0
- 10X PBS buffer: 1.37 M NaCl, 27 mM KCl, 100 mM Na₂HPO₄, 18 mM KH₂PO₄, pH 7.4.
- 1X TBS/FBS buffer: 50 mM Tris-HCl, 150 mM NaCl, 0.05% FBS, pH 7.5

2.1.2 Reagents for SPR gold surfaces fabrication

The SPR sensing platforms were fabricated by combining laser interference lithography (LIL) performed at TASC-IOM-CNR laboratories (Basovizza, TS, Italy) and soft lithography techniques performed at

LaNN laboratories (Veneto Nanotech s.c.p.a., Padova). S1805 photoresist was purchased from Microposit (Shipley European Limited, UK), while MF319 Developer and PGMEA (propylene glycol monomethyl ether acetate) were purchased from MicroChem Corp (Newton, MA, USA).

PDMS (polydimethylsiloxane; Sylgard 184) was purchased from Dow-Corning Corp. (Midland, MI, USA), and the thiolene resin, used for the lithographic master replica, NOA 61 (Norland Optical Adhesive) was purchased from Norland Products Inc. (Las Vegas, NV, USA).

2.1.3 Instruments

Below all the main instruments used for this Thesis are indicated:

- Versarray Chipwriter Pro System (BioRad Laboratories, Hercules, CA, USA)
- TeleChem SMP 2 Stealth Pins (Arrayit Corporation, Sunnyvale, CA, USA)
- Microarray High-Speed Centrifuge (Arrayit Corporation, Sunnyvale, CA, USA)
- Genepix 4000B laser scanner and Software (Molecular Devices, Sunnyvale, CA, USA)
- NanoPhotometer Classic (Implen, Munich, Germany)
- Agilent 2100 Bioanalyzer (Agilent Technologies, Santa Clara, CA)
- Array Booster AB410 hybridization station (Advalytix, Munich, Germany)
- Advawash Station AW400 (Advalytix, Munich, Germany)
- Leica Microsystems confocal microscope TCS SP5 II mounted on Leica DMI6000 CS (Wetzlar, Germany)
- Tescan Vega II LMU scanning electron microscope (SEM) (VEGA TS 5130 LM, Tescan, Czech Republic)
- VEECO D3100 Nanoscope IV atomic force microscope (AFM) (VEECO, Plainview, NY, USA)
- Dual beam FEI Nova 600i scanning electron microscope (FEI, Hillsboro, OR, USA)
- VASE ellipsometer (J.A. Woollam Co., Lincoln, NE, USA)

2.2 Fabrication

2.2.1 Commercial slides (e-Surf LifeLine)

Commercial e-Surf microarray slides (25x75 mm) were purchased from LifeLineLab (Pomezia, Italia). e-Surf is an innovative, high performance activated substrate for protein and nucleic acid microarray applications, since it binds either amino-modified DNA or proteins via $-NH_2$ groups and is therefore suitable for both oligonucleotides and proteins deposition.

The proprietary functional 3D polymer is an innovative concept, offering many advantages over the traditional 2D sylanised glasses. The polymeric glass coating is obtained by physical adsorption of a N,N-dimethylacrylamide (DMA), N,N-acryloyloxysuccinimide (NAS), and [3-(methacryloyloxy)propyl]trimethoxysilyl (MAPS) copolymer. Each monomer confers to the copolymer a specific feature, in particular:

- NAS: reactive group able to bind amino-modified DNA and primary amines of lysines and arginines in proteins.
- DMA: forms the polymer backbone, facilitates polymer adsorption on the glass surface.
- MAPS: covalently reacts with free silanols and stabilizes the coating.

The 3D polymer ensures an optimal biomolecules orientation, allowing ligands to maintain their native configuration and to be available for subsequent binding.²⁹

2.2.2 Gold surfaces

Flat and sinusoidal gold surfaces were kindly provided by Dr. Agnese Sonato and Dr. Gabriele Zacco, operating at TASC-IOM-CNR laboratories and at LaNN laboratories.

The metal used for SPR surfaces must be capable of resonating with the incoming light at a suitable wavelength, in addition, the metal on the sensor surface must be free of oxides, sulphides and it must not react with other molecules on exposure to the atmosphere or liquid. Of the metals, gold is the most suitable choice, since it is very resistant to oxidation and other atmospheric contaminants but is compatible with many chemical modification systems.

The sensing surface consists of a thiolene resin sinusoidal grating ($\sim 6 \text{ cm}^2$) coated by a bi-metallic layer (Chromium (5 nm)/Gold (40 nm)) and supported onto a glass slide. Concerning plasmonic surfaces, the grating geometry was the following: period of 500 nm and amplitude of 40 nm. Surface fabrication process is illustrated in *Figure 10* and summarised in the following steps and in *Figure 10*:

1) *Laser interference lithography (LIL)*

A S1805/PGMEA solution (2:3) was spun onto a silicon wafer with a spin speed of 6000 rpm for 30 s. The sample was exposed to a 50 mW helium cadmium (HeCd) laser emitting a TEM_{00} (Transverse electromagnetic) single mode at a 325 nm light source with a beam incidence angle of 19° and an exposure dose of 70 mJ/cm^2 . Resist developing was performed by immersing the samples in a MF319/Milli-Q water (10:1) solution for 15 s. Exposure and process parameters (i.e., beam incidence angle, exposure and developing time) were chosen in order to obtain a sinusoidal grating with a period of 500 nm and a peak-to-valley amplitude of 40 nm.

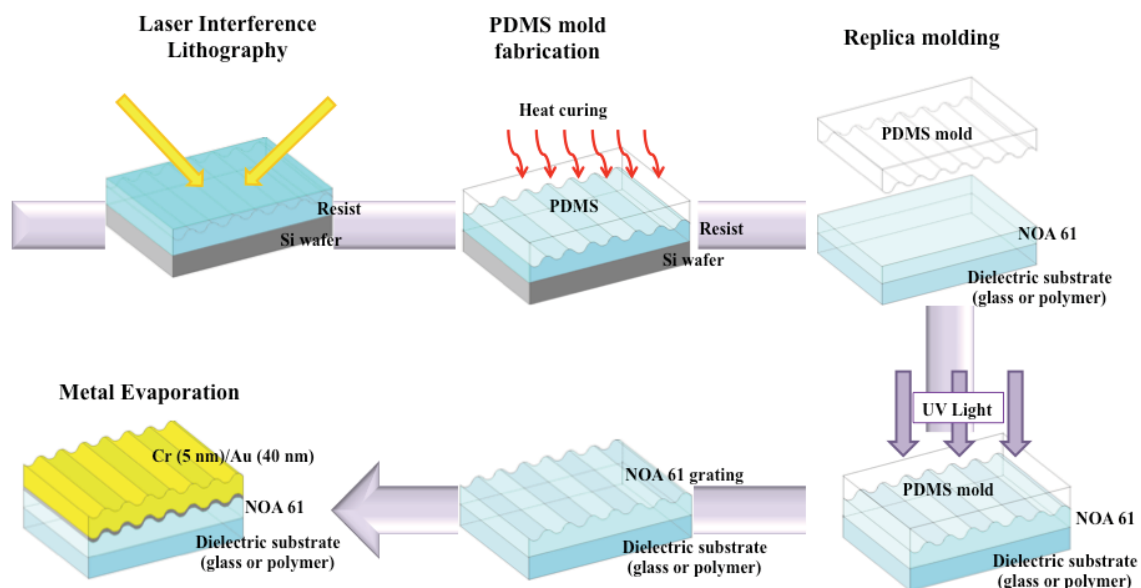


Figure 10. Fabrication strategy adopted for the realisation of the sensing substrates. Sinusoidal gratings were realised through laser interference lithography and replicated through soft lithography. Metal evaporation was finally performed onto the surface.

2) *Soft lithography*

Soft lithography is a non-photolithographic technology based on self-assembly and replica molding for carrying out micro- and nanofabrication and it provides a convenient, effective, and low-cost method for the formation and manufacturing of micro- and nanostructures.

For the replica of the prepared nanostructure, a PDMS mold was realised curing the PDMS layer dropped onto the resist grating at 60 °C for 4 h. The nanopattern was imprinted onto a thiolene resin film (NOA 61) supported onto a microscope glass slide, illuminating the PDMS mold with UV light ($\lambda = 365$ nm) for 30 s, using a standard metal halide 50 mW/cm² lamp (DYMAX UV light flood lamp curing system, DYMAX, Torrington, CT, USA). A 12 hour thermal treatment at 50 °C was then performed in order to increase the resin adhesion onto the glass substrate. The final plasmonic substrate consisted of two identical gratings imprinted onto a microscope glass slide of 75 mm \times 25 mm.

3) *Thermal evaporation*

A gold layer (40 nm) was evaporated above the patterned resin film and a thin chromium film (5 nm) was used as adhesion layer between the metal and the underlying dielectric medium. A VEECO D3100 Nanoscope IV atomic force microscope (AFM) and a dual beam FEI Nova 600i scanning electron microscope were adopted to characterise the substrate topography and sinusoidal profile: results are reported in *Figure 11*: a period of 500 nm and a peak-to-valley amplitude of 40 nm were obtained.

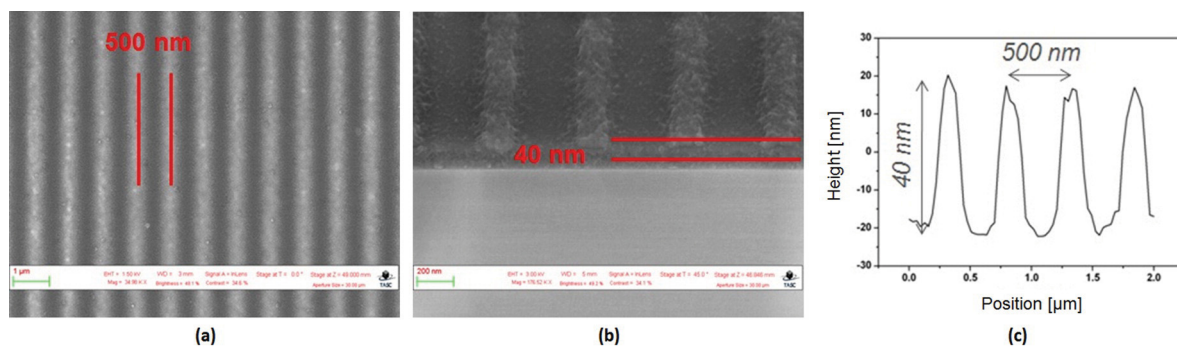


Figure 11. Surface topography SEM images of the sinusoidal plasmonic substrates realised in this work (a, b). The sinusoidal profile was collected by AFM measurements (c).

2.3 Substrates functionalisation

2.3.1 Gold substrates cleaning and SH-PEG-COOH functionalisation

Thiolated PEG (polyethylene glycol) was used as antifouling layer to assure high surface protection from non-specific adsorptions: it is widely accepted that a hydrophilic polymeric layer should be inserted between the recognition element of the biosensor and the metal surface to prevent these interaction and to optimise sensing performances (*Figure 12*). Among all, PEG is one of the most effective agents used for this purpose, as demonstrated by wide literature evidences³⁰⁻³⁶, such that it has often been defined the “gold standard” of antifouling polymers, and its antifouling efficacy depends on the polymer chain length, its surface packing density and the fouling protein size.^{37,38}

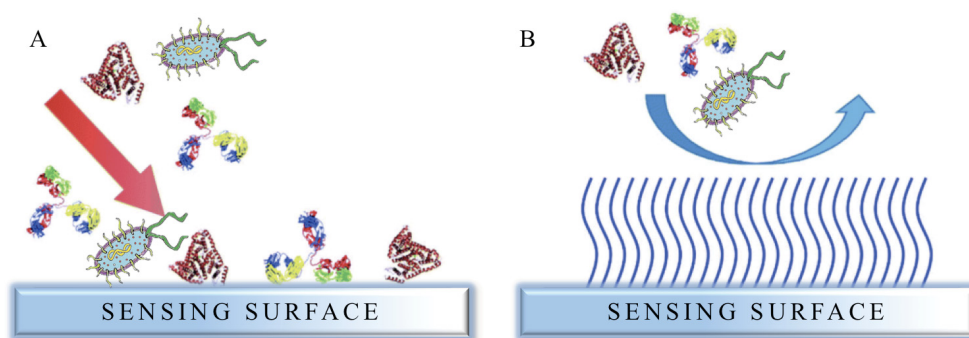


Figure 12. (A) A sensing surface without an antifouling polymer coating is quickly coated in proteins when it comes into contact with samples (containing DNA, proteins, cells, etc...). (B) Passivating the surface with PEG or PEG derivatives reduces aspecific adsorption to the surface. Adapted from³⁷.

Although silver is known to have optimal plasmonic properties⁷, sensing substrates were fabricated with gold and PEG was anchored to the gold surface via self-assembly of thiol species onto the surface: gold binds thiols with high affinity (~40-44 kcal/mol) and it does not undergo any undesired reactions with them, it is chemically stable and essentially inert, it does not oxidize at temperature below its melting point (1064,18 °C), and it does not react with atmospheric oxygen neither with most chemicals.³⁹⁻⁴²

These properties make it possible to handle and manipulate gold samples under atmospheric conditions and allow the usage of liquid cleaning solutions containing for example oxygen peroxide, alcohol or ammonium.

In this work, gold substrates were preliminary cleaned through immersion into Basic Piranha solution for 10 minutes at room temperature (RT) to avoid possible interference caused by organic residues: attention needs to be paid due to the corrosive nature of this solution. Substrates were then rinsed, dried under nitrogen flux, and kept in a clean and dry environment.

A hetero bifunctional PEG (SH-PEG-COOH) was used to functionalise the surface, upon an incubation of 24 hours in humidified environment of a 1mM aqueous solution. The molecule has a MW of 3.4 kDa (Laysan Bio, Arab, AL, USA) and its structure is depicted below in *Figure 13*.

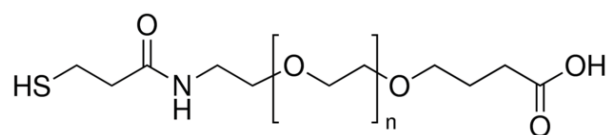


Figure 13. *O*-(3-Carboxypropyl)-*O'*-[2-(3-mercaptopropionylamino)ethyl]-polyethylene glycol (MW 3400 Da).

As can be seen, this molecule carries both a –SH group and a –COOH group: the approach consisted in the formation of a covalent bond between the –SH and the gold surface, and then obtain a –COOH functionalised surface that can be used for the subsequent activation and binding of –NH₂ modified DNA probes or proteins through a peptide bond.

2.3.2 Evaluation of the –COOH functionalisation

To verify the deposition of the –COOH layer obtained after SH-PEG-COOH incubation, the TBO (Toluidine Blue O) colorimetric quantitative assay can be performed. TBO test was performed on a representative number of nanostructured and not nanostructured gold PEGylated surfaces: the reagent

(Figure 14) is a cationic dye able to bind equimolar (1:1) to $-\text{COOH}$, through electrostatic interactions, when it is in the deprotonated form (pH 10).⁴³

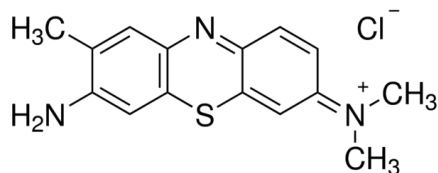


Figure 14. Toluidine Blue O (MW 305.83 Da).

Changing pH from basic to acid (pH 2), the ionic interaction between the $-\text{COOH}$ and TBO is lost causing the detachment of the dye from the surface and its dispersion in solution. The amount of detached TBO can therefore be measured and correlated with the $-\text{COOH}$ surface density.

In particular, surfaces were immersed for 5 hours at 30°C in a TBO solution (5×10^{-4} M, pH 10). The solution was then removed and the surfaces were firstly washed with potassium hydroxide (NaOH 10^{-4} M, pH 10) to remove non-bounded dye, and then incubated with a known volume of acetic acid (CH_3COOH 50%, pH 2) to detach the interacting dye.

TBO concentration was then determined measuring the solution optical density at $\lambda = 633$ nm - using Implen NanoPhotometer Classic. Through an appropriate calibration curve (obtained using TBO in 50% acetic acid solution, pH2) and normalising the results considering the sample surface area, it was possible to obtain the number of $-\text{COOH}$ groups, and thus of HS-PEO-COOH molecules adsorbed onto the surface per cm^2 .

The TBO test was performed on gold nanostructured gratings ($n = 6$) and the estimated density of carboxyl groups resulted to be in the order of 3×10^{15} $-\text{COOH}/\text{cm}^2$ ($\pm 10\%$): this density appears to be sufficient for the anchoring of biomolecules and in accordance with the literature reported data.⁴⁴ A theoretical estimation of appropriate surface biomolecules density was evaluated and reported: in particular, concerning antibodies - considering that the average molecular weight of an immunoglobulin is 170 kDa - and estimating that the average volume that will be used to fill a microwell (9mm*9mm - 81 mm^2) will be

40 μl , with an antibody concentration of 1-0.5 mg/ml, the amount of antibody molecules/cm² will be about 3 orders of magnitude (1000 times) lower than the -COOH groups available on the surface and estimated by TBO assay, i.e. approximately 10¹² molecules of antibody/cm² vs 10¹⁵ -COOH groups/cm². These indications are satisfactory for the effective biofunctionalisation of the substrates.

2.3.3 Biomolecules coupling to activates surfaces trough microarray printing

Concerning e-Surf microarray slides, amino-modified oligonucleotides or proteins can directly be bound to the surface, in the appropriate buffer, since these slides expose NAS, the reactive group that is able to bind amino modified DNA and primary amines of lysines and arginines in proteins. Concerning instead gold surfaces, after SH-PEG-COOH functionalisation, a preliminary activation needs to be performed to allow subsequent biomolecules coupling.

2.3.3.1 EDC-mediated activation of -COOH functionalised gold surfaces

Carbodiimide compounds provide the most popular and versatile method for labelling or crosslinking to carboxylic acids. The most readily available and commonly used carbodiimide for aqueous crosslinking is the water-soluble EDC.

Carbodiimide conjugation works by activating -COOH for direct reaction with primary amines via amide bond formation. Because no portion of their chemical structure becomes part of the final bond between conjugated molecules, carbodiimides are considered zero-length carboxyl-to-amine crosslinkers.

EDC crosslinking is most efficient in acidic conditions and must be performed in buffers devoid of extraneous carboxyls and amines. MES buffer pH 6 (4-morpholinoethanesulfonic acid) is a suitable carbodiimide reaction buffer. Phosphate buffers and neutral pH (up to 7.2) conditions are compatible with the reaction chemistry, albeit with lower efficiency; increasing the amount of EDC in a reaction solution can compensate for the reduced efficiency.

N-hydroxysuccinimide (NHS) or its water-soluble analog (Sulfo-NHS) is often included in EDC coupling protocols to improve efficiency or create dry-stable (amine-reactive) intermediates. EDC couples NHS to

carboxyls, forming an NHS ester that is considerably more stable than the O-acylisourea intermediate while allowing for efficient conjugation to primary amines at physiologic pH (Figure 15).

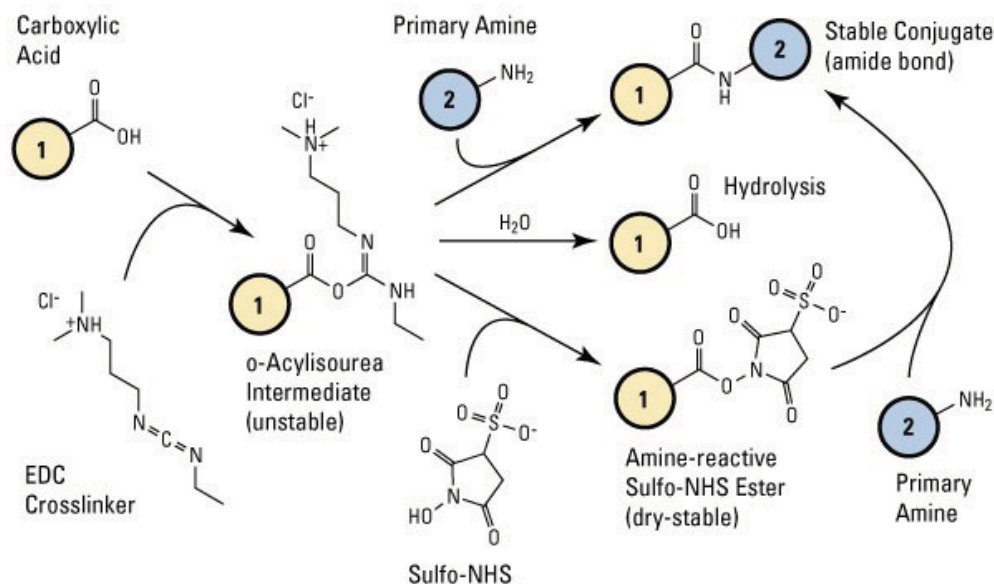


Figure 15. Sulfo-NHS plus EDC crosslinking reaction scheme. Carboxyl-to-amine crosslinking using the carbodiimide EDC and sulfo-NHS. Addition of NHS or Sulfo-NHS to EDC reactions (bottom-most pathway) increases reaction efficiency.

For the experiments of this work, PEGylated gold surfaces were therefore incubated with a fresh prepared EDC-SNHS solution (in MES buffer, pH6) for 15 minutes at RT, to obtain a semi-stable amine-reactive NHS-ester. The activated surfaces were subsequently rinsed with Milli-Q water, N₂ dried (or centrifuged with Microarray High-Speed Centrifuge) and immediately functionalised with the biomolecules of interest, in order to obtain a stable amine bond between -COOH and -NH₂ groups.

2.3.3.2 Coupling of biomolecules to e-Surf microarray glass slides or gold activated slides

Amino modified DNA probes or proteins were covalently bound directly to e-Surf microarray slides, or prior EDC-mediated activation to gold slides.

In particular, amino-modified oligonucleotides were firstly resuspended at 100 μM concentration in Milli-Q, then diluted in Oligo microarray Printing Buffer 1X to a final concentration of 20 μM , and finally deposited on the slide trough microarray spotter. Proteins/antibodies were instead diluted to the appropriate concentration (0,1-1 mg/ml) in Protein microarray print buffer 1X and finally deposited on the slide trough microarray spotter.

The printing protocol was the same both for DNA oligo and for proteins and it is summarised below:

1. Printing and coupling

- a) Print DNA solution/protein solution on activated slides to form microarrays
- b) Place printed slides in a slide storage box
- c) Set uncovered storage box in a saturated NaCl chamber. Over night incubation must be performed at an adequate humidity percentage: for this work, μBox with slideholders (*Figure 16*, QUANTIFOIL Instruments, Jena Germany) was used.
- d) Seal chamber and allow to incubate over night at room temperature. Store coupled slides at ambient condition until use.



Figure 16. The μ BOX will protect the glass slides or micro well plates, as they are watertight, crushproof and have an automatic pressure purge valve. The μ BOX is equipped with speed lock and will hold up to 2 slideholders (each capable of holding up to 4 standard 75 x 25 mm slides). A moist sponge or paper towels soaked with a NaCl saturated solution is placed in the bottom of the chamber to create a humid environment.

The post-coupling processing was instead different, depending on the immobilised biomolecules, in particular:

2a. Post-coupling processing for DNA oligonucleotides

- a) Place the slides in a slide rack and block residual reactive groups using pre-warmed 1X Oligo microarray blocking solution at 50°C for 15 minutes (extend to 30 minutes if not warm).
- b) Discard the blocking solution.
- c) Rinse the slides twice with water.
- d) Wash slide with Oligo microarray washing solution (pre-warmed to 50°C) for 15 to 60 minutes on the shaker.
- e) Discard wash solution and rinse the slides twice with water.

2b. Post-coupling processing for proteins and antibodies

- a) Place the slides in a slide rack and block residual reactive groups using Protein microarray blocking buffer for 1 hour.
- b) Discard the blocking solution.
- c) Rinse the slides twice with 1X Protein microarray washing solution or 1X PBS solution.

The microarray deposition was performed by contact printing with TeleChem SMP 2 Stealth Pins (*Figure 17*), using Versarray Chipwriter Pro System at controlled humidity condition (relative humidity 35%-45%) to properly control spot morphology and geometry.

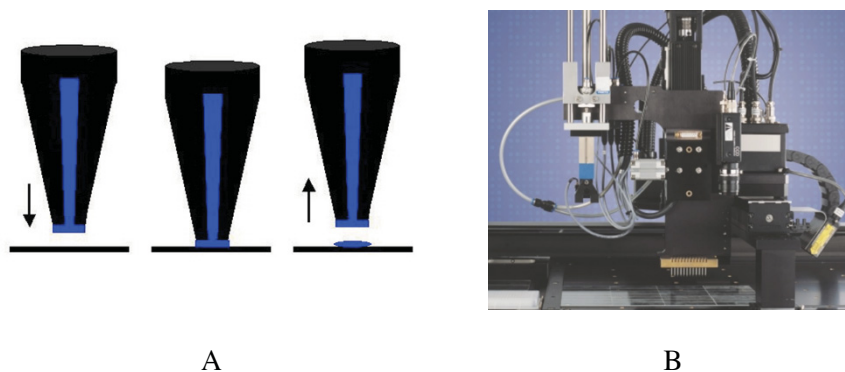


Figure 17. Microarray printing mechanism. A) Arrayit's printing technology (U.S. patent 6,101,946) enables high-speed manufacture of microarrays. The pins have flat tips and defined uptake channels, which allows a thin (25 μm) layer of sample to form at the end of the pin, and printing to proceed by gentle surface contact. Printing occurs as a simple 3-step "ink-stamping" process as follows: (left) downstroke, (centre) contact, and (right) upstroke. B) VersArray ChipWriter Pro System.

Printing scheme was designed to deposit geometrically defined blocks, to obtain 48 identical sub-arrays, organised in 4 columns and 12 lines. This will allow the subsequent hybridisation or incubation of up to 64 different samples or replicas, using a specific mask, the ProPlate 64 slide chamber multi-wells (*Figure 18*, ProPlate, Sigma Aldrich), optimising experimental time, reagents consuming and avoiding replica-to-replica variations.

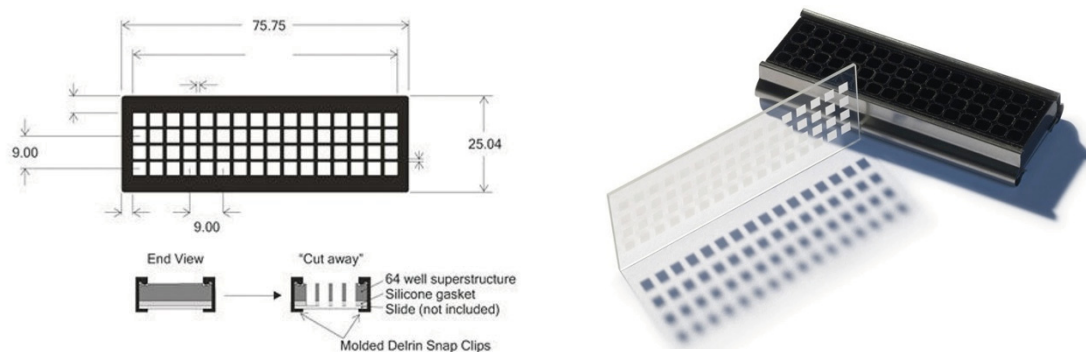


Figure 18. Grace Bio-Labs ProPlate® microarray system, Wells dimension $W \times L$ 3.5 mm \times 3.5 mm.

2.3.4 Samples labelling and incubation

Depending on sample nature and characteristics (DNA, proteins, cells, etc...), different labelling and incubation protocols were optimised and used. Details will be given in 3 and 4 specific Sections.

2.3.5 Microarray fluorescent measurements

Fluorescent measurements on hybridised arrays were performed using a Genepix 4000B laser scanner (Molecular Devices, Sunnyvale, CA) and the Gene Pix Pro software using both 532 and 635 nm wavelengths. Fluorescent spot intensities were quantified using the Gene Pix Pro software after normalising the data by subtracting local background from the recorded spot intensities. For each samples, five replicas were performed, each of them consisting in a subarray with a set of triplicate probes for each analysed mutation.

2.3.6 Surface plasmon resonance measurements

A J.A. Woollam Co. VASE ellipsometer with angular and wavelength spectroscopic resolution of 0.005° and 0.3 nm, respectively, was used for the reflectivity measurements on the SPR surface (*Figure 19*). A goniometer with a precision of 5' mounted onto the sample holder allowed the sample azimuthal orientation control. Reflectivity measurements of the plasmonic gratings were performed in the dry state.

The setup consisted in a Xenon-Neon lamp (75W) as a light source with a monochromator and focusing system that allow selecting wavelengths in the range 270 – 2500 nm. Polarization state was controlled with a first polarizer and the output light that hits the sample was reflected into a detector arm, consisting in a rotating polarizer (analyser) and a photodiode system for signal conversion and amplification.

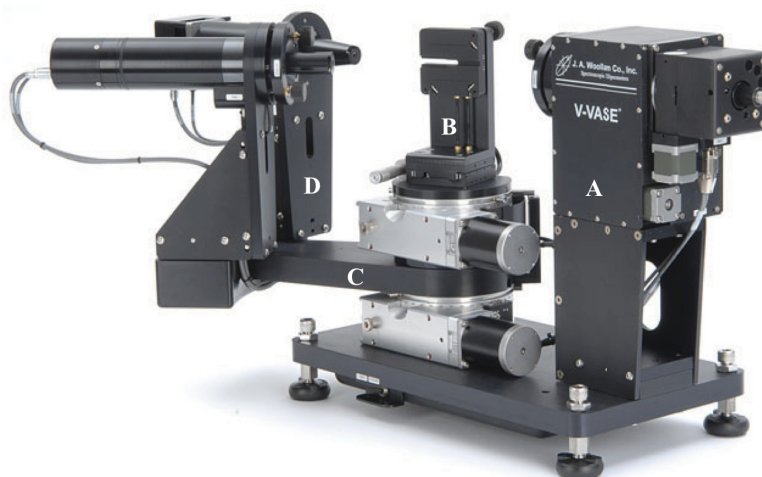


Figure 19. VASE spectroscopic ellipsometer used in this work. (A) Optical bench for focusing and polarization control of the output light (monochromatised by a gating monochromator, located in sequence to a Xe-Neo 75 W lamp), (B) sample holder, (C) rotating goniometer for incidence angle scan, (D) detector.

2.3.6.1 SPR interrogation parameters for DNA platform – angular interrogation

Concerning DNA platform, for the rotated azimuth configuration, incident wavelength λ was set to 625 nm, the azimuthal angle (ϕ) to 45° , and the incident light polarisation (α) to the value of 140° in order to optimize dip depth ($\alpha = 0^\circ$ corresponds to transverse-magnetic - TM - polarisation). In the azimuthally rotated GC-SPR, in fact, TM polarisation is no longer the optimal one for SPP coupling, and the polarisation angle should be tuned according to the formula $\tan \alpha = -\tan \phi \cos \theta$, θ being the resonance polar angle.⁴⁵ Incident angles range from 20° to 80° by a step of 0.2° .

Each surface was characterised before dressing procedures and after each functionalisation step. For each well, the analysis time required was 1 min per step. For each sample, two replicas were performed on each grating, and four replicas were therefore available in a single slide, composed by two gratings.

2.3.6.2 SPR interrogation parameters for antibody platform – wavelength interrogation

Concerning antibody platform, for the rotated azimuth configuration incident wavelength λ ranged from 600 to 800 nm, the azimuthal angle (ϕ) was set to 45° and the incident light polarisation (α) to the value of 140° in order to optimize dip depth ($\alpha = 0^\circ$ corresponds to transverse-magnetic - TM - polarisation). The incident angle was set to 70° . Each surface was characterised before dressing procedures and after each functionalisation step.

The wavelength interrogation – and not the angular one – was used for antibody platform since, for biosafety reasons, a microfluidic cell was used to perform the experiment, as will be described in Section 4. This device allowed the usage of single incident angle (70°) therefore SPR measurements were performed through wavelength interrogation.

3. DNA platform for Cystic Fibrosis

causing mutations detection

In this Section, a strategy for the investigation of some of the most frequent mutations responsible for cystic fibrosis (CF) among the Italian population is described. For the detection of the CF mutations, a highly sensitive Grating Coupled–Surface Plasmon Resonance enhanced spectroscopy method for label-free molecular identification was applied, exploiting a conical illumination configuration. Gold sinusoidal gratings were used as sensing surfaces, and the specific biodetection was achieved through the coupling with DNA hairpin probes designed for single nucleotide discrimination. Such substrates were used to test unlabeled PCR amplified homozygous wild type (wt) and heterozygous samples, deriving from clinical samples, for the screened mutations.

Hybridisation conditions were optimised to obtain the maximum discrimination ratio (DR) between the homozygous wild type and the heterozygous samples. SPR signals obtained from hybridising wild type and heterozygous samples showed DRs able to identify univocally the correct genotypes, as confirmed by fluorescence microarray experiments run in parallel. Furthermore, SPR genotyping was not impaired in samples containing unrelated DNA, allowing the platform to be used for the concomitant discrimination of several alleles also scalable for a high throughput screening setting.

3.1 Introduction

3.1.1 Cystic fibrosis disease

Cystic fibrosis (CF) is one of the most common lifeshortening inherited diseases among the Caucasian population, as its incidence is 1 in 2000– 2500 live births. CF, inherited in a Mendelian autosomal recessive way, is caused by mutations in the cystic fibrosis transmembrane conductance regulator (CFTR) gene. The gene was identified in 1989^{46,47}, located on the long arm of chromosome number 7 (band q31)

and coding for a chlorine ion channel protein^{48,49}, a 1480 amino acid membrane bound glycoprotein with a molecular mass of 170,000 Da (Figure 20).

An abnormal CFTR protein results in defective electrolyte transport and defective chloride ion transport in the apical membrane epithelial cells of the sweat gland, airway, pancreas, and intestine.

As recessive diseases, CF presents “carrier” individuals: these are genetically heterozygous for a specific mutation on CFTR gene, i.e. only one of the two CFTR alleles carries the mutation (wild type/mutant alleles: wt/mut). Heterozygotes are phenotypically normal, as healthy as individuals with both wild type alleles (wild type/wild type alleles: wt/wt), defined as wt homozygous. When a particular mutation is instead present on both alleles of the CFTR gene, a mut homozygous condition is recognised (mutant/mutant alleles: mut/mut), and individuals with this genetic profile are phenotypically affected by CF disease.

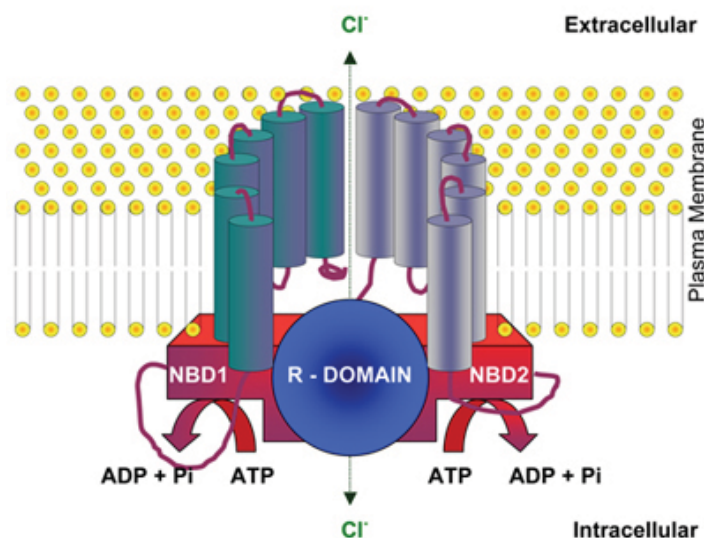


Figure 20. CFTR has been proposed to have two transmembrane (TM) domains (TM1 and TM2) (in green and grey) predicted to contain six hydrophobic membrane-spanning regions, two nucleotide-binding (NB) domains (NBD1 and NBD2) (in red) and one regulatory (R) domain (in blue). R domain contains several potential sites for phosphorylation by cAMP dependent PKA or PKC. The activity of CFTR as an ion channel depends upon phosphorylation of the R domain and binding of ATP to the nuclear binding domains. Figure adapted from⁴⁷.

Almost 1000 different mutations have been identified in the CFTR gene, however, the vast majority of them are at frequencies lower than 0.1%. Mutations of the CFTR gene can be classified into five classes according to the mechanism by which they disrupt the synthesis, traffic and function of CFTR protein.⁵⁰ Class I and II represent approximately 12% and 87% of the CFTR mutations that cause CF in patients worldwide, respectively, while class III, IV and V represent 5% each (*Figure 21*).

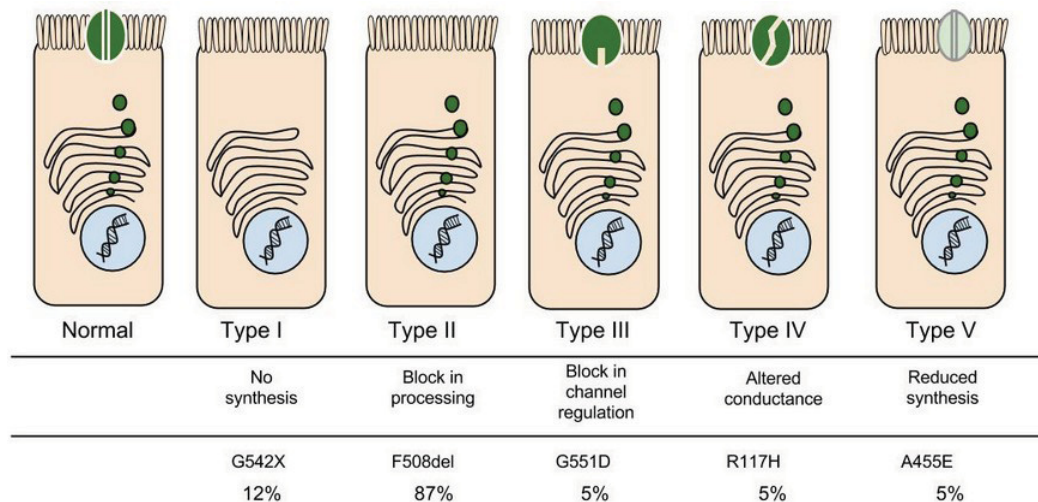


Figure 21. Classification of CFTR mutations. Figure adapted from⁵¹.

The most frequent mutation, $\Delta F508$, accounts for 30% – 88% of CF chromosomes worldwide (*Figure 22*), depending upon race/ethnicity. This mutation consists in a deletion of the three nucleotides that comprise the codon for phenylalanine (F) at position 508. Among the Italian population, $\Delta F508$ has a frequency in carriers of more than 40%, followed by two other mutations with a frequency in carriers of 5 – 6% each: R1162X and N1303K.^{52,53}

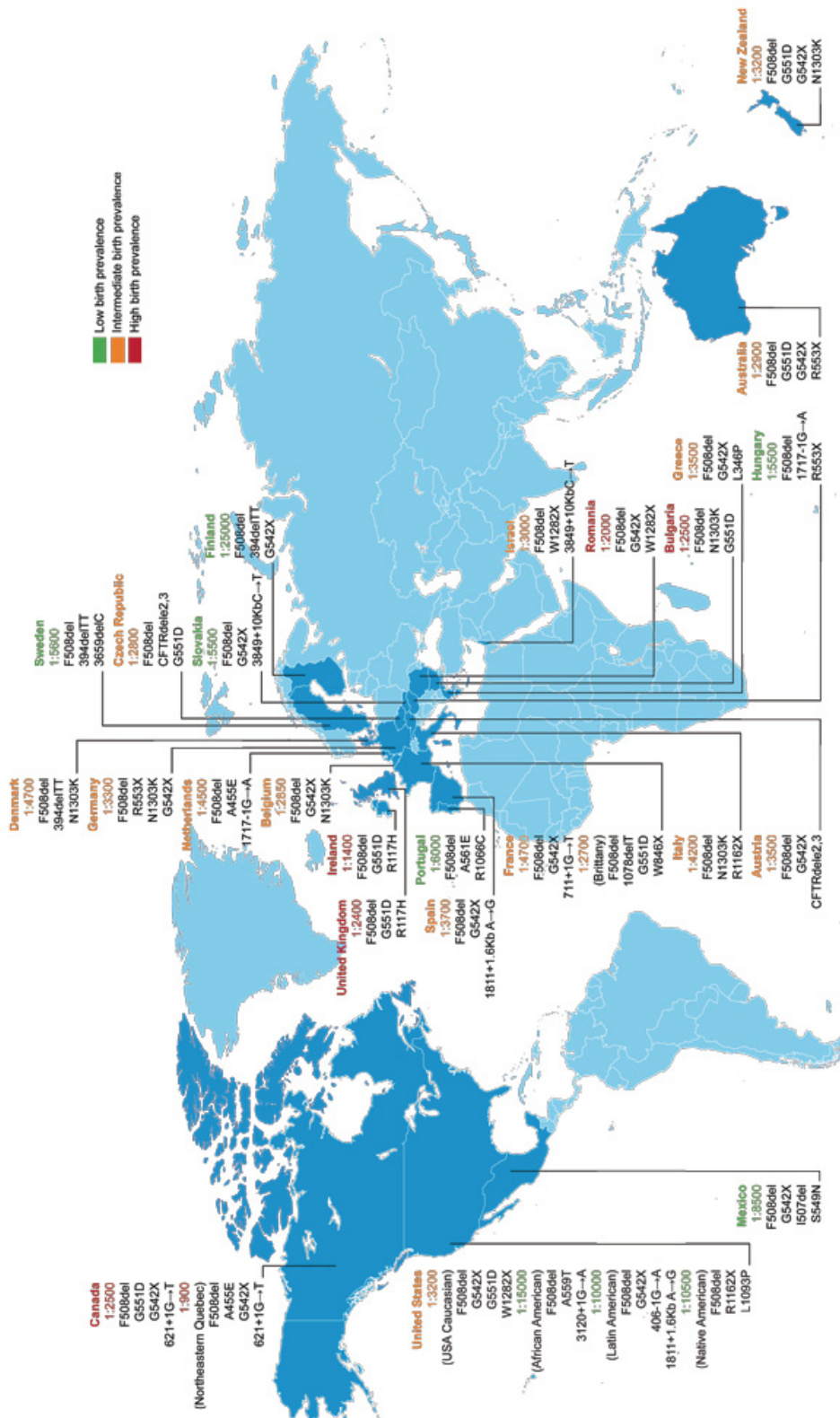


Figure 22. Most common CFTR mutations around the world: birth prevalence is reported as number of live births per case of CF. Common/important mutations in each region are listed below the prevalence.

Adapted from⁵⁴.

3.1.2 Cystic fibrosis genotyping

CF genotyping has seen rapid and efficient growth in recent years since, more than the most commonly used CF diagnostic techniques, novel assays and methods might be employed to enhance the detection throughput performances. The most widely traditional used techniques to diagnose CF are ASO (allele-specific oligonucleotide) dot-blot, based upon hybridisation of a labelled oligonucleotide probe with the target DNA anchored to a membrane, and reverse dot-blot, in which oligonucleotide probes are bound to the membrane on which the biotinylated amplified target DNA is hybridised.⁵⁵⁻⁵⁸ Other detection techniques based on nucleic acid specific amplification and identification include amplification refractory mutation system (ARMS) or allele specific amplification^{59,60}, oligoligation assay (OLA)⁶¹, polyacrylamide gel electrophoresis (PAGE) separation of the heteroduplexes⁶², single-stranded conformation polymorphism (SSCP)^{63,64}, and denaturing gradient gel electrophoresis (DGGE).⁶⁵

More recently, biosensor-based techniques for the detection of CF mutation were reported, as electrochemical biosensors based on methylene blue-DNA interaction⁶⁶, DNA microarrays⁶⁷⁻⁷¹, or biospecific interaction analysis (BIA) monitored through surface plasmon resonance based technology⁷²⁻⁷⁷, performed both through the usage of DNA and PNA molecules.^{78,79}

SPR is a promising high-sensitivity, fast, and low cost technique that meets the requirements for the development of reliable accurate methods in the detection of CF mutations. Most of the literature results based on the SPR technique are performed using the prism-coupling detection method (PC-SPR) and synthetic complementary oligonucleotides as target DNA: in these works limited evidence is available assessing the performances of SPR-based biosensors on clinical samples. Typically, in these studies, a single mutation is analysed at a time, to discriminate between homozygous and heterozygous states, e.g. in CFTR^{74,75,77}, in BRCA1⁸⁰, or in p53 gene.⁸¹

3.1.3 Aim of the study

The present study is focused on the development of a DNA azimuthally rotated grating-coupled surface plasmon resonance-based sensor²¹ for the detection of some of the most common CFTR related mutations.

GC-SPR under azimuthal control, as demonstrated in its first application in simple chemical systems^{21,22}, gives the possibility to enhance the SPR detection sensitivity up to 1 order of magnitude (up to 600 and 800°/RIU) with respect to standard GC- and PC-SPR methods (typically 50–150°/RIU).⁸² In addition, more SPPs can be supported with the same illuminating wavelength. On top of that, through symmetry breaking after grating rotation, polarization assumes a fundamental role on surface plasmon polaritons excitation, and it must be properly tuned in order to optimize the coupling strength.

Allele specific oligonucleotide stem-loop probes have been designed to achieve precise CF genotyping due to the presence of a hairpin-forming region. In the presence of a full complementary DNA, the probe loses its closed structure, allowing the formation of a stable hybrid, while in the presence of mismatched or non-complementary DNA it maintains its secondary structure.^{83,84}

Clinical PCR amplified samples - derived both from homozygous wild type (wt/wt) and clinical heterozygous samples (wt/mut) - were used to set up the SPR system, and results were compared also to fluorescent-based microarray experiments in terms of genotyping ability and discrimination power. Experiments were also performed using PCR amplified samples mixed with fragmented human genomic DNA as an interferent to verify the efficacy of the detection performances of the SPR sensor. These results successfully proved the reliability of the SPR platform in discriminating between the presence of a wild type or mutant allele in the samples.

3.2 Materials and Methods

3.2.1 Primers and Allele Specific Oligonucleotide DNA probes design

The three most frequent mutations among the Italian population of the CFTR gene were selected (Δ F508, R1162X, N1303K), and their localization was verified through the CFTR mutation database (<http://www.genet.sickkids.on.ca/app>). For each mutation, a pair of primers able to amplify the genomic portion of interest through PCR was selected (*Table 3*). Selected primers were purchased from IDT Integrated DNA Technologies (Leuven, Belgium).

Based on the genomic regions identified by the relative primers, specific wild type (wt) and mutant (mut) probes for DNA microarrays were selected, using Array Designer software (Premier Biosoft, CA, USA). Selected probes were also checked for their specificity through the Basic Local Alignment Search Tool (BLAST). For the complete ASO probe design, a portion of each hairpin was defined with a length of six base pairs. The stability of the secondary structure was examined in order to standardize the T_m and ΔG of the hairpin region of all the created structures. Results obtained for the hairpin selected portions and for the final probes are summarised in *Table 4*. Probes were purchased from IDT Integrated DNA Technologies with a 5' C6-NH₂ modification, to allow subsequent surface functionalisation.

Hybridisation conditions for the CFTR microarray were first set up through the preliminary usage of complementary fluorescent (Cy3 and Cy5) oligonucleotides (HPLC purified), purchased from IDT.

3.2.2 Surface functionalisation

Commercial microarray glass slides and gold slides were functionalised as described in Section 2. Concerning gold substrates, probes were anchored through ECD-mediated coupling with the usage of a ProPlate 64 slide chamber multiwells: up to 16 wells of 3.5 mm \times 3.5 mm are obtained for each grating. Each well was functionalised with a single specific probe, leaving two empty cells per grating as measurement references: an example of plasmonic surface organization is showed in *Figure 23*: up to 14 samples can be tested per grating, and up to 28 per slide.

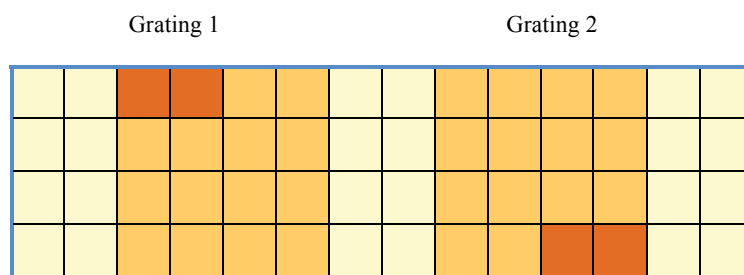


Figure 23. Example of SPR surface scheme created on a microscope glass slide (75mm x 25mm), with 2 gratings having 16 wells each. Flat gold wells (light pink) divide the two gratings, in which reference cells (2 per grating) are highlighted in orange and test cells (14 per grating) are in light orange.

Concerning instead commercial microarray slides, in a single slide up to 48 subarrays were printed; six replicas of alignment probes were spotted, plus three replicas of each investigated wt or mut probe, to ensure proper statistical analysis: the resulting scheme is depicted in *Figure 24*.

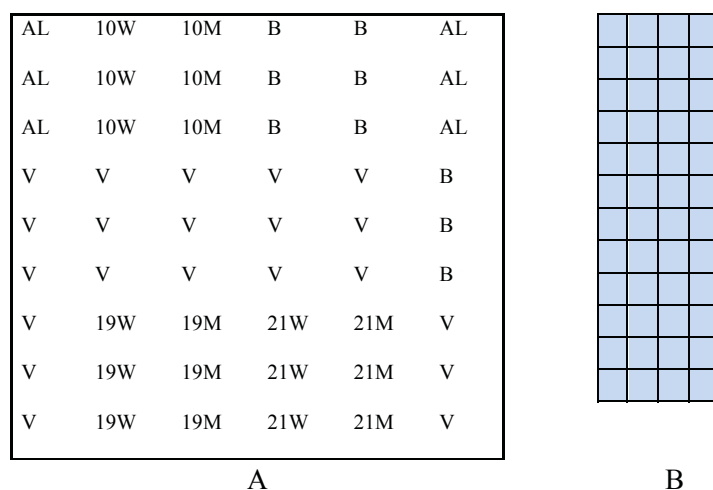


Figure 24. A) Deposition scheme of each of the 48 subarrays adopted for microarray printing on e-surf LifeLine slides. V = empty spots, B = buffer, AL = alignment spots. 10W = $\Delta F508$ wt probe; 10M = $\Delta F508$ mut probe; 19W = R1162X wt probe; 19M = R1162X mut probe; 21W = N1303K wt probe; 21M = N1303K mut probe. B) Scheme of a complete slide, including 48 identical subarrays.

3.2.3 Samples preparation and hybridisation

Human DNA extracts were kindly provided by Dr. L. Picci (Pediatric Department, Padua Hospital, University of Padova). In particular, a homozygous wild type (wt/wt alleles) and a heterozygous (wt/mut alleles) sample for each of the three analysed mutations were obtained after verification through DNA sequencing. No homozygous mutant samples were available.

DNA samples were PCR amplified using AmpliTaq Gold 360 DNA polymerase reagents (Applied Biosystem, Life Technologies, Milan, Italy).

Reagents concentration and PCR amplification conditions are illustrated below (*Table 1*):

Table 1 PCR reagents concentration (left) and amplification conditions (right).

<i>Components</i>	<i>Final concentration</i>
DNA template	Variable
25 uM Forward Primer	0,5 uM
25 uM Reverse Primer	0,5 uM
10X PCR Buffer	1X
25 mM MgCl ₂	1,5 mM
10 mM dNTPs	200 uM
<i>Taq</i> Polymerase (5 U/ μ l)	2,5 U
Milli-Q H ₂ O	to volume

<i>Thermocycling conditions</i>		
Step	Temperature	Time
Initial Denaturation	95 °C	5 min
Amplification 40 Cycles	95 °C (denaturation)	30 sec
	50 °C (amplification)	30 sec
	72 °C (extension)	1 min
Final Extension	72 °C	7 min
Hold	4 °C	∞

PCR products were purified with silica spin columns (PureLink PCR Purification Kit, Life Technologies) and analysed through an electrophoretic run on an Agilent Bioanalyzer with a DNA chip (*Figure 25*).

Fluorescent PCR products were obtained using a mix of dCTP-Cy3 or dCTP-Cy5, for wild type or heterozygous samples, respectively (GE Healthcare, Little Chalfont, UK). Fluorophore incorporation was verified spectrophotometrically.

Human genome from the lymphoma cell line (BL41 cell line, LGC standards, UK) was extracted with QIAamp DNA Mini Kit (Qiagen, Hilden, Germany) and fragmented with double strand DNA Fragmentase using the conditions indicated by the supplier (New England Biolabs, Ipswich, MA, USA). Obtained

fragments ranged from 300 bp to 600 bp, as verified by capillary gel electrophoresis with the Agilent Bioanalyzer, and were used as interferent DNA in the subsequent preparations.



Figure 25. Agilent 2100 Bioanalyzer workstation.

CFTR PCR fragments, Cy3/Cy5-labeled or unlabeled, were incubated on e-surf microarray slides and on gold plasmonic slides, respectively. Mixtures were denatured, cooled, and hybridised for 3 h at 37 °C, in an optimised hybridisation buffer (2X SSC, 0.1% SDS, 0.2 mg/mL Bovine Serum Albumin, 20% formamide), in the Array Booster AB410 hybridisation station (*Figure 26 A*). ProPlate 64 multiwells slide chambers were used to physically isolate each subarray during incubation with different samples.

For fluorescent analysis, one PCR sample could be simultaneously tested for the mutation of interest in the whole subarray that included the six specific probes (three wild type and three mutants, each in triplicate, see *Figure 24*).

For SPR experiments, instead, each PCR product obtained for all of the three loci was split into two wells to analyse separately sample hybridisation on the wild type or on the mutant probe anchored on different wells on the sensing surface.

After hybridisation, slides were washed in the Advawash Station AW400 (*Figure 26 B*) for 5 min in 1X SSC 0.1% SDS at 37 °C, 2 min in 0.2X SSC at RT, 2 min in 0.1X SSC at RT and 30 s in Milli-Q H₂O at

RT, spin-dried using Microarray High-Speed Centrifuge and submitted to SPR analysis or scanned for fluorescent emission.



Figure 26. A) Array Booster AB410 hybridisation station and B) Advawash Station AW400.

3.2.4 SPR and fluorescence measurements

SPR and fluorescence measurements were performed as described in Section 2. In particular, concerning SPR measurements, substrates were characterised after each experimental step with the parameters of *Table 2*:

Table 2. Characterisation parameters used for SPR measurements.

Incident wavelength [nm]	625
Light incidence angle [°]	32-46
Azimuth [°]	45°
Polarization [°]	140°

Reflectivity measurements were carried out in the following steps:

- after piranha cleaning;
- after PEG functionalization;
- after probe anchoring;

- after target hybridization

The described procedure allowed to control all the experimental steps with high precision and accuracy in order to be able to reproduce the optimised experimental conditions.

3.3 Results and Discussion

3.3.1 Primers and Allele Specific Oligonucleotide DNA probes design

For each of the 3 mutations to be analysed, a pair of primers able to amplify the genomic portion of interest through PCR was selected (*Table 3*).

Table 3. PCR primers for CFTR genomic regions' amplification.^a

<i>Name</i>	<i>Sequence 5'-3'</i>	<i>nt</i>	<i>GC%</i>	<i>T_m °C</i>	<i>Amplicon length (wt/mut)</i>
ΔF508 (ex10) F	ATGATGGGTTTTATTCCAGAC	22	36.4	50.9	271/268
ΔF508 (ex10) R	ATTGGGTAGTGTGAAGGGTTC	21	47.6	54.6	
R1162X (ex19) F	GCCCGACAAATAACCAAGTGA	21	47.6	55.5	454/454
R1162X (ex19) R	GCTAACACATTGCTTCAGGCT	21	47.6	55.8	
N1303K (ex21) F	AATGTTCCACAAGGGACTCCA	20	45.0	53.9	473/473
N1303K (ex21) R	CAAAAGTACCTGTGCTCCA	20	45.0	52.9	

^aPrimer sequences were adapted from sequences reported by⁸⁵. *nt*: nucleotide length. *GC%*: guanine-cytosine percentage. *wt*: wild type DNA. *mut*: mutant DNA.

Concerning microarray probes, hairpin-shaped molecule were designed to discriminate between wild type and mutant sequences: they consisted of a probe sequence embedded between complementary sequences that form a hairpin stem, attached to the microarray surface by only one of its strands. In the absence of an amplified DNA (target), probe is held in the closed state, while when the target binds perfectly to its probe (no mismatch), the greater stability of the probe-target helix forces the stem to unwind, resulting in an opening of the probe, permitting hybridisation (*Figure 27*).

It would be therefore possible to increase specificity differentiating between two DNA targets that differ by as little as a single nucleotide.⁸⁶⁻⁸⁸

According to literature's information, a length of 18–22 nucleotides was chosen as optimal for probes' design, to discriminate single base mutations with high accuracy. It should be noted that the probes' design

was highly constrained by the position of the mutation itself, which should be placed in the central position of the probe, in order to maximize mutation discrimination capability^{89,90}, and by the nucleotide composition of the sequence surrounding the mutation itself.

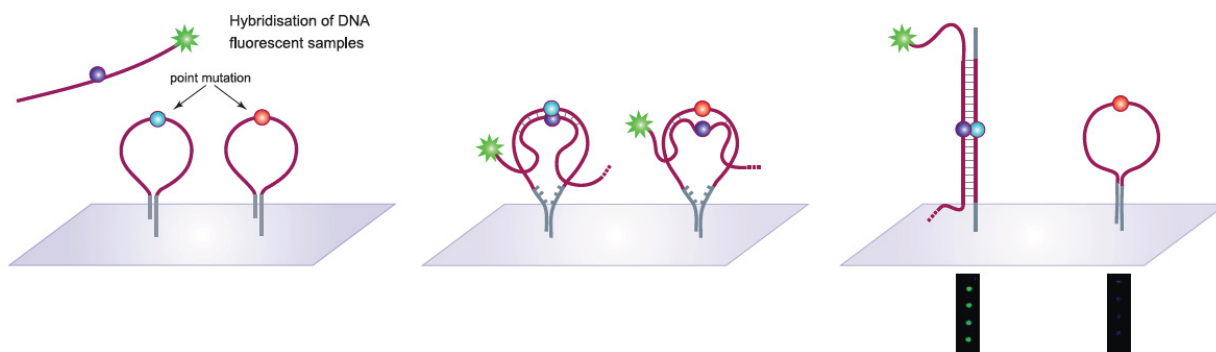


Figure 27. Cartoon depicting the hybridisation mechanism of ASO hairpin probes for the discrimination of single nucleotide mutations.

The portion of each hairpin probe was designed as indicated in literature regarding the length of the portion and a length of 6 bp is set^{55,56}, carefully evaluating the stability of the structure in order to standardize the T_m and ΔG of the hairpin regions. For the ASO probes, design results are summarised in *Table 4*: the hairpin portion is indicated in bold and underlined; probes with the hairpin portion show excellent uniformity in chemical–physical characteristics, especially concerning the average T_m . The hairpin regions with stem-loop motif were designed in order to obtain a narrow range of melting temperature for all of the probes, as well as for the stem region, and comparable structure and ΔG .

Table 4. Sequences of Microarray ASO Probes.^b

Name	Sequence 5'-3'	Structure	Nt	T _m °C	GC%	ΔG hairpin portion kcal/mol	T _m hairpin portion °C	ΔH hairpin portion kcal/mol	ΔS hairpin portion kcal/mol
$\Delta F508$	<u>CAATCGAAT</u> ATCATCTTT GGTGTTC <u>TCGATTG</u>		34	59,2	38,2	-3,2	44,7	-51,5	-162,02
$\Delta F508$ mut	<u>CAATCGATA</u> TCATTGGTG TTTCCTATG <u>TCGATTG</u>		34	59,0	38,2	-4,87	43,6	-83	-262,07
R1162X	<u>CCATCATCT</u> GTGAGCCGA GTCTTTGA <u>TGG</u>		30	62,1	50,0	-2,24	41,5	-42,8	-136,02
R1162X mut	<u>CCATCAATC</u> TGTGAGCTG AGTCTTTAT <u>GATGG</u>		32	60,1	43,8	-2,47	42,9	-43,6	-137,96
N1303K	<u>CAAGCATT</u> AGAAAAAAC TTGGATCCC <u>TTGCTTG</u>		34	60,2	38,2	-2,52	42,7	-44,9	-142,15
N1303K mut	<u>CAAGCATT</u> AGAAAAAA GTTGGATCC <u>CTTGCTTG</u>		34	60,2	38,2	-2,52	42,7	-44,9	-142,15

^bThe hairpin region with the mutated oligonucleotides is represented in red, and the hairpin portion is bold and underlined. Thermodynamic analysis was performed using IDT DNA software (<http://eu.idtdna.com/analyzer/applications/oligoanalyzer/>), evaluating with software default parameters (oligo concentration = 0.25 μ M, Na⁺ concentration = 50 mM) the whole probe sequence and the hairpin structure (T = 25 °C, Na⁺ concentration = 25 mM, suboptimality = 50%).

3.3.2 Hybridisation conditions setup and optimization through fluorescent analysis

Hybridisation conditions for the CFTR microarray were first set up through the preliminary usage of complementary fluorescent (Cy3 and Cy5) oligonucleotides (Table 5). These perfect match oligos were used to preliminary test the ability of the deposited ASO probes to recognize specifically the wt or mut sequence, and potentially to correctly genotype the subsequent samples.

Table 5. Oligonucleotide sequences of DNA fluorescent (Cy3 or Cy5) complementary targets.

Name	Sequence 5'-3'
Δ F508	Cy3/AGGAAACACCAAAGATGATATT
Δ F508 mut	Cy5/CATAGGAAACACCAATGATAT
R1162X	Cy3/AAAGACTCGGCTCACAGA
R1162X mut	Cy5/TAAAGACTCAGCTCACAGAT
N1303K	Cy3/AGGGATCCAAGTTTTTCTAAA
N1303K mut	Cy5/AGGGATCCAAGTTTTTCTAAA

The performances of the chosen hybridisation setting were subsequently confirmed using fluorescently labelled PCR products deriving from clinical samples to analyse the screening potential of the platform. Several conditions were deeply investigated, applying variations to SSC and formamide concentrations and to hybridisation temperature to achieve optimal genotyping.

Conditions were optimised for oligos hybridisation, considering the contribution to the T_m given by monovalent cations concentration (Na⁺), formamide percentage, probe length and GC%. T_m was calculated using the following formula for DNA:DNA hybrids:⁹¹

$$T_m = 81,5 + 16,6 * \log (Na^+ \text{ Molarity}) + 0,41 * GC\% - 0,72 * \text{formamide}\% - 500 / \text{oligo length}$$

Hybridisation temperature (T_{hyb}) was calculated to obtain a Δ between T_m and T_{hyb} of 20-25°C (moderate stringency) or between 15-20°C (high stringency).

Buffer composition was set to operate with an hybridisation temperature ranging from 25°C to 37°C (range temperature lower than theoretical melting temperature of the hairpin probes) in order to ensure hairpin's probe structure maintenance, and thus the possibility to obtain a theoretical optimal discrimination between perfect match and mismatch, and at the same time to operate with a possible portable device at or above room temperature.

Some of the most promising oligos hybridisation settings were tested on PCR amplified clinical samples, fluorescently labelled with Cy3 or Cy5 d-CTP. The hybridisation protocol that allowed detecting the proper allele with the higher specificity included a buffer composition with SSC 2X and formamide 20%, at a hybridisation temperature of 37 °C. Fluorescence microarray hybridisation results were collected, and the ratio between the signal on the mutated probe and the one on the wild type probe was calculated, obtaining the discrimination ratios (DR) for each analysed locus, as shown in *Figure 28*. These ratios indicate the ability to discriminate between a perfect and a mismatched target sequence and are necessary to establish a univocal way to genotype unknown samples.

For wt samples (wt/wt), DRs more close to zero are expected for an optimal genotyping indicating that the wt DNA is almost completely hybridised on the wt probe. Reported DRs demonstrate that, for all the wt tested samples, obtained values were suitable for genotyping. In particular, for wt Δ F508 and wt R1162X, all reported values are included between 0.01 and 0.08.

Regarding the N1303K wt sample, the obtained DR is 0.4, relatively higher if compared to the DR rates obtained for the other wt samples, but still able to genotype correctly the sequence. This can be attributed to the chemico-physical characteristics of N1303K wt and mut probe couple, constrained by the mutation position itself, and by the surrounding nucleotides.

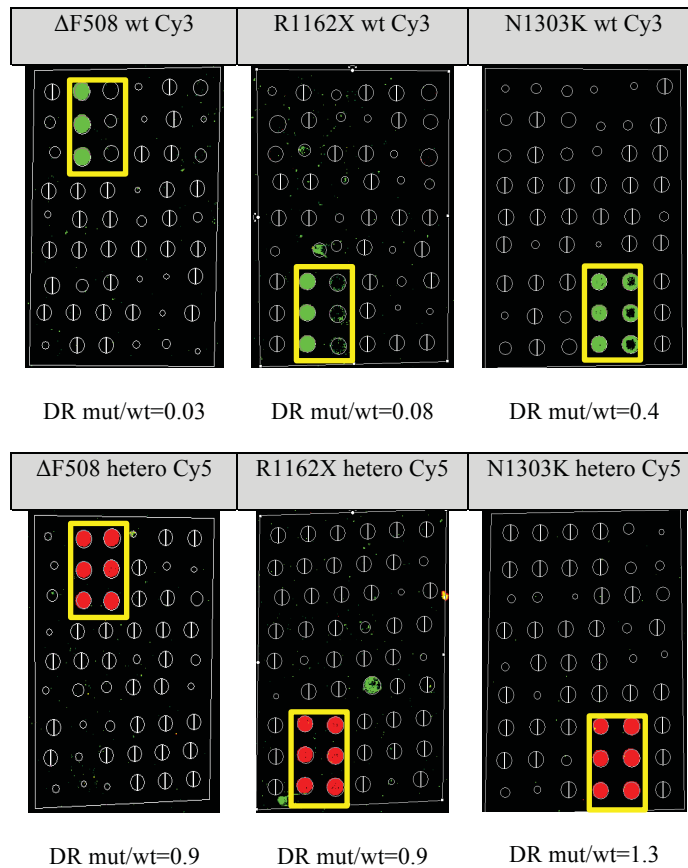


Figure 28. Microarray hybridization results obtained with PCR fragments, labelled with Cy3 (green, wt samples) or with Cy5 (red, heterozygous samples) under the optimised hybridization conditions (SSC2X, formamide 20%, hybridization temperature 37 °C 3h). Results are shown both as images and numerically as discrimination ratios (DR). Yellow boxes: include wt and mut probe for the analysed mutation. wt: wild type samples. hetero: heterozygous samples.

For heterozygous samples (wt/mut), DRs more close to 1 are expected for an optimal genotyping, indicating that the heterozygous sample is equally hybridised on the two probes (wt and mut). Concerning heterozygous samples, for all the tested samples, DRs between 0.9 and 1.3 were achieved: obtained DRs are in line with the expected DR value and are particularly suitable to achieve a precise genotyping of the heterozygous samples.

3.3.3 SPR response to PCR amplified clinical samples

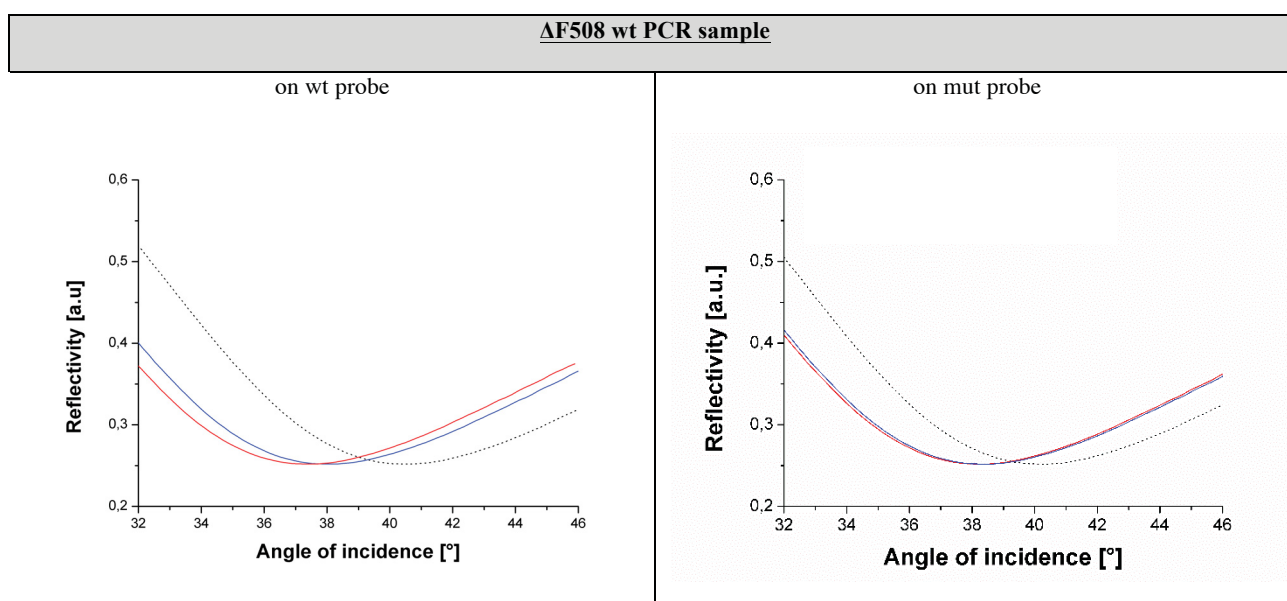
Hybridisation of CFTR unlabeled PCR products was performed on plasmonic slides, with the same condition used and optimised for fluorescent readout. Results are numerically expressed in *Table 6* and representative graphs are shown in *Figure 29*.

Experiments were performed always in parallel with hybridisation on microarray of labelled PCR, as control. Shifts were collected after substrate cleaning, surface biofunctionalisation, and sample incubation.

Table 6. SPR shifts obtained after hybridisation of CFTR related PCR products.^a

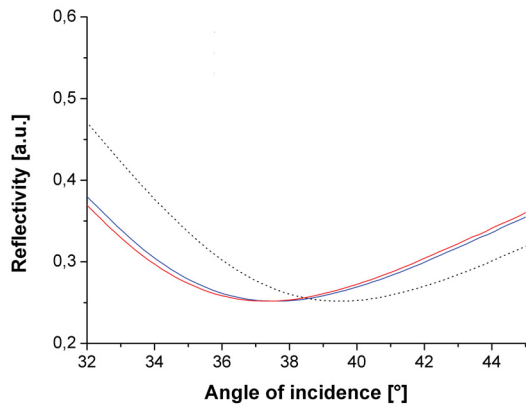
		Screened Mutation					
		$\Delta F508$		R1162X		N1303K	
hybridised on	PCR	wt PCR	hetero PCR	wt PCR	hetero PCR	wt PCR	hetero PCR
	wt probe		$0.64^\circ \pm 0.06^\circ$	$0.26^\circ \pm 0.06^\circ$	$0.51^\circ \pm 0.06^\circ$	$0.24^\circ \pm 0.07^\circ$	$0.45^\circ \pm 0.07^\circ$
mut probe		$0.13^\circ \pm 0.06^\circ$	$0.19^\circ \pm 0.07^\circ$	$0.05^\circ \pm 0.06^\circ$	$0.77^\circ \pm 0.07^\circ$	$0.08^\circ \pm 0.06^\circ$	$0.38^\circ \pm 0.06^\circ$
DR range ^b		0.1–0.2	0.7–3	0.1–0.2	0.7–3	0.1–0.2	0.9–2

^aEach sample is incubated both on wt and on mut related probe. Values of the shifts are representative of one experiment. ^bDRs are mediated on results of three independent experiments.

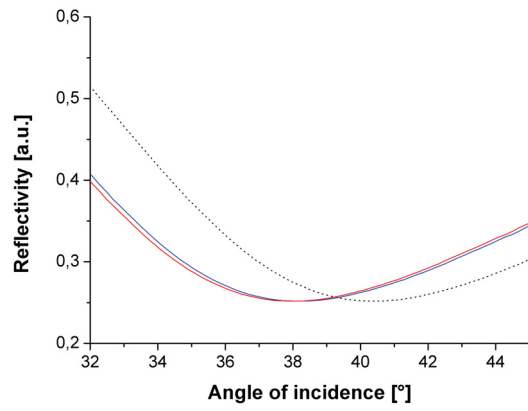


Δ F508 heterozygous PCR sample

on wt probe

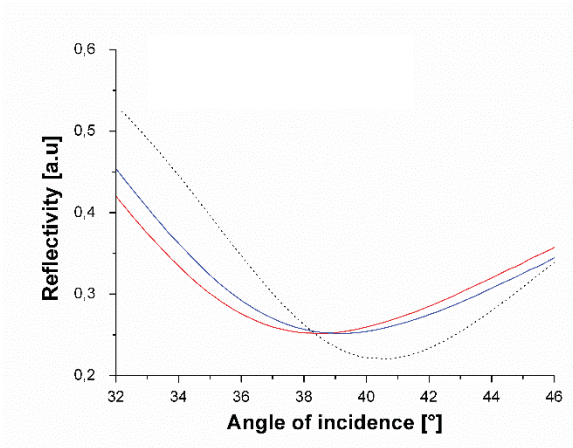


on mut probe

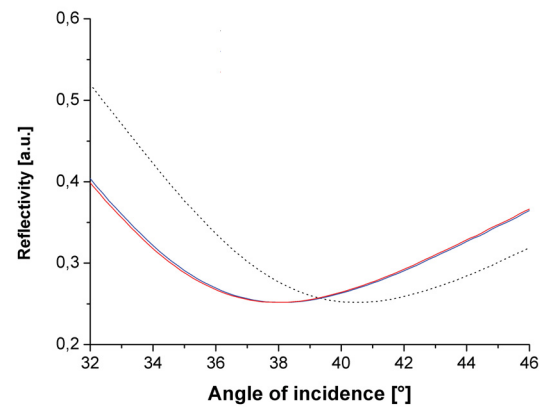


R1162X wt PCR sample

on wt probe

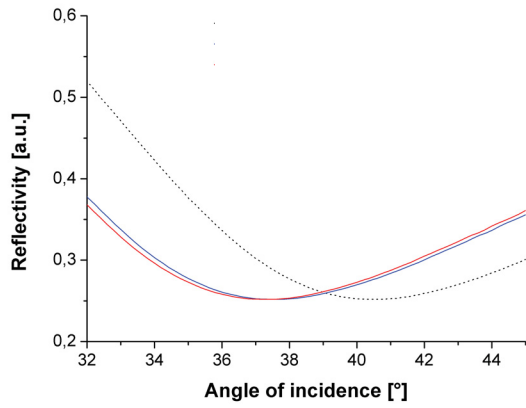


on mut probe

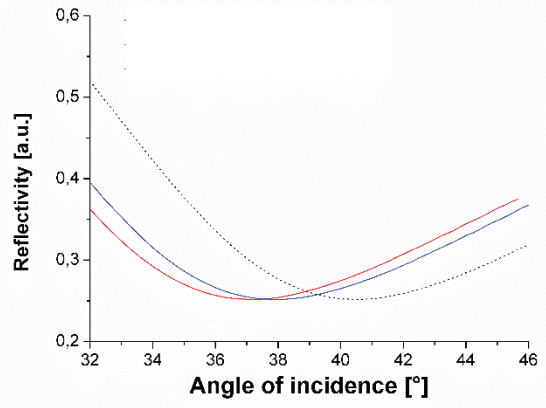


R1162X heterozygous PCR sample

on wt probe



on mut probe



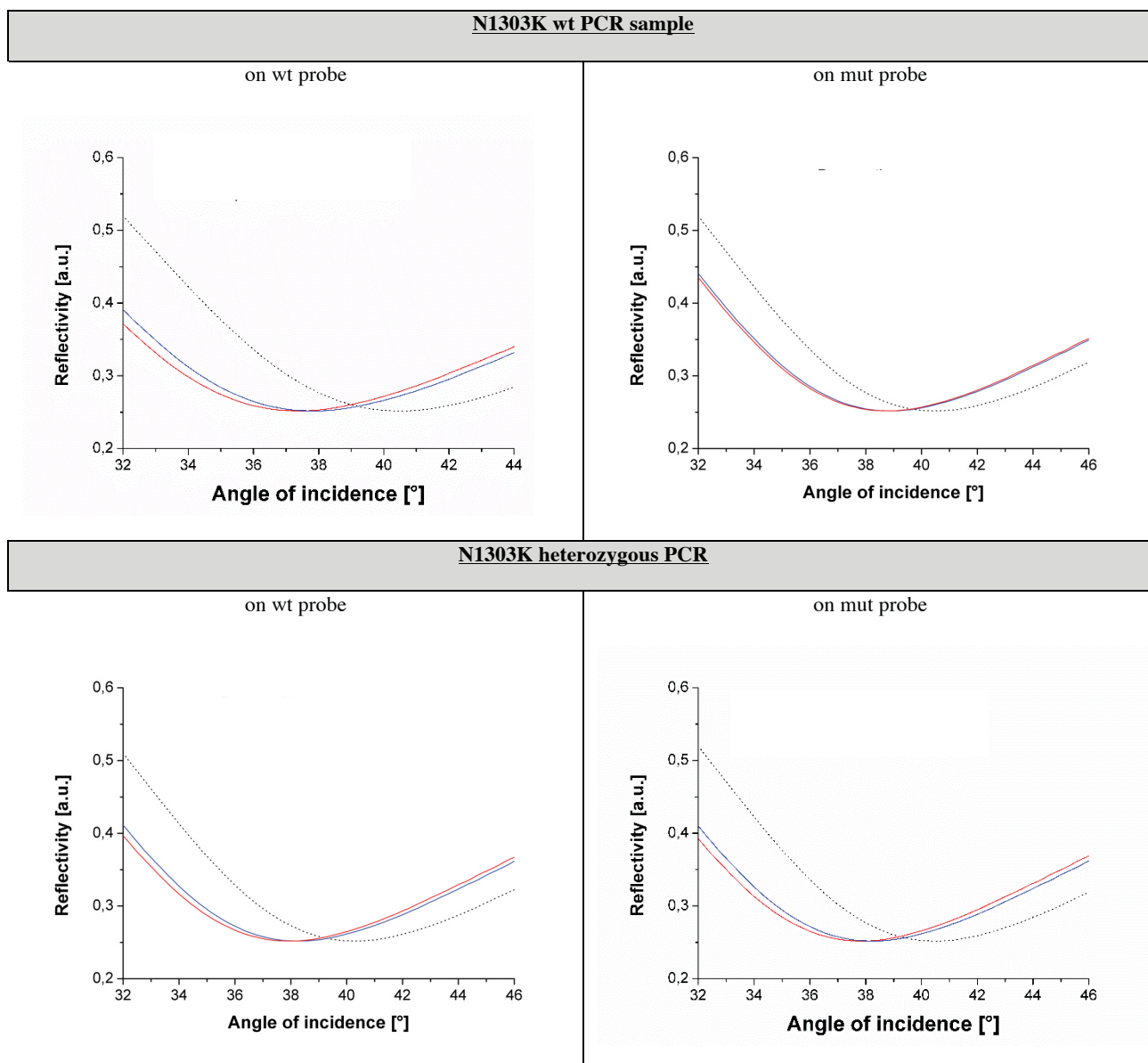


Figure 29. SPR shifts obtained after hybridisation of CFTR related PCR products. Reflectivity curves were collected for the bare grating after substrate cleaning (black dots), after SH-PEG-COOH plus -NH₂ modified probe immobilization on the surface (blue line), and after sample incubation (red line). Three measurements per point were performed. The curves were fitted using a Lorentz function; the error was propagated and then mediated on all the measurements. The reflectivity minimum was derived from the fitting procedure.

For tested wt samples, a significant shift was recorded after incubation of the sample on the related wt probe (0.45°–0.64°), while no significant signal, i.e., a signal comparable to the measurement error (up to 0.15°), was detected on the mut one (0.05°–0.13°).

In the case of heterozygous samples, resonance angle shifts were collected on both relative probes (0.19°–0.77°). DRs for wild type and heterozygous samples were calculated from the shift ratios.

In the case of wt samples DR is included between 0.1 and 0.2 for all the tested samples, underlining genotyping ability of all wt probes in the SPR configuration. Concerning mut probes DR ranges from 0.7 to 3, underlying that also in this case precise genotypisation can be achieved.

3.3.4 SPR response in presence of interferent DNA

A series of experiments were performed to verify the system genotyping ability in presence of a more complex sample, resembling the ones routinely used for molecular CF detection, i.e. samples containing several PCR amplified CF related sequences. For this purpose, complex samples containing the target sequences and fragmented human genomic DNA were used. As shown in *Table 7*, the presence of interferent DNA did not mislead the genotypisation of the unknown samples.

Table 7. Hybridisation shift obtained incubating the target PCR amplicons alone or mixed with interferent unrelated genomic DNA sequences.^a

Target wt/wt DNA									
	ΔF508			R1162X			N1303K		
Probe	wt	mut	DR	wt	mut	DR	wt	mut	DR
Interferent ^b									
without	0.56° ± 0.08°	0.13° ± 0.06°	0.23 ± 0.11	0.45° ± 0.06°	0.11° ± 0.07°	0.24 ± 0.16	0.45° ± 0.07°	0.08° ± 0.06°	0.18 ± 0.14
with	0.70° ± 0.07°	0.07° ± 0.06°	0.10 ± 0.09	0.53° ± 0.06°	0.04° ± 0.08°	0.08 ± 0.15	0.45° ± 0.07°	0.12° ± 0.06°	0.27 ± 0.14

^aTarget DNA amplicons derived from homozygous wt/wt samples. ^b Interferent: fragmented genomic DNA (80 ng) and/or unrelated PCR amplicons (300 pg each).

The shift signals did not differ between samples and DR values were all around the threshold value of 0.2 as for the reference non-complex samples (row without interferent), supporting the correct identification of wild type samples for all of the three investigated alleles.

Further analyses are on-going to verify the lower limit in sample cellularity in order to reliably detect the presence of mutated sequences in the CFTR gene responsible for CF disease without PCR-mediated amplification.

3.3.5 System cut-off evaluation and test with blind samples

After the evaluation of the DRs deriving from all the genotyping experiments performed and summarised in the previous paragraphs, DR cut-offs were established and are reported in *Table 8*. A DR cut-off for wt sample genotypisation can be set at 0.4: all the obtained DRs below 0.4 univocally genotype a wt sample; vice versa a DR above 0.5 genotypes univocally the presence of a mutant allele. In particular, the presence of a heterozygous sample is characterised by a DR value in the range between 0.5 and 3.0, as verified in the performed experiments.

Table 8. Summary of genotypisation DRs cut-off range obtained using fluorescent technique (a) or SPR technique (b).

<i>(a) fluoro analysis</i>			<i>(b) SPR analysis</i>		
DR output results			DR output results		
	wild type	Hetero		wild type	hetero
mut/wt probe signal	<0.4	0.5–1.5	mut/wt probe signal	<0.4	0.5–3.0

To validate the genotypisation-established cut-offs, human DNA samples were PCR amplified and analysed through the SPR platform, in a blind experiment, running a fluorescent microarray experiment as a control.

In particular 4 samples - $\Delta F508$ wild type and heterozygous samples plus N1303K wild type and heterozygous samples - were analysed in duplicate on the plasmonic gratings. Results are reported in *Figure 30*, in which shifts are represented as dots on a graph delimited by the DR cut-off lines. For all the

analysed sample's replicas, a correct genotyping is achieved, as shown in the graph. The shifts of wild type samples are below the 0.4 line, while all heterozygous samples present signals above the 0.5 line.

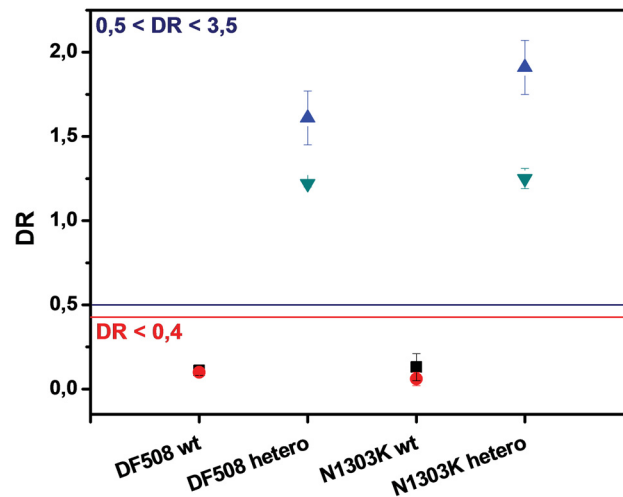


Figure 30. Genotyping of CF samples for the positions related to $\Delta F508$ or N1303K alleles in a blind experiment. The red line represents the DR cut-off for wild type samples, while the blue line points to the lower limit of the DR for heterozygous samples. Red dots and black squares represent replicas of the relative wild type samples, while green and blue triangles represent replicas of the relative heterozygous samples.

3.4 Conclusions

In this Section experiments aimed at the set-up of a plasmonic-based platform for the identification of the most common CF causing mutation among the Italian population were described.

Probes for CFTR screening were chosen, and their structure was evaluated. A precise and reproducible method for plasmonic gold surface functionalization was optimised for the genotyping of the three most frequent CFTR in the Italian population. Hybridisation conditions for correctly genotyping PCR fragments deriving from DNA extracted from clinical samples were properly set using a fluorescent microarray technique. Once optimised, hybridisation conditions were used for samples analysis on SPR substrates.

Data obtained from plasmonic analysis demonstrated to be fully consistent and homogeneous between replicas, indicating the correct genotypisation of the selected alleles. These results clearly showed the possibility of employing azimuthally controlled GC-SPR for the genotypisation of CF mutations, and the discrimination between homozygous and heterozygous state could be improved further by finely controlling hybridization parameters to increase the number of the simultaneously detectable mutations. Moreover, the presence of interferent unrelated DNA did not affect the genotyping ability of the optimised SPR system.

Further analyses will be performed to establish if the SPR technique could correctly identify mutations also in non-amplified samples, possibly even with the introduction of SPR enhancers.

Results shown in the experiments of the present Section are the starting point for the realization and improvement of a GC-SPR based sensor that could be easily integrated in a diagnostic prototype thanks to the high sensitivity reached by the azimuthally rotated approach and to the system scalability. In fact, even if all the SPR measurements were performed by using a spectroscopic ellipsometer, requiring an expensive and quite complex readout, the detection system could be easily miniaturised developing a compact prototype as demonstrated in previous works^{18,23}, leading to a low cost, label-free mutation screening, with the possibility of integrating the system in a lab-on-a-chip device with temperature and microfluidic control, and suitable also to be used by non-qualified personnel.

In addition, using a CCD camera for the plasmonic signal collection, a parallel readout of multiple reactions onto the same substrate could be possible, making the sensing system comparable and

complementary to the fluorescence-based detection method. The ability of SPR technique to correctly identify unamplified samples is now under investigation to reduce the test running time.

The results of this work produced the following publications:

Peer Reviewed Journal:

- Meneghello, A. et al. “*Label-Free Efficient and Accurate Detection of Cystic Fibrosis Causing Mutations Using an Azimuthally Rotated GC-SPR Platform.*” **Analytical Chemistry**. 86, 11773–11781 (2014).²⁵

Abstract in International Conference Proceeding:

- International Conference: “NanotechItaly 2013”, Venezia, Italy (2013):
Meneghello, A. et al. “*Surface Plasmon Resonance platform for the efficient and sensitive detection of Cystic Fibrosis causing mutations.*”

4. Antibody platform for *Legionella pneumophila* bacteria detection

In this Section, a work aiming at the exploitation of the SPR phenomenon to develop a fully automated platform for fast optical detection of *Legionella pneumophila* pathogens is described.

The legal limit of *L. pneumophila* concentration in a high-risk hospital environment in Italy is 10^2 CFU/L (colony forming unit per litre), and the gold standard for its identification is a time consuming microbiological culture method. Starting from these considerations a sensitive azimuthally-controlled GC-SPR system was applied to the detection of *L. pneumophila* to test the detection limit of the developed sensing device in term of specificity and sensitivity. The detection was accurately set up and precisely optimised firstly through the usage of flat gold functionalised slides to be then translated to sinusoidal gold gratings for label-free grating-coupled plasmonic (GC-SPR) detection using ellipsometer, in order to ensure reproducible and precise bacteria identification.

Through azimuthally-controlled GC-SPR 10 *Legionella pneumophila* CFU were detected, while in the case of fluorescence analysis results, a negative readout is obtained if incubating less than 10^4 CFU.

This detection platform could be further implemented as a prototype in which water and air samples will be sequentially concentrated, injected into a microfluidic system, and delivered to the SPR sensor for analysis.

4.1 Introduction

4.1.1 Pathogen biosensing: overview and focus on Legionella

In the last decades there has been an increasing interest in sensitive, specific and fast biosensors to address several industrial and societal needs. In particular, reliable and fast detection of pathogenic bacteria in food, water, and air is a key challenge in biosensing due to the strong impact on health. Standard

microbiological methods based on cell culture and plating are highly efficient in the identification of bacterial strains, but they are very time consuming as identification and enumeration of the investigated bacteria require several days. In addition, most of these conventional methods require a biological facility, thus they are not suitable for on-site analysis and cannot be carried out by untrained personnel. Therefore, new biosensing devices, capable of detecting pathogens in a faster and equally accurate manner, are needed and, for this purpose, a multidisciplinary approach is essential to develop such platforms for contributing to solve significant societal challenges.

Among pathogenic bacteria, *Legionella pneumophila* is of particular concern because its ability to colonise water systems, pools, air-conditioning systems (Figure 31) and thus spreading in close environments, it can endanger the health of individuals such as elderly and immunocompromised people (Figure 32).⁹² Thus, a more accurate microbiological control is required, most notably in hospitals (operating rooms, laboratories, critical asepsis rooms, wards, common areas), but also in industrial and travel-associated environments as suggested by ECDC (European Centre for Disease Prevention and Control) data (<http://ecdc.europa.eu/en/Pages/home.aspx>).

Favourable conditions for bacteria growth are also found in plants for the production of sanitary hot water and in evaporative cooling towers (30-50 °C with a relative humidity of 60-99%).

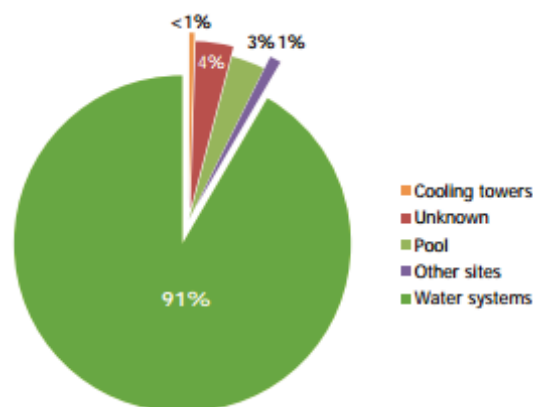


Figure 31. Distribution of sampling sites testing positive for *Legionella*, EU/EEA, 2013.

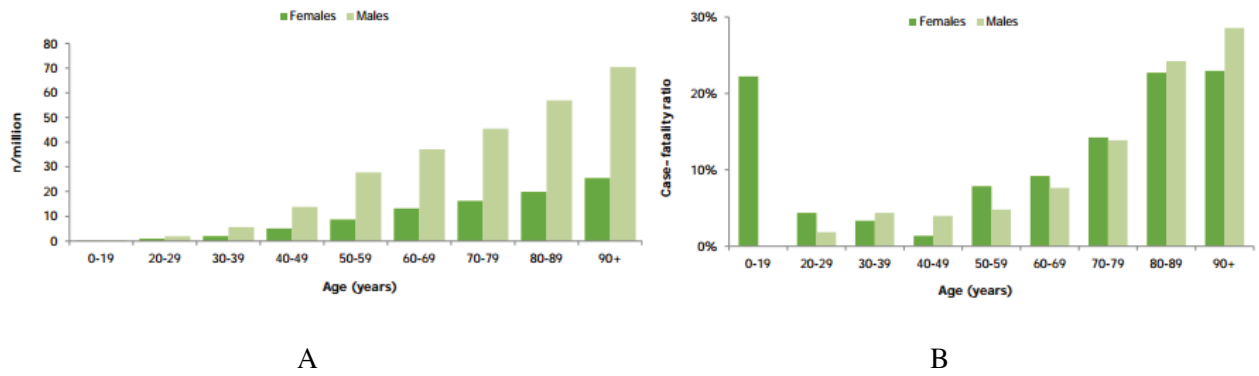


Figure 32. A) Notification rates of Legionnaires' disease per million, by sex and age group, EU/EEA, 2013. B) Reported case-fatality of Legionnaires' disease by sex and age group, EU/EEA, 2013.

According to EU 2013 data (Figure 33) the three largest reporting countries (France, Italy and Spain) accounted for 58% of cases, and the six largest countries (France, Italy, Spain, Germany, the Netherlands and the United Kingdom) together reported 83% of cases. Italy accounted for the majority of the reported cases (1345 cases per million).

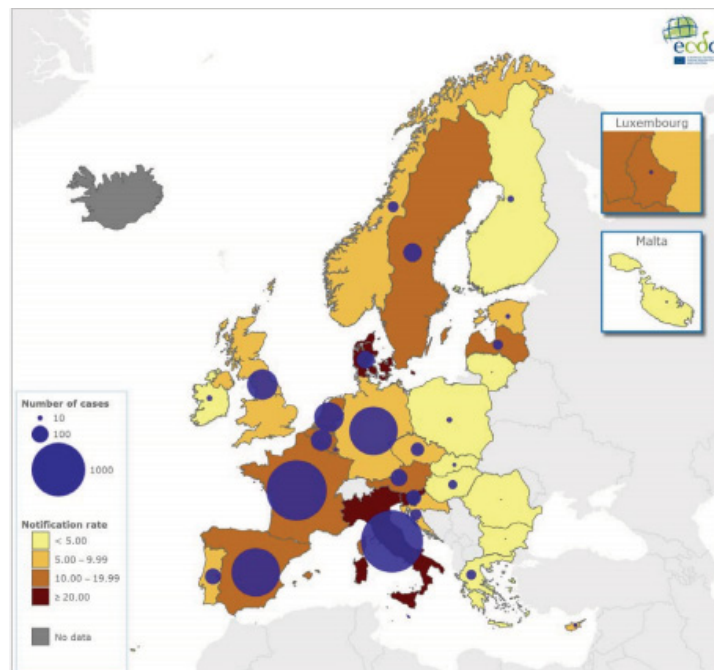


Figure 33. Reported cases and notifications of Legionnaires' disease per million, by reporting country, EU/EEA, 2013.

The perspective of this study consists in performing the whole SPR-based protocol for pathogen detection, from air/water sampling to *L. pneumophila* detection, in a fully automated prototype system and with specificity and sensitivity consistent with EU guidelines (The European Working Group for Legionella Infections (EWGLI) <http://www.ewgli.org>; ESCMID Study Group for Legionella Infections (ESGLI) https://www.escmid.org/research_projects/study_groups/legionella_infections).

Even though several SPR-based sensors are already on the market for the detection of biomolecules, the development of an SPR sensor for detection of bacteria faces significant challenges, as:

- High sensitivity and low detection limit of the biosensor are of key importance: because pathogenicity is very high, even the presence of small amounts of pathogens (<100 bacterium cells) can be a risk for health and therefore must be traced.
- Selectivity towards target pathogen detection is critical to avoid both false-positive and false-negative results: in order to have a reliable readout, the sensitive surface must be selective for *L. pneumophila* bacterium cells, show non-selective adsorption of species and include positive and negative internal control.
- Short analysis times (i.e. requiring hours instead of days of present microbiological techniques) are essential to trigger a quick response and put into action the necessary measures, such as water/air disinfection and physical examinations on the exposed humans.
- Ease of use, possibility of on-site monitoring and automation of the sample manipulation and detection procedure are significant factors for frequent environmental monitoring and use by untrained personnel.
- The whole delivery of samples from the sampling unit to the sensing unit must ensure efficient delivery of the bacteria.
- The size of the device should allow samples to be analysed at the point of need rather than in a separate laboratory, allowing reduction of cost per single measurement and increase in throughput.

Biochemical and molecular sensing of pathogens can be roughly divided into immune sensing and amplified nucleic acid detection. Whereas the latter approach detects specific DNA or RNA sequences of target cells/bacteria, and typically requires an amplification/labelling step of the target nucleic acids prior

to measurement, immunosensing is based on the strong interaction between antigens on the target cells and specific antibodies immobilised on the sensing surfaces, through which antibody-antigen conjugates are formed. These conjugates can be detected using different methods, including fluorescence, luminescence^{93,94}, electrical or electrochemical impedance⁹⁵, cantilever^{96,97}, quartz crystalline microbalance (QCM)⁹⁶, magneto-resistivity⁹⁸ and SPR.⁹³

Among these sensing techniques, SPR sensors provide an extremely sensitive and versatile tool for miniaturised label-free sensing platforms integrated into lab-on-chip systems for potential applications in environmental monitoring, biotechnology, medical diagnostics, drug screening, food safety and security.⁷ Currently, SPR is widely adopted for the detection of biomolecules or to study binding interactions between biomolecules such as nucleic acid-nucleic acid, nucleic acid-proteins, carbohydrate-protein, and lipid-protein.⁷ Detection and investigation of viruses, bacteria and eukaryotic cells is nowadays becoming a rapidly growing field in SPR biosensing (*Figure 34*).

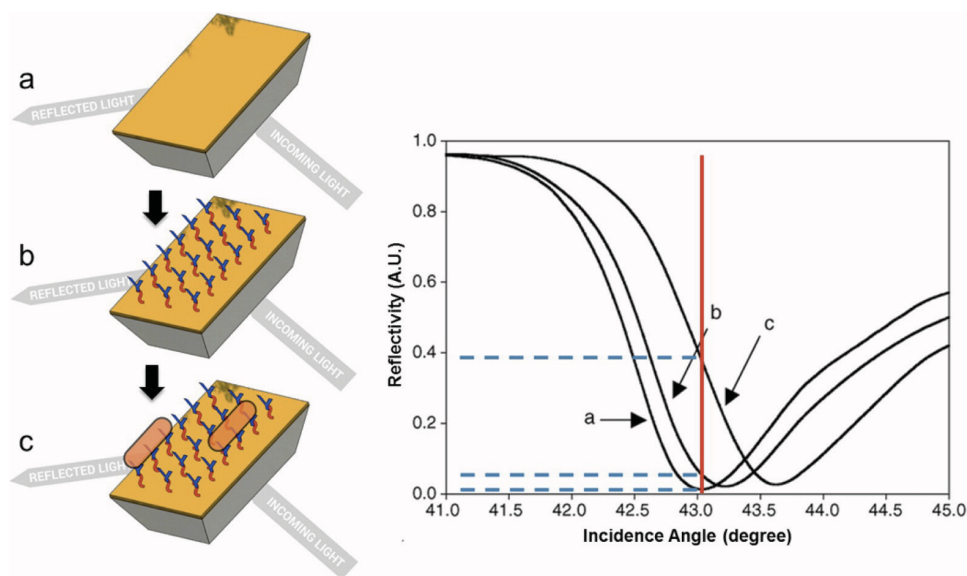


Figure 34. A schematic of a standard surface plasmon resonance (SPR) detection principle and readout. (a) A resonance angle can be identified for incident light shining on a thin metal surface such that the light is converted to surface plasmons and very little light is reflected back from the surface. (b) When recognition elements, such as antibodies, are attached, the refractive index at the surface changes and the resonance angle shifts, causing an increase in the reflectivity for a fixed incident light angle. (c) The

*resonance angle shifts again when cells bind to the antibody. The shift is proportional to the size and surface density of the attaching objects. Figure adapted from*⁹⁹.

Several studies have been published on SPR-based methodologies for detection of various bacterial species such as *Escherichia coli* O157:H7^{100–102}, *Staphylococcus aureus*¹⁰³, methicillin-resistant *Staphylococcus aureus*¹⁰⁴ or *Vibrio cholerae*¹⁰⁵ but the detection was only achieved in laboratory settings. This limitation should be overcome by a new device architecture providing simultaneous positive and negative control to yield reliable measurement readouts in presence and absence of *Legionella* bacterial cells.

Different SPR sensing architectures and transduction systems have been explored to improve sensing performance. A novel grating-coupled SPR (GC-SPR) configuration under azimuth and polarization control will ensure sensitivity, as well as provide the requirements for new compact and integrated systems. A typical feature of SPR is its label-free approach: labelling of the analyte with a chemical or optical tag is not required, which is a clear advantage considering that the labelling procedure may modify and/or disrupt the target-probe interaction, and the lack of a labelling step simplifies automation.

Due to the enhanced sensitivity of this configuration compared with conventional SPR, the possibility of detecting low amounts of biological species with high accuracy has already been demonstrated.^{97,98} This feature will be exploited for the detection of *L. pneumophila* within the concentration limits fixed by EU guidelines.

Specificity will be provided by the immuno-functionalization of the plasmonic surface using anti-*L. pneumophila* antibodies. In order to take complete advantage from SPR sensitivity, the surface of the optically-active surface needs to be suitably coated with a biorecognition element able to bind the specific analyte, and to be passivated to prevent non-specific adsorption onto the plasmonic sensitive surface. The work was focused on a case study involving the *L. pneumophila* pathogen, but one future application could include the extension of the proposed GC-SPR-based approach to other pathogens' monitoring, through possible modulation of SPR grating parameters and instrumental settings in a multiplexing format.

4.1.2 *Legionella pneumophila* and legionellosis

Legionella pneumophila is a thin, aerobic, pleomorphic, flagellated, non-spore forming, Gram-negative bacterium of the genus *Legionella*. Bacteria dimensions range from size from 0.3 to 0.9 μm in width and from 1.5 to 5 μm in length (Figure 35), while in culture filamentous forms up to 20 μm can be frequently found. The cell wall of these organisms is characterised by the presence of branched-chain fatty acids that are not usually present in Gram-negative bacteria.¹⁰⁶

L. pneumophila, an intracellular parasite of free-living protozoa, is the causative agent of Legionellosis (Legionnaires' disease) that is a serious form of pneumonia, with a case-fatality ratio on the order of 10-15%. Recognised risk factors for Legionnaires' disease - which could increase the fatality rate up to 80% - include belonging to an older age group (>50 years), male, having a chronic underlying disease with or without an associated immunodeficiency and being a heavy cigarette smoker.¹⁰⁷

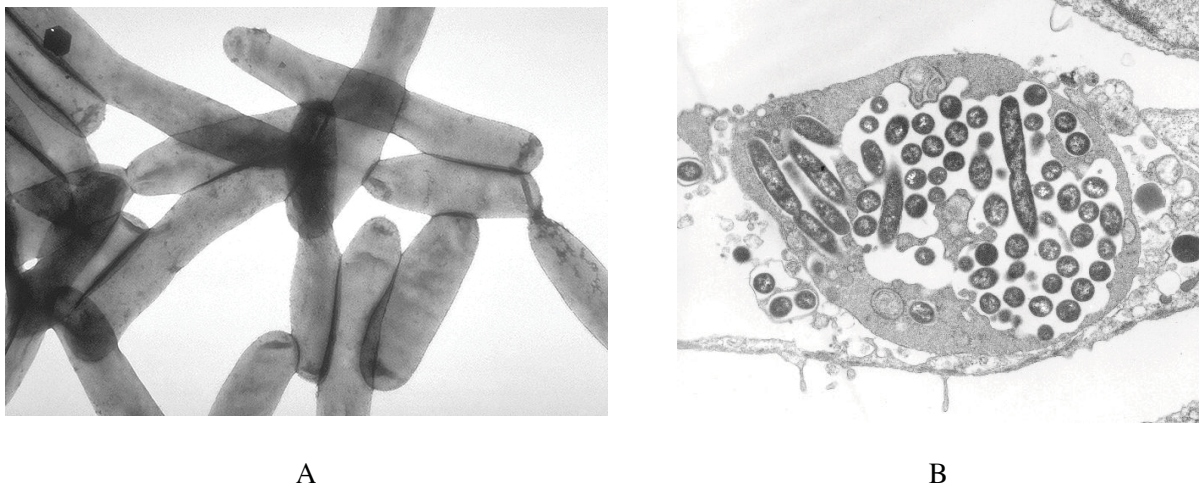


Figure 35. A) TEM image of *Legionella pneumophila* bacilli (picture from CDC/ Dr. Francis Chandler, ID#: 1187); B) TEM image of *Legionella pneumophila* multiplying inside a cultured human lung fibroblast. Multiple intracellular bacilli, including dividing bacilli, are visible in longitudinal and cross section (picture from CDC/ Dr. Edwin P. Ewing, Jr., ID#: 934).

Although 42 different species of *Legionella* have been described, not all associated with human disease¹⁰⁸, *L. pneumophila* is the species most often detected in diagnosed cases. The European Working group for

Legionella Infections (EWGLI) and the European Legionnaires' Disease Surveillance Network (ELDSNet) have reported 4897 cases of Legionellosis in 2011 in EU Member States, Iceland and Norway.^{109,110}

L. pneumophila is found in aquatic habitats, especially in potable water, air conditioning, hot and cold water systems, cooling towers, evaporative condensers, spa/natural pools, healthcare facilities and, more in general, in high accommodation capacity structures.¹¹¹ Legionnaires' disease is normally acquired through the respiratory system by breathing in air that contains *L. pneumophila* in an aerosol, especially made of droplets with a diameter of less than 5 µm, that can reach the lower airways more easily.

The standard technique for detection and monitoring of this pathogen is microbiological bacterial culture, which is based on the *in vitro* selective growth of bacteria (ISO 11731: 1998 and ISO 11731-2: 2008). Whereas this approach is very accurate and allows for extremely low detection limits (a single CFU can be detected), it has essentially three disadvantages: (1) it requires dedicated microbiology laboratories, (2) it must be performed by highly specialised personnel, and (3) delivery of test results may take up to several days (more than 7 days are usually required).

Whereas the sensitivity and detection limit of bacterial culture tests can be hardly achieved by other instrumental techniques, such detection approach is not suitable for high-frequency *L. pneumophila* environmental monitoring (i.e. delivery of results on the order of hours and tests repeated on a daily basis). Since Legionella is a widespread pathogen and has a relatively high case-fatality ratio, it should be clear that outbreaks should be caught at their early onset in order to trigger a quick response, putting into action the necessary countermeasures as soon as possible, such as water/air disinfection and physical examinations on the exposed humans. This is even more evident considering that crowded environments and large infrastructures might exacerbate the consequences of an outbreak, in particular when hospitalised debilitated patients are involved or other risk groups such as children and the elderly. Standard culture methods, therefore, appear unsuited for the environmental monitoring against Legionella threats.

4.1.3 Aim of the study

Based on the considerations illustrated above concerning Legionella, the existence of a gap between the actual health risk and the possibility to manage this risk, e.g. enforcing suitable disinfection and treatment countermeasures, is a major concern: the need to close this technological gap responds to the societal challenge of having safer and more healthy environments.

The study was focused on the development of a sensitive azimuthally-controlled grating coupled-SPR system for the identification of *L. pneumophila*. Experimental protocols were first set up with fluorescent microarray technique firstly through the usage of flat gold functionalised slides. Results were translated to sinusoidal gold gratings for label-free GC-SPR detection using ellipsometer, in order to ensure a reproducible and precise bacteria identification and take advantage of the high sensitivity of the GC-SPR configuration to increase the performances of our sensing device in terms of detection limit (detectable bacterium CFUs) and output time.

Experimental validation of the functionalised sensing surface demonstrated the high specificity of the platform in detecting *L. pneumophila* with low cross-reaction signals due to the presence of other Legionella species and no signal when bacteria other than Legionella were present in the sample. Moreover the sensing GC-SPR unit was able to recognize the presence of as few as 10 CFUs of *L. pneumophila* in the incubated sample. These results indicate the possibility to scale the sensing unit in an automated and controlled device for *Legionella pneumophila* detection.

4.2 Materials and Methods

4.2.1 Marketing antibodies evaluation and deposition

Anti *Legionella pneumophila* antibody were selected among commercially available molecules, from most competitive suppliers in terms of quality/cost ratio.

Required characteristics to satisfy experimental needs were:

- polyclonal: for the recognition of multiple epitopes to ensure efficient capturing and detection
- unconjugated: acting as capture antibody for the label-free detection (cost reduction)
- obtained immunising with whole cells/live cells: to allow the recognition of native antigens and intact whole cells that will be present in the environment

Two anti *Legionella pneumophila* antibodies with the desired features were chosen (Table 9):

- rabbit polyclonal antibody
- unconjugated
- obtained immunising with a whole cell preparation of *L. pneumophila* (ATCC #33152)
- not absorbed
- one of the 2 indicating as reactive towards *L. pneumophila* serogroups 1-12 in IFA. Recognizes all antigens of intact microorganism

Gold slides were cleaned, PEGylated, functionalised and blocked as described in Section 2, as well as e-surf microarray slides, used as parallel fluorescence microarray control.

Concerning gold slides, two types of substrates were used:

- *gold flat slides*: they present a planar surface, the antibody was deposited through the microarray spotter and they were analysed through microarray laser scanner.
- *gold sinusoidal slides*: the antibody was deposited through the usage of the ProPlate multi-well mask in order to have multiple wells to be incubated and analysed through label-free SPR.

Table 9. Specifications of the two anti *L. pneumophila* selected antibodies.

	<i>Virostat Legionella pneumophila</i> IgG polyclonal antibody (#6051)	<i>Abnova Legionella pneumophila</i> polyclonal antibody (#PAB13999)
Host animal	Rabbit	Rabbit
Immunogen	A whole cell preparation of <i>Legionella pneumophila</i> ; ATCC #33152	Native from <i>Legionella pneumophila</i>
Specificity	All antigens of intact microorganism	Reacts with <i>L. pneumophila</i> serogroups 1-12 in IFA. Recognizes all antigens of intact microorganism. Antiserum is not absorbed and may cross-react with related microorganisms
Cross reactivity	Antiserum is not absorbed and may cross-react with related microorganisms	Antiserum is not absorbed and may cross-react with related microorganisms
Storage buffer	phosphate saline buffer (0.01M, pH 7.2) containing 0.1% sodium azide	10 mM PBS, pH 7.2 (0.09% sodium azide)
Concentration	1 ml, 4-5 mg/ml	100 µl, 4-5 mg/ml

The following antibodies were used:

- Virostat (Portland, ME, USA) IgG α *Legionella pneumophila* polyclonal antibody (#6051)
- Abnova (Taipei, Taiwan) IgG α -*Legionella pneumophila* rabbit polyclonal antibody (#PAB13999)
- Invitrogen IgG1 anti-biotin mouse monoclonal antibody (clone Z021), 1 mg/ml, as negative control
- Invitrogen Goat anti-mouse IgG Secondary Antibody, Alexa Fluor® 532 conjugate (#A-11002) or Alexa Fluor® 647 conjugate (#A-21235), as fluorescence controls.

Up to 48 identical sub-arrays were spotted per slides.

4.2.2 Protocols for bacteria culture, processing and identification

4.2.2.1 Bacteria strains and culture

The following bacteria strains were used:

- *Legionella pneumophila* subsp. *pneumophila* (ATCC 33152) serogroup 1 (BSL2)
- *Fluoribacter dumoffii* (ATCC 33343) (BSL2)

- *E. coli* DH10-β (New England Biolabs, Ipswich, MA USA): as negative control (BSL1)

Legionella - defined as fastidious bacterium i.e. a bacterium that has a complex nutritional requirement - do not grow on standard culture media¹¹², but needs L-cysteine and iron to grow. Culture media and supplement for Legionella, purchased from Biolife Italia (Milano, Italy), whose formula is reported in *Table 10*, were the following:

- Legionella BCYE (Buffered Charcoal Yeast Extract) Agar Base
- Legionella BCYE α-Growth Supplement

Table 10. Legionella BCYE Agar Base formula (left) and Legionella BCYE α growth supplement (right).

<i>Legionella BCYE Agar Base</i>	
Typical Formula	mg/litre
Activated charcoal	2.0
Yeast extract	10.0
Agar	13.0

<i>Legionella BCYE α growth supplement (vial contents for 500 ml of medium)</i>	
Typical Formula	mg/litre
ACES Buffer/Potassium hydroxide	6.4 g
α -ketoglutarate	0,5 g
Ferric pyrophosphate	125.0 mg
L-Cysteine HCl	200.0 mg

Legionella selective agar was prepared following the supplier protocol:

Suspend 12.5 g in 450ml of cold distilled water. Heat to boiling with agitation and sterilise by autoclaving at 121°C for 15 minutes. Cool to 50°C and add the contents of one vial Legionella BCYE α Growth Supplement reconstituted with 50 ml of sterile, warm distilled water (50°C). Mix well and distribute into sterile Petri dishes. Final pH 6.9 ± 0.1.

The colony morphology of *Legionella pneumophila* on the plating media after 48-72 hours of incubation is as follows: diameter 1-2 mm (increase in size on further incubation), white, glistening, circular, smooth, raised with entire edge.

E. coli was cultured in TSA (*Table 11*), prepared following the supplier protocol (Biolife Italia):

Suspend 40 g in 1000 ml of cold distilled water. Heat to boiling with agitation and sterilise by autoclaving at 121 °C for 15 minutes. Cool to 50 °C, mix well and distribute into sterile Petri dishes. Final pH 7.3 ± 0.2.

Table 11. TSA formula.

TSA	
Typical Formula	mg/litre
Tryptone (Pancreatic Digest of Casein)	15.0
Soytone (Papaic Digest of Soybean Meal)	5.0
Sodium Chloride	5.0
Agar	15.0

4.2.2.2 Colony forming unit (CFU) number evaluation

For correctly testing the system sensitivity, the measurement of the content of colony forming units per ml of a solution was made dissolving specific colonies in physiological solution (NaCl 0.9 % w/v) and correlating the solution optical density (OD_{600}) to the number of colonies on agar plates seeded with dilutions starting from known OD, after 72 hours of incubation. Counting the number of colonies corresponding to each dilution, the content in CFU for a specific OD was therefore defined, and data are summarised in *Table 12*.

Table 12. OD_{600} -CFU correlation for the investigated bacteria.

Specie	CFU/ml at $OD_{600} = 0.15$
<i>Legionella pneumophila</i>	$1.5 \cdot 10^8$
<i>Legionella dumoffii</i>	$1.2 \cdot 10^8$
<i>Escherichia coli</i>	$0.2 \cdot 10^9$

4.2.2.3 Labelling and binding protocol for bacteria cells

Protocols and procedures were tested and optimised to properly manipulate and label bacteria cells. Selected colonies were picked and dissolved in physiological solution. To remove any agar residual, colonies were washed 2 times in 1X PBS + 0.5% FBS (Fetal Bovine Serum), pH 7 and kept at 4 °C for few days or frozen in a solution of 1XPBS, 10% FBS and 15% glycerol.

Fluorescent labelling of bacteria was performed as follow: colonies were recovered, washed and resuspended in 1X TBS/FBS buffer (50 mM Tris-HCl, 150 mM NaCl, 0.05% FBS, pH 7.5). OD₆₀₀ was spectrophotometrically determined and solution was diluted to the appropriate OD₆₀₀ corresponding to the desired CFU amount. Bacteria labelling was performed with NHS ester (succinimidyl ester) of Alexa Fluor® 555 or 647 (Invitrogen): these esters are popular tool for conjugating Alexa dye to a protein or antibody through their primary amines, obtaining a conjugate with bright fluorescence and great photostability. Known amount of bacteria cells (typically 10⁸ CFU) were labelled with 30 µg of NHS ester Alexa (resuspended in 5 µl of DMSO) for 1h at room temperature and under gentle shaking.

Cells were then washed 3 times in 1X TBS/FBS 1X to remove the excess of unbound fluorophore and then resuspended in 1X TBS/1% BSA, buffer selected for bacteria incubation on the slides, that was performed for 1 h at RT in gentle shaking. After incubation, solutions were removed and wells were washed once with Protein washing buffer (50 mM Tris, 250 mM NaCl, 0.05% Tween 20, pH 7.0) and twice in 1X PBS. Slides were finally spin dried and analysed for fluorescence response through laser scanner. Unlabelled cells were manipulated and diluted in the same way except for the labelling step, and slides were analysed for SPR response through ellipsometer.

4.2.2.4 Antibody labelling for “sandwich” fluorescent detection

Concerning fluorescent detection, bacteria cells were recognised directly - through fluorescent cell labelling - or indirectly - through fluorescent antibody labelling. Antibody labelling was performed as follow: 2 µg of antibody per well were labelled with NHS ester of Alexa Fluor® in a 1:4 molar ratio. Labelling was performed for 1 hour at RT and the mix was diluted in 1X TBS/1% BSA to stop the reaction, that was incubated on the slides as described previously.

4.2.2.5 Bacteria cell fragmentation

Bacteria cell fragmentation was achieved resuspending cells in physiological saline solution and performing three freezing cycles (-80 °C for 30 minutes and 37 °C for 5 minutes with subsequent vortexing for 2 minutes). Viable CFU evaluation after such treatment was performed by plating treated samples: the

fragmentation treatment efficiency was higher than 99.99%. Fragmented cells were used to validate the antibody ability to recognize and bind fragmented *versus* whole cells.

4.2.3 Microfluidic cell for SPR measurements

For *Legionella* incubation on functionalised gratings and subsequent reflectivity measurements, a microfluidic cell (*Figure 36*) (JA Woollam and Co., Inc. - CA, USA) was used to perform the acquisition of SPR spectra.

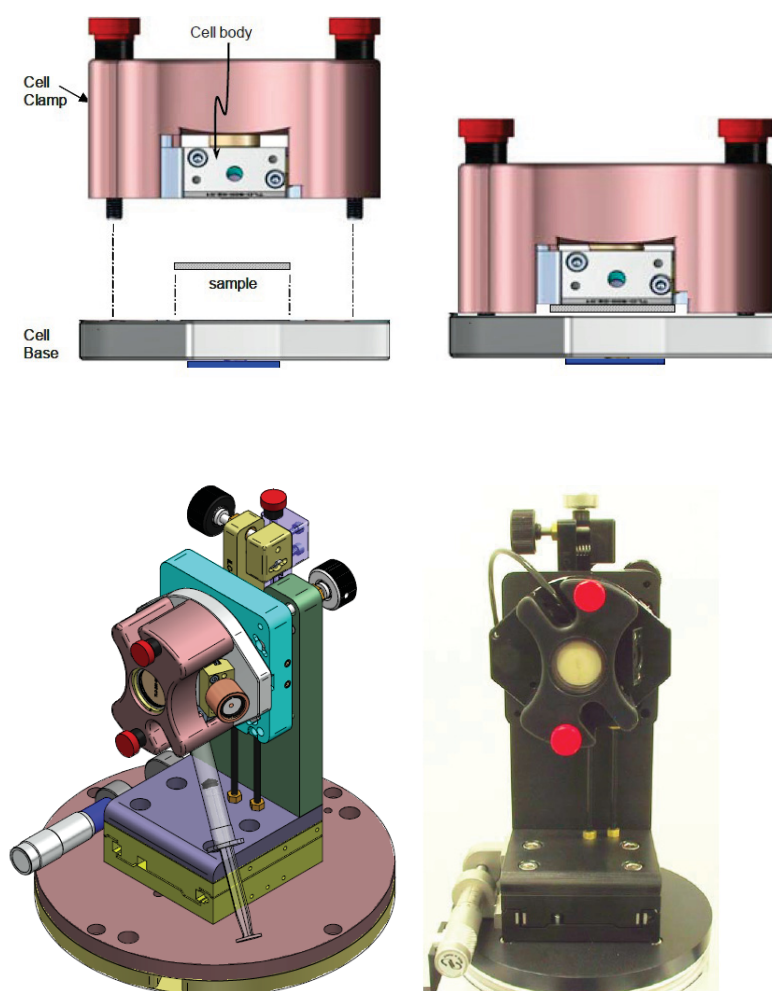


Figure 36. Microfluidic cell used for SPR experiment (*LiquidCell Manual TLC-300, J.A. Woollam and Co., Inc.*).

Due to the closed structure of the cell and the presence of a single inlet and outlet port, the incident light beam enters the microfluidic cell according to a fixed angle, determining the possibility of analysing one sample at a time. Therefore, in every experimental session one single grating was employed, anchored to the base of the cell in a stable way for the whole experimental procedure and analysis.

SPR measurements were performed as described in Section 2, in particular substrates were characterised after each experimental step with the parameters of *Table 13*.

Table 13. Characterisation parameters used for SPR measurements.

Incident wavelength [nm]	600-800
Light incidence angle [°]	70
Azimuth [°]	45°
Polarization [°]	140°

Reflectivity measurements were carried out in the following steps:

- after piranha cleaning, substrate anchoring to the cell base and definition of a grating experimental area;
- after PEG o/n functionalisation, washing and drying, antibody deposition o/n inside the experimental area and blocking;
- after *L. pneumophila* incubation on the functionalized area, washing, frozen ethanol fixation and drying.

The described procedure allowed to control all the experimental steps with high precision and accuracy in order to be able to reproduce the optimised experimental condition. A well-defined functionalisation area was delimited by the o-ring (*Figure 37*).

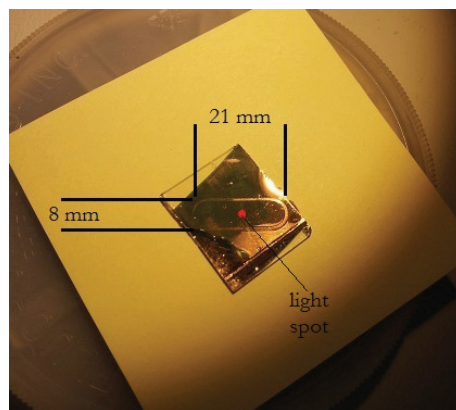


Figure 37. *Picture of an SPR where the o-ring delimited region (8x21mm) and the incidence light spot are visible. The functionalisation area was defined by drawing an ellipse-like shape with an alcohol resistant pencil.*

4.3 Results and Discussion

4.3.1 POSEIDON Project (ICT-26 Horizon 2020)

During my PhD work I've been involved in Surface Plasmon Resonance project for the detection of *Legionella pneumophila*: obtained results were used as preliminary data for the preparation and submission of a Horizon 2020 project, which has been approved and started on January 2015.

The results illustrated in this Section (4.3 Results and Discussion) have been therefore obtained as preliminary data and internal results of POSEIDON project (*Plasmonic-based autOated lab-on-chip SEnsor for the rapid In-situ Detection of LegiONella*), focused on the specific detection of *Legionella pneumophila* (ICT-26-2014-I RIA, G.A. 644669).

The project aims at the exploitation of the SPR phenomenon to develop a fully automated platform for fast optical detection of *L. pneumophila*. This detection platform will be implemented as a prototype in which water and air samples are sequentially concentrated, injected into a microfluidic system, and delivered to the SPR sensor for analysis. The designed system will allow for its future integration in water distribution and HVAC (heating, ventilation and air conditioning) for prevention of *L. pneumophila* outbreaks. A schematic overview of the project approach is summarised in *Figure 38*.

The partnership is composed by: *Italy* (Veneto Nanotech s.c.p.a., Clivet s.p.a., ARC - Centro Ricerche Applicate s.r.l.), *Spain* (CatLab), *Sweden* (Uppsala University) and *Netherlands* (Metrohm Applikon). From December 2015 Veneto Nanotech is no more involved in the project because of company financial issues, and working packages involving Veneto Nanotech expertise were moved to other partners, and a new Italian partner, Protolab s.r.l., has been involved in the project.

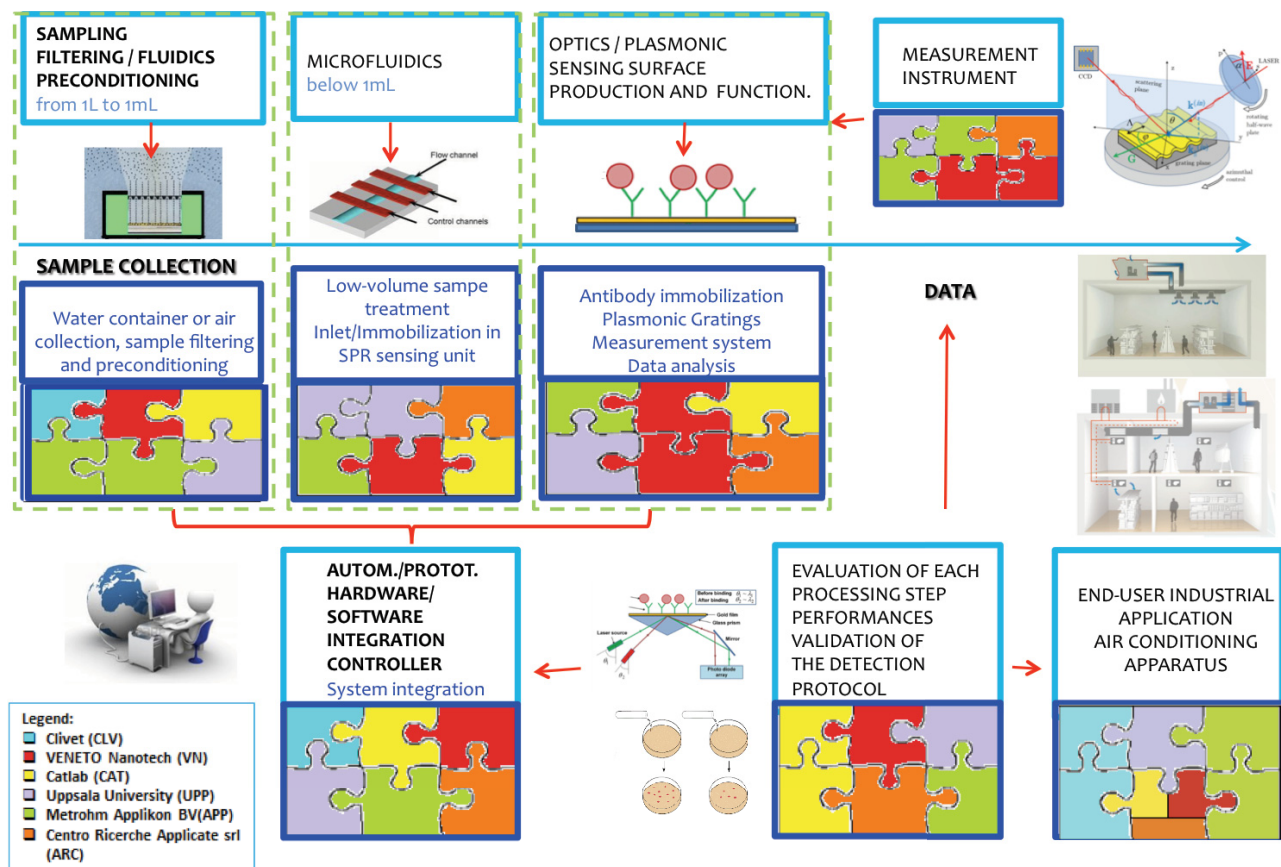


Figure 38. Schematic overview of POSEIDON project depicted visualising the different system components and the partners' involvement in their development (see legend) and the connection in the workflow.

4.3.2 Antibody binding evaluation

A first set of experiments was performed to verify the antibodies ability to recognize *Legionella pneumophila* and *dumoffii* cells. Recorded fluorescence values were compared to define the discrimination ability of the two selected antibodies. In these first experiments, standard e-surf slides were used, since their characteristics of reliability and reproducibility were already know in the laboratory.

Colonies of *Legionella pneumophila* or *Legionella dumoffii* were diluted in physiologic solution, quantified through OD₆₀₀, labelled and incubated as described in Materials and Methods section.

The two selected anti-*Legionella* antibodies (purchased by Viostat and Abnova) were able to recognize with completely overlapping efficiency *Legionella pneumophila* cells. A partial reactivity was observed also when incubating *Legionella dumoffii* cells, and the two antibodies shows also in this case similar

binding capability. Data are reported graphically in *Figure 39* and are representative of at least three independent replicas.

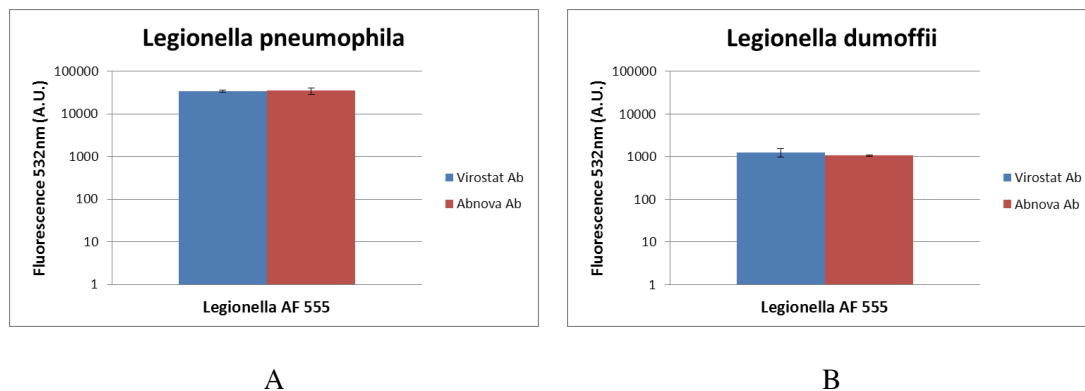


Figure 39. Binding efficiency recorded on microarray e-surf slides functionalised with anti-*Legionella* antibodies (Virostat - in blue versus Abnova - in red) when incubating the same amount of fluorescently labelled (Alexa Fluor 555) *L. pneumophila* (A) or *L. dumoffii* (B) cells.

As can be observed by the recorded fluorescence intensity, selected polyclonal antibodies were able to recognize in a highly specific way *L. pneumophila* cells (A.U. $35000 \pm 10\%$) if compared to *L. dumoffii* ones ($1100 \pm 10\%$), with a signal at least 1 order of magnitude higher when recognising *L. pneumophila*.

Also if specific information about the cross-reactivity ability of the two antibodies is not fully characterised by the supplier, both antibodies are produced from rabbit immunised with *L. pneumophila* ATCC 33152, can react with all the 12 serogroups of *L. pneumophila*, and can partially cross-react with other *Legionella* species.

Fluorescence signals recorded incubating labelled *Legionella* on negative control antibody are not significant (A.U. <100), as expected, revealing absence of cells aspecific interaction (data not shown).

4.3.3 Bacteria capturing demonstration through confocal and scanning electron microscopy

After demonstrating the antibody binding ability concerning Legionella detection, a further demonstration of bacteria capturing was achieved directly, through both confocal and scanning electron microscopy (SEM).

A microarray slides properly functionalised with α -Legionella antibody and incubated with Alexa 555-labelled *L. pneumophila* cells was used for the imaging experiment, reported in *Figure 40*.

Both fluorescence confocal microscopy and scanning electron microscopy images were collected. Used scanning electron microscope is designed for high as well as low vacuum operating, giving the possibility of examination of non-conducting, water containing specimens in their natural state at low vacuum conditions in microscope chamber.

As can be nicely seen, a peculiar green fluorescent pattern is revealed through confocal microscopy, due to bacteria capturing only on the region delimited by the microarray spots, and the same peculiar pattern is revealed after metallisation and scanning electron microscopy. No signal is detectable on the surrounding regions, demonstrating an optimal surface passivation and absence of aspecific interactions with the background surface.

L. pneumophila cultured cells appear, as reported in literature¹¹³, mainly as filamentous clusters and in minor part as rod-shaped bacteria.

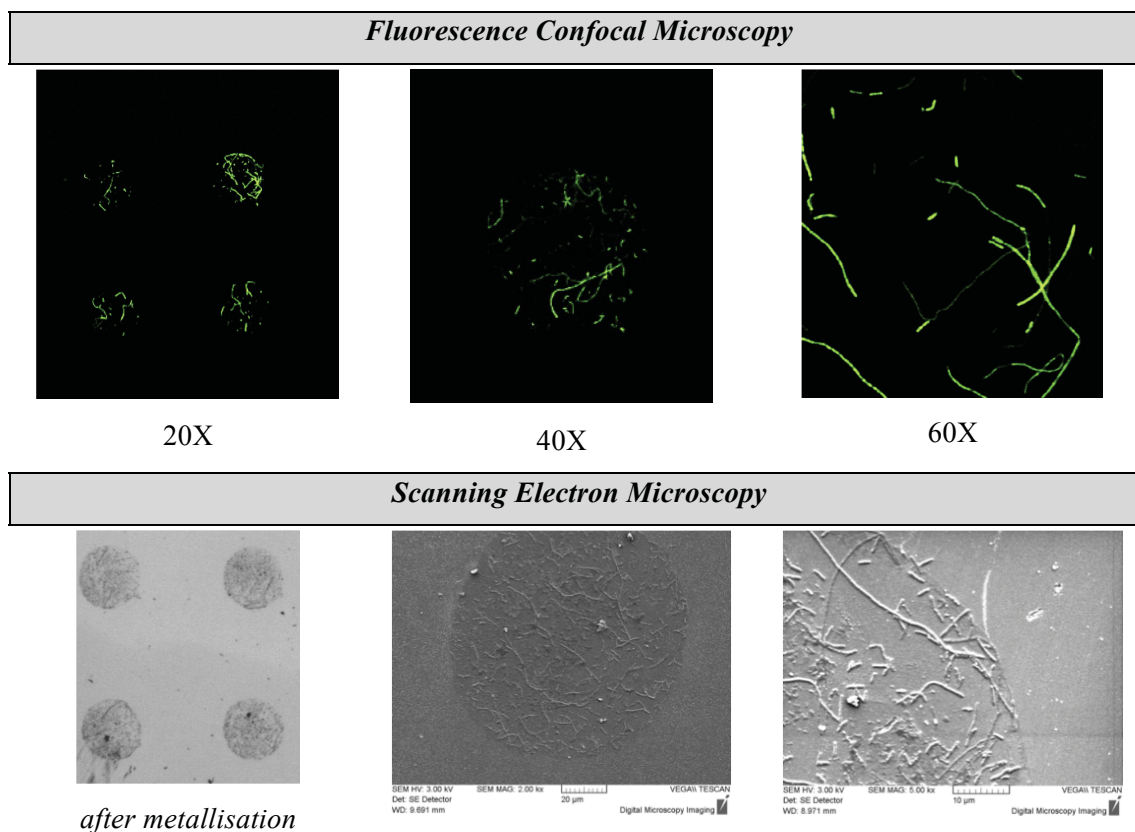


Figure 40. Fluorescence confocal microscopy (upper panels) and Scanning electron microscopy (lower panels) of *Legionella pneumophila* cells incubated on α -*Legionella* functionalised microarray slides.

4.3.4 Direct vs indirect bacteria detection

Antibody selection performances were evaluated directly, using fluorescently labelled bacteria, or indirectly, performing a “sandwich” indirect detection. *Legionella* cells were incubated as Alexa Fluor 555 labelled or unlabelled. For the “sandwich” detection the two α -*Legionella* polyclonal antibodies were labelled with Alexa Fluor 647 and used as detection probe.

This experiment was performed to analyse if the “sandwich” detection could result in better performances when compared to the direct one, and if the bacteria labelling step could impair or worsen antibody recognition in a significant way. The experiment was performed to compare also in this setting the performances of the two selected α -*Legionella* polyclonal antibodies, used in alternative combination as capturing or as detecting molecules.

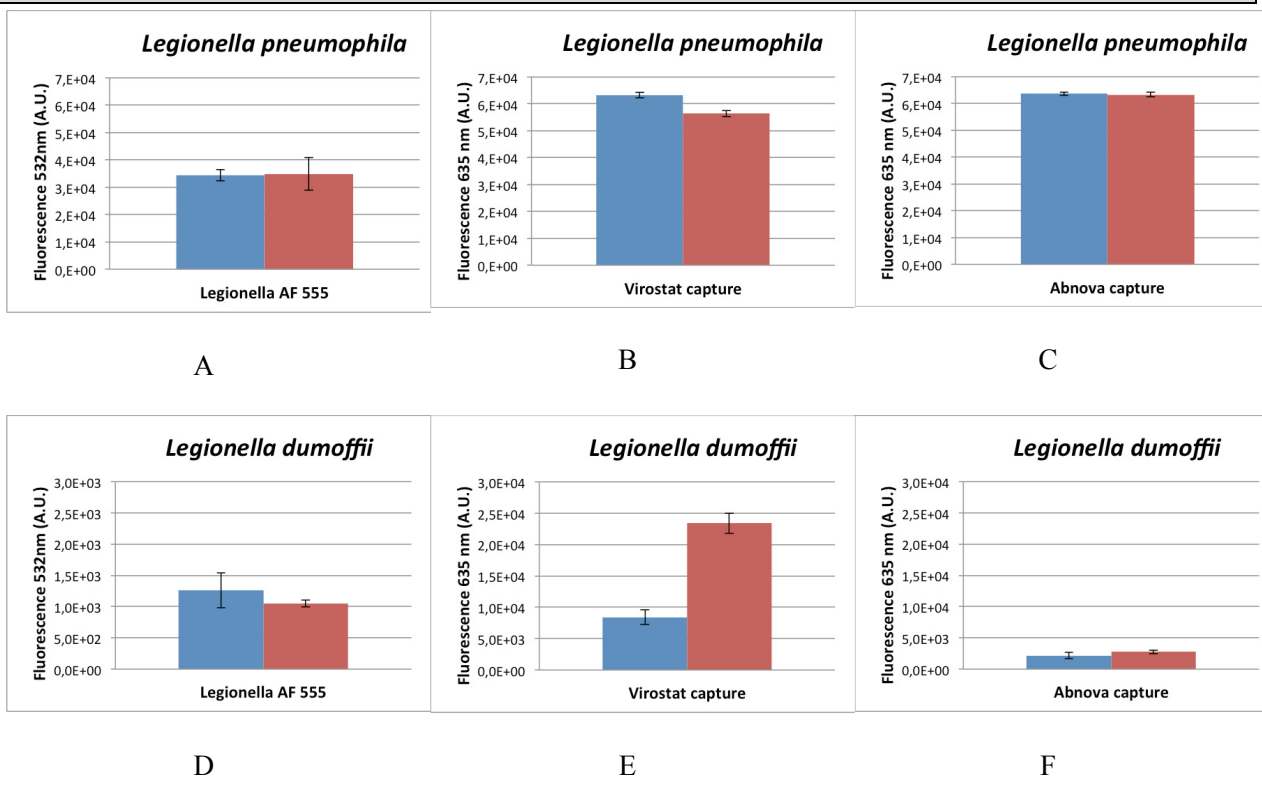
Obtained results are reported graphically *Figure 41 A, B and C* concerning *L. pneumophila* cells and in *Figure 41 D, E and F* concerning *L. dumoffii* cells. Detection of labelled cells through a “sandwich” strategy is correctly obtained, and it is not significantly different if using Virostat or Abnova antibody, neither as capturing or detecting molecule. Only if detecting *L. dumoffii* using Abnova as detecting antibody and Virostat as capturing one (*Figure 41 E*) an improvement of the fluorescent readout is achieved, nevertheless comparable performances between the two antibodies are observed when performing a direct detection of *L. dumoffii* labelled cells (*Figure 41 D*).

For the subsequent label-free SPR application a direct recognition performed can therefore be foreseen with one of the two antibodies as capturing layer, without specific preferences.

Experiments were also performed with unlabelled cells recognised by labelled antibodies and demonstrate that fluorescent signals obtained with labelled cells plus labelled antibodies are not significantly different from the one obtained with unlabelled cells plus labelled antibodies (*Figure 41 G and H*): this result indicates that bacteria labelling – with the optimised fluorescent molecules ratio – did not impair antibody binding and did not lead to aspecific interactions.

Eventual aspecific binding was also verified incubating labelled bacteria on unrelated antibody (α -biotin) with or without subsequent incubation with labelled α -Legionella antibody: in none of the cases a significant fluorescent signal was detected (*Figure 42*), demonstrating the absence of aspecific interaction events.

1. Fluorescent microarray readout incubating Alexa Fluor 555 labeled Legionella cells detected directly or through a “sandwich” Alexa Fluor 647 labeled antibody.



2. Fluorescent microarray readout incubating unlabeled Legionella cells detected through a “sandwich” Alexa Fluor 647 labeled antibody.

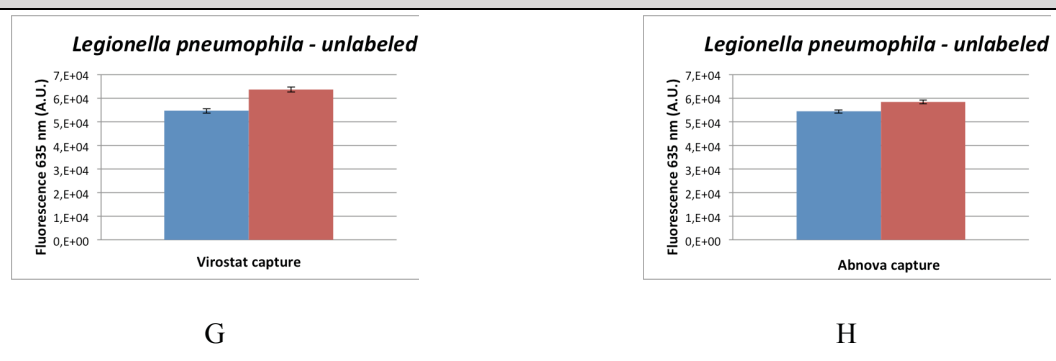


Figure 41. Graphical representation of direct vs indirect Legionella cells detection experiments. Blue histograms: Virostat antibody; red histograms: Abnova antibody. 1. A, B, C: *L. pneumophila* cells detection; 1. D, E, F: *L. dumoffii* cells detection. A and D: green fluorescent signal deriving from Alexa Fluor 555 bacteria labelling (direct detection) captured by Virostat antibody (blue) or Abnova (red). Red fluorescent signal deriving from Alexa Fluor 647 Antibody labelling (indirect detection) detecting labelled bacteria captured with Virostat antibody (B and E) or with Abnova antibody (C and F) or detecting unlabelled bacteria captured with Virostat antibody (G) or with Abnova antibody (H).

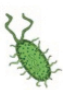
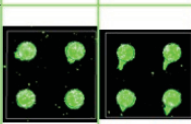
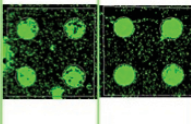
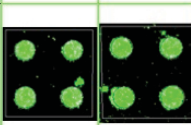
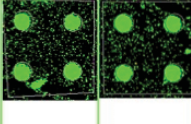

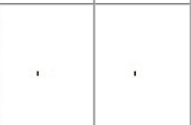

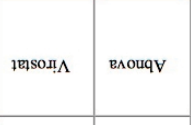

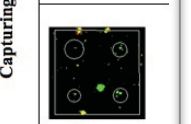
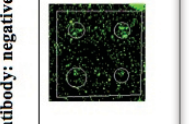
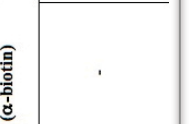

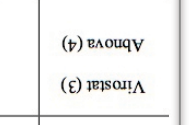
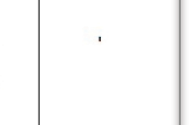
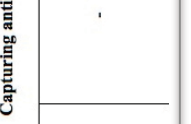


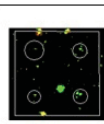
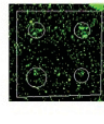


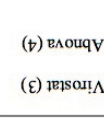

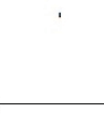
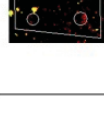
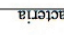
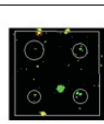
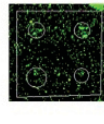


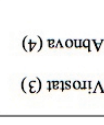

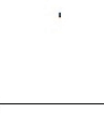
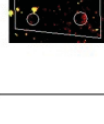
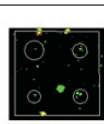
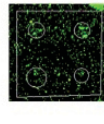


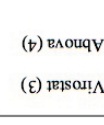

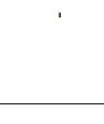
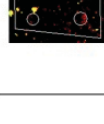
← INCUBATED TARGET		Incubation of Legionella cells on α -Legionella capture antibody				← DETECTION Ab 647			
		Capturing antibody: Virostat		Capturing antibody: Abnova		Capturing antibody: Virostat		Capturing antibody: Abnova	
		<i>L. pneumophila</i>	<i>L. dumoffii</i>	<i>L. pneumophila</i>	<i>L. dumoffii</i>	<i>L. pneumophila</i>	<i>L. pneumophila</i>	<i>L. pneumophila</i>	<i>L. dumoffii</i>
	Labeled bacteria								
	Unlabeled bacteria								
	Labeled bacteria								
	bacteria								
		Capturing antibody: negative control (α -biotin)				Capturing antibody: negative control (α -biotin)			
									

Figure 42. Fluorescent microarray results obtained for direct vs indirect Legionella cells detection. Bacteria cells were used as Alexa Fluor 555 labelled or unlabelled. Detecting antibodies were used as Alexa Fluor 647 labelled.

4.3.5 Sensitivity evaluation of the fluorescent set-up

Once confirmed and evaluated the ability to specifically recognize *Legionella* cells of the two selected α -*Legionella* antibodies, experiments were performed to establish the fluorescent system sensitivity in terms of minimum detectable amount of bacteria CFU.

Experiments were performed both on e-surf microarray glass slides and on flat gold slides, in order to evaluate and compare fluorescent signals, availability and performances of antibody anchored on gold through a SH-PEG-COOH linker: results obtained in terms of spots shape and quality appear to be improved when using gold slides, probably due to the compact antifouling PEG layer created on the slides, if compared to the polymeric layer available on commercial e-surf slides surfaces (data not shown). For this reason, results obtained on gold slides only are reported in this paragraph.

L. pneumophila and *L. dumoffii* bacteria colonies were collected, quantified, labelled with Alexa Fluor 555 and appropriately diluted through serial dilution from known OD₆₀₀, starting from 2×10^8 CFU/ml down to 2×10^4 CFU/ml. Cells were finally incubated on the platform and results are reported both graphically (Figure 43) and as microarray fluorescent images (Figure 44): data are representative of at least three independent experiments.

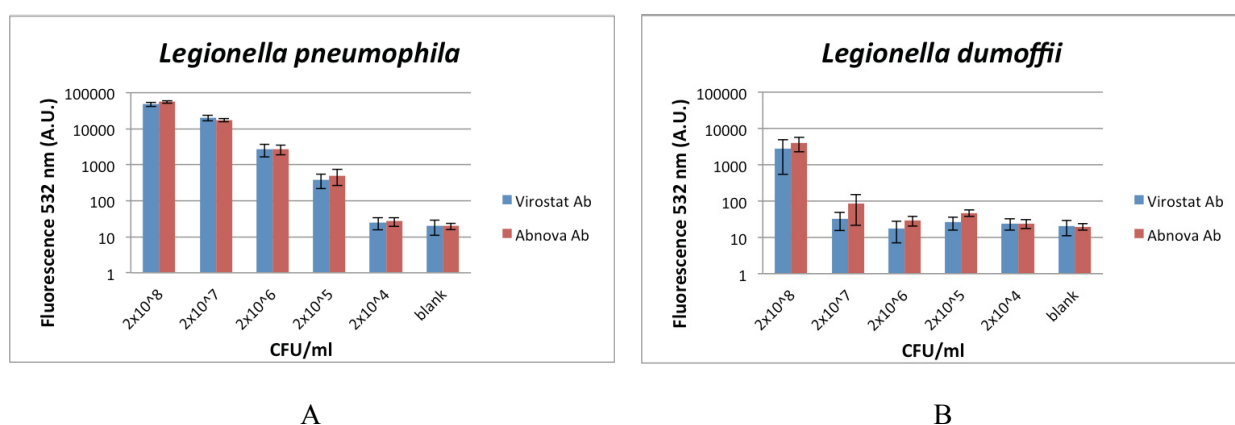


Figure 43. Graphical representation of sensitivity performances of α -*Legionella* antibodies incubated with serial dilutions of Alexa Fluor 555 labelled *L. pneumophila* (A) and *L. dumoffii* cells (B).

Concerning fluorescent readout sensitivity for *L. pneumophila* up to 2×10^4 CFU/ml can be detected while for *L. dumoffii* fluorescent readout is not significant below 2×10^7 CFU/ml. As previously illustrated, the

two selected α -Legionella antibodies can react only partially and with low efficiency with *L. dumoffii* cells if compared to *L. pneumophila* cells, being them raised specifically for *L. pneumophila* specie, as indicated by the specifications and confirmed by fluorescence experiments.

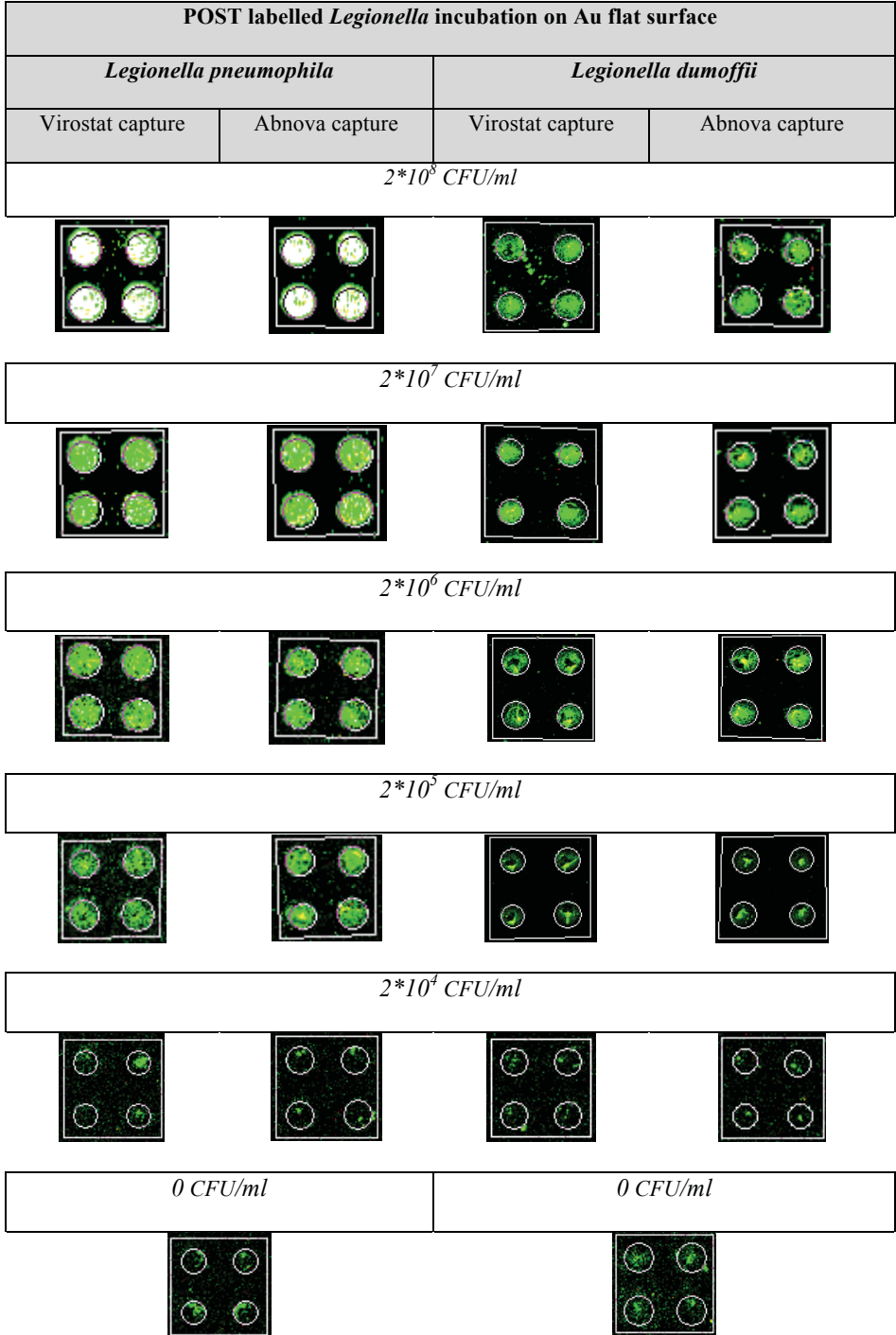


Figure 44. Microarray fluorescence images of sensitivity performances of α -Legionella antibodies incubated with serial dilutions of Alexa Fluor 555 labelled *L. pneumophila* and *L. dumoffii* cells.

4.3.6 Evaluation of ethanol fixation effect on sensitivity

To test the bond stability and the possibility to block and stabilise bacteria on the slide, after bacteria cells incubation gold slides were analysed for fluorescence, and then fixed in absolute ethanol (100%) for 15 minutes at -20 °C. The experiment was performed on *L. pneumophila* incubated array. Slides were finally dried and fluorescence signals were acquired and compared with the signals recorded prior to fixation.

As can be seen from *Figure 45*, the fluorescence signals recorded after ethanol fixation are not significantly different from the ones recorded prior to fixation (differences below 10%); in addition, there were no significant differences related to the usage of Virostat or Abnova antibodies: data represented in the graph are related to the usage of Virostat antibody as capture probe.

Ethanol fixation has therefore been used for all the subsequent experiments prior to SPR measurements, to ensure a proper cell fixation.

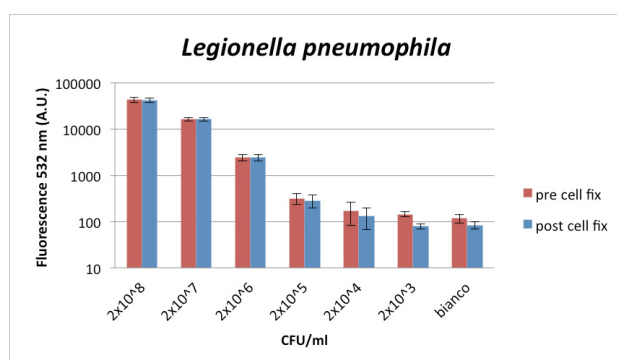


Figure 45. Graphical representation of sensitivity performances of α -*Legionella* antibodies (Virostat) incubated with serial dilutions of Alexa Fluor 555 labelled *L. pneumophila* pre (red) versus post (blue) ethanol fixation.

4.3.7 Evaluation of system performances with whole vs fragmented cells

An evaluation of the platform possibility to recognize also fragments of bacterial microorganisms was performed by cell fragmentation with an optimised freezing and thawing protocol described in Materials and Methods Section.

The analysis of cell viability after fragmentation has demonstrated a fragmentation efficiency > 99.99%: in *Figure 46* vital Legionella colonies appear rich in long flagella around the cells (A and C) while after fragmentation cells are found only as fragmented portions or debris (B and D). The experiment was performed for both Legionella species.

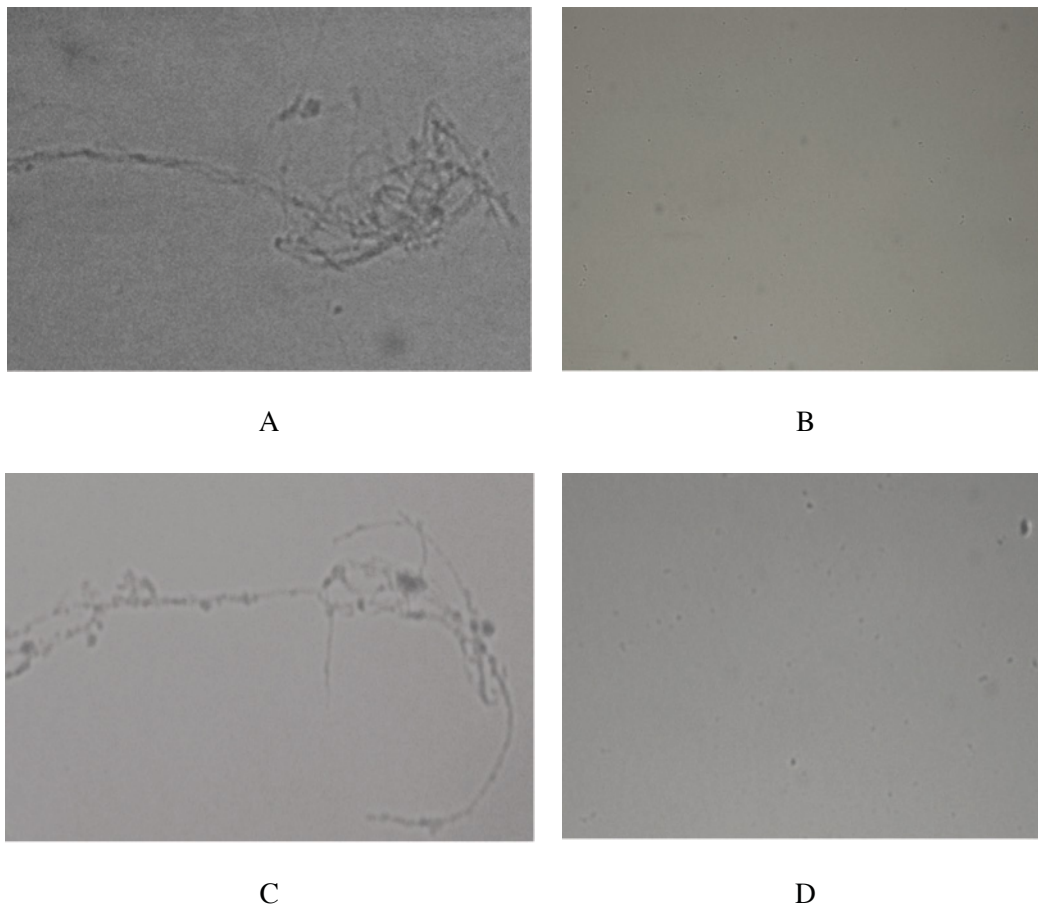


Figure 46. Whole Legionella cells (A: *L. pneumophila*, C: *L. dumoffii*) versus fragmented cells (B: *L. pneumophila*, D: *L. dumoffii*). 10X magnification.

After fragmentation cells were fluorescently labelled and incubated on microarray - at the concentration of $2 \cdot 10^8$ CFU/ml and $2 \cdot 10^7$ CFU/ml - in parallel with unfragmented cells at the same concentration: recorded fluorescent intensities from fragmented cells are lower to the one recorded from whole cells for both species, of at least 50%. Furthermore, whole cells appear on the spots as compact fluorescent discrete

structures while fragmented ones appear as a fluorescent homogeneous spot, without particular distinguishable tridimensional structure (data not shown).

Results indicate the ability of the platform to detect also the presence of fragments labelled cells, also if with lower efficiency.

4.3.8 Florescence system performances with antibody deposition in microwells

To simulate the pattern of antibody deposition that will be used for SPR setting, i.e. antibody deposited not as spots but incubating the deposition solution in the whole microwell, α -Legionella antibody was appropriate diluted and deposited on the slide delimited by cells of 12.25 mm² (square of 3.5 mm * 3.5 mm) through ProPlate 64 slide chamber multiwells. Slides were incubated overnight in a humidity chamber at 75% saturation, and then stored as previously described.

Bacterial cells were labelled and properly diluted with concentrations ranging from $2 \cdot 10^8$ CFU/ml to $2 \cdot 10^4$ CFU/ml. With wells functionalization it is not possible to perform a precise fluorescence quantification since the software is devoted to microarray spots analysis, but only a qualitative analysis comparing background wells and negative control wells (were no significant fluorescent signal is recorded) is possible. In this experimental setting it was possible to record a distinguishable fluorescence signal up to $2 \cdot 10^5$ CFU/ml for *L. pneumophila* samples and up to $2 \cdot 10^8$ CFU/ml for *L. dumoffii* (Figure 47).

Since for this experimental setting only a qualitative analysis was possible, this experiment demonstrate the correct antibody functionalisation and bio-recognition also when depositing the antibodies on the whole microwell: this functionalization will therefore be used for the subsequent SPR gold grating functionalization, in parallel with spots functionalisation on flat gold slides as fluorescence control, for each experimental SPR session.

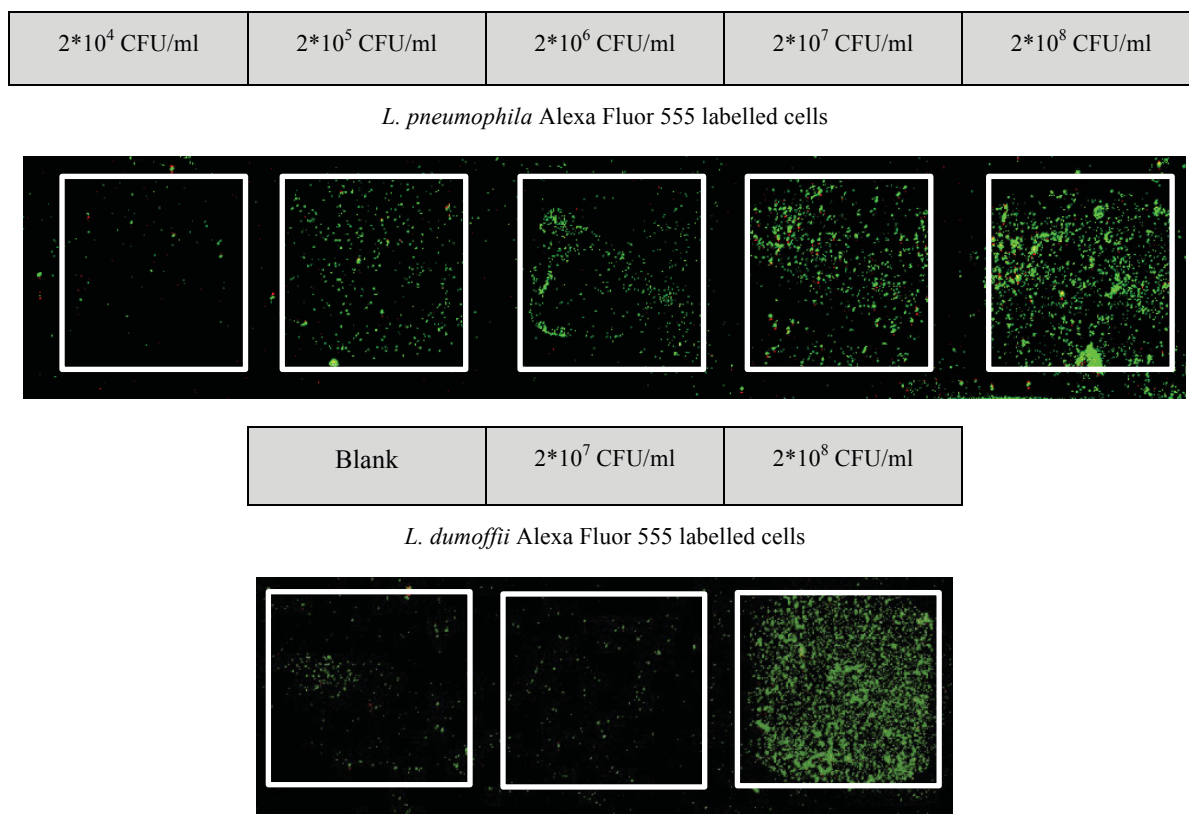


Figure 47. Fluorescence images recorded on wells functionalised with α -Legionella antibody deposition in the microwells and incubated with different concentration of *L. pneumophila* and *L. dumoffii* Alexa Fluor 555 labelled cells.

4.3.9 Grating functionalisation and SPR measurements setup with microfluidic cell

The functionalisation of gold gratings used for bacteria detection experiments was optimized through a series of procedures to verify and define the manipulation techniques of a substrate anchored to the base of the cell adopted for these experiments. In this way it was also possible to define the procedure “checkpoints” that need to be recorded and verified through SPR measurement. Results allowed to define: 1) functionalisation volumes, 2) functionalisation procedures, 3) washing procedures and 4) analysis area delimitation. All the procedures must ensure adequate precision, repeatability and safety of sample manipulation and analysis.

The following steps were performed and SPR measurements were recorded along the protocol, after each specific step, to collect statistical data and to evaluate the substrate behaviour:

- SPR measurement (1) after piranha cleaning - bare grating
- over night PEGylation
- washing, drying and SPR measurement (2)
- -COOH groups activation and overnight antibody binding
- washing, drying and SPR measurements (3 not blocked)
- surface BSA blocking, washing, drying and SPR measurement (3 blocked)
- working area delimitation with alcohol-resistant pencil and SPR measurement (4)
- surface ethanol fixation (4 EtOH)

Each step was clearly detectable and statistical analysis was performed to obtain predictable and reproducible shift range representative of each step. Finally, an incubation protocol of *Legionella* cells on plasmonic gratings was defined as follow:

- a) grating cleaning and anchoring to the cell base; definition of a grating experimental area (with alcohol-resistant pencil); 1° SPR measurement (bare): recorded shift included between 0 and 0.1 nm.
- b) surface o/n PEGylation, washing and drying; antibody deposition inside the delimited area (o/n RT) and blocking; 2° SPR measurement (PEG+Ab+blocking): recorded shift included between 6 and 7 nm.
- c) *L. pneumophila* incubation on the functionalized area; washing, frozen ethanol fixation and drying; 3° SPR measurement (PEG+Ab+blocking+bacterium): recorded shift proportional to the amount of incubated bacteria.

4.3.10 *Legionella pneumophila* SPR detection - sensitivity and specificity

Bacterium concentrations of 10^6 , 10^4 , 10^2 , 10 CFU of unlabelled or Alexa Fluor-647 labelled cells – from the same cell batch - were tested for SPR and fluorescent analyses run in parallel, respectively. Negative

control samples were set using 10^4 CFU of *E. coli* as controls for anti-Legionella antibody capturing specificity.

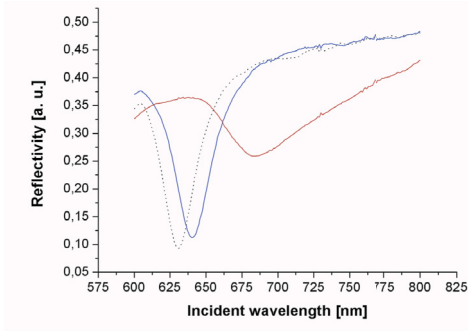
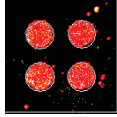
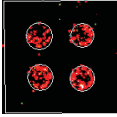
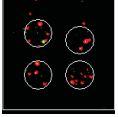
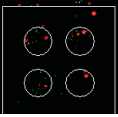

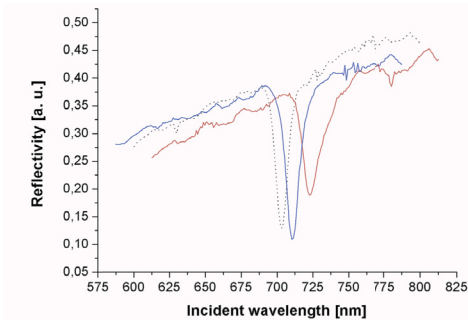
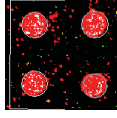
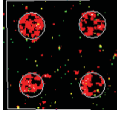
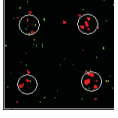
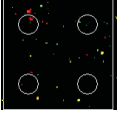
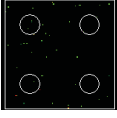
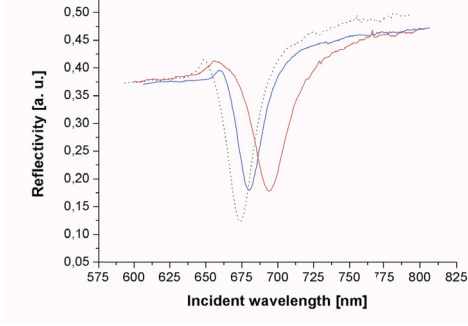
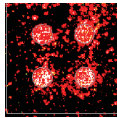
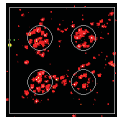
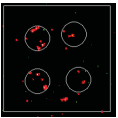
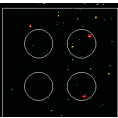
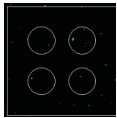
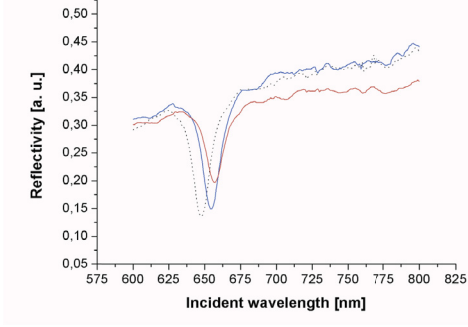
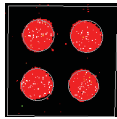
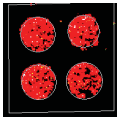
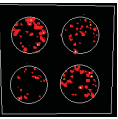
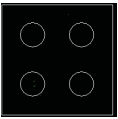
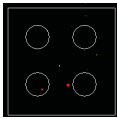
Results are reported graphically - for SPR - or as fluorescent images – for microarray - in *Figure 48* and numerically in *Table 14*.

As can be observed in all the replicas, through azimuthally-controlled GC-SPR it was possible to detect a concentration of 10 CFU, while in the case of fluorescence analysis results, a negative readout is obtained if incubating less than 10^4 CFU. The SPR shift corresponding to 10 CFU (i.e. 2.46 ± 0.04) could allow to further improving the SPR detection sensitivity since negative controls recorded shift (i.e. 0.07 ± 0.03 , obtained using bacteria not belonging to the Legionella genus) was comparable to the measurement instrumental error (hundredth of nm).

Possible variations between experimental sessions concerning the size of the functionalization areas – manually drew – could cause experimental variability related to the different dispersion surface of the incubating solutions. The different dispersion of the sample and therefore its local concentration may in fact be responsible for the lack of proportionality of the SPR shifts related to 10^4 and 10^2 CFU.

Although SPR detection experiments concerning 10^4 and 10^2 CFU need to be further analysed since recorded data are not proportional for these dilutions, the results are reliable shift values are significantly higher than the ones recorded on negative controls, demonstrating the platform specificity. Post functionalisation shifts for all analysed grating are coherent and included in the range of 6.5-9.5 nm.

Further tests will be performed for Legionella detection in microfluidic-integrated system, allowing validation and parallel analysis of samples/replicas and quality control for each experimental session.

SPR spectra - <i>L. pneumophila</i>	Fluorescent microarray – <i>L. pneumophila</i>				
	10 ⁶ CFU	10 ⁵ CFU	10 ⁴ CFU	10 ³ CFU	Blank
<p style="text-align: center;">10⁶ CFU</p>  <p>Reflectivity [a. u.]</p> <p>Incident wavelength [nm]</p>					
<p style="text-align: center;">10⁴ CFU</p>  <p>Reflectivity [a. u.]</p> <p>Incident wavelength [nm]</p>					
<p style="text-align: center;">10² CFU</p>  <p>Reflectivity [a. u.]</p> <p>Incident wavelength [nm]</p>					
<p style="text-align: center;">10 CFU</p>  <p>Reflectivity [a. u.]</p> <p>Incident wavelength [nm]</p>					

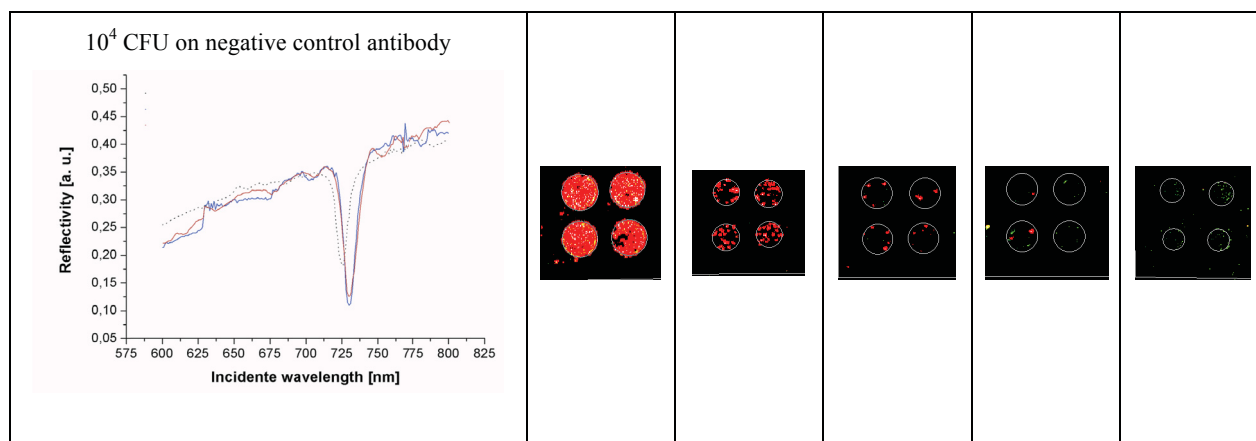


Figure 48. SPR shift measurements performed on gratings for *Legionella pneumophila* detection. Each SPR experiment was run in parallel with a fluorescence microarray control experiment with the same cells' batch. Different serial dilution and negative control are reported. Black dotted line: bare grating, blue line: functionalised grating (PEG+Antibody+Blocking), red line: test grating (bacterium incubation).

Table 14. SPR platform results obtained incubating known amount of *L. pneumophila*. *E. coli* was used as negative control.

Target	Antibody	Resonance wavelength shift after PEG, antibody and blocking [nm]	Resonance wavelength shift after bacteria incubation [nm]
<i>L. pneumophila</i> 10 ⁶ C.F.U.	α Legionella	9,68±0,04	46,30±0,12
<i>L. pneumophila</i> 10 ⁴ C.F.U.	α Legionella	6,15±0,12	12,64±0,11
<i>L. pneumophila</i> 10 ³ C.F.U.	α Legionella	7,04±0,05	13,60±0,05
<i>L. pneumophila</i> 10 C.F.U.	α Legionella	6,65±0,05	2,46±0,04
<i>L. pneumophila</i> 10 ⁴ C.F.U.	no antibody	4,67±0,16	0,06±0,16
<i>E. coli</i> 10 ⁴ C.F.U.	α Legionella	6.76±0.04	0.07±0.03

4.4 Conclusions

In this Section, a sensitive GC-SPR system was optimised and applied to the detection of *L. pneumophila* to test the detection limit of the developed sensing device in term of detectable bacterium CFU. Through azimuthally-controlled GC-SPR, 10 CFU were detected, while in the case of fluorescence analysis results, a negative readout is obtained if incubating less than 10^4 CFU: bacteria concentration detected using GC-SPR system was lower than the concentration detected through fluorescence microarray control method, allowing the overcoming of experimental limits. Negative control experiments, run in parallel with the *E. coli*, allowed also to verify the specificity of the detection method.

This detection platform is going to be implemented as a prototype in which water and air samples will be sequentially concentrated, injected into a microfluidic system, and delivered to the SPR sensor for analysis, through the European Horizon 2020 project “Poseidon”.

The results of this work produced the following publications:

Peer Reviewed Journal:

- Meneghello, A. et al. *Paper under preparation.*

Abstract in International Conference Proceeding:

- International Conference: Advances in Biodetection & Biosensors, co located event with Advances in Microarray Technology, Single Cell Analysis Europe and Lab-on-a-Chip. Berlin, Germany (2014).

Meneghello, A. et al. “*Detection of nosocomial infections related pathogens through a novel plasmonic biosensor device.*” **Awarded as:** Best poster in “Advances in Biodetection & Biosensors” conference.

- International Conference: EuroNanoForum, Riga, Latvia (2015):

Pierobon, R. et al. “*POSEIDON: Plasmonic-based automated lab-on-chip Sensor for the rapid In situ Detection of LegiONella.*”

- International Conference: Nanotech Italy 2015, Bologna, Italy (2015):

Rinaldi, M. et al. “*POSEIDON: Plasmonic-based Automated Lab-on-chip Sensor for the Rapid in Situ Detection of LegiONella*”.

5. Conclusions

My PhD Thesis work was aimed at the exploitation of the Surface Plasmon Resonance (SPR) phenomenon for the set-up of biosensing platforms for clinical and environmental applications.

In particular, two types of SPR-based platforms were set-up and optimised: the first one was an oligonucleotide-based platform for the detection of Cystic Fibrosis (CF) causing mutations while the second one was an antibody-based platform for the detection of *Legionella pneumophila* whole cells.

Sensing detection of cystic fibrosis DNA showed the possibility of employing azimuthally-controlled GC-SPR for the genotyping of human DNA PCR amplified sample from wild type and heterozygous samples.

Data obtained from plasmonic analysis demonstrated to be fully consistent and homogeneous between replicas, indicating the correct genotyping of the selected alleles. These results clearly showed the possibility of employing azimuthally controlled GC-SPR for the genotyping of CF mutations. Furthermore, SPR genotyping was not impaired in samples containing unrelated DNA, allowing the platform to be used for the parallel discrimination of several alleles also scalable for a high throughput screening setting. Results shown in the experiments of the present Section are the starting point for the realization and improvement of a GC-SPR based sensor that could be easily integrated in a diagnostic prototype thanks to the high sensitivity reached by the azimuthally rotated approach and to the system scalability.

Concerning antibody platform for *Legionella pneumophila* bacteria detection, a strategy for the exploitation of the SPR phenomenon to develop a fully automated platform for fast optical detection of *Legionella pneumophila* pathogens was investigated. Through azimuthally-controlled GC-SPR, 10 CFU were detected, while in the case of fluorescence analysis results, a negative readout is obtained if incubating less than 10^4 CFU. Successful results were obtained when incubating environmental derived samples. This detection platform could be further implemented as a prototype in which water and air samples will be sequentially concentrated, injected into a microfluidic system, and delivered to the SPR sensor for analysis.

Concluding, the peculiar Grating Coupled–Surface Plasmon Resonance sensing method applied for this Thesis work has revealed to be an accurate and highly sensitive strategy – with multiplexing possibility - for the sensing and detecting of different kind of biomolecules, from DNA fragments to whole bacteria cell, and in different kind of applications, from genetic disorders' diagnostics to microbiological monitoring.

6. Acknowledgements

The work of this Thesis has been supported by:

- Excellence Project - Progetto di Eccellenza SPLENDID “Surface PLasmonics for Enhanced Nano Detectors and Innovative Devices.” (Fondazione CARIPARO and University of Padova).
- POR CRO 2007-2013 Misura 1.1.3: “Sviluppo di sensori plasmonici per la rivelazione batterica ambientale”.
- POSEIDON Project (Horizon2020-ICT-2014-1): “Plasmonic-based autOated lab-on-chip Sensor for the rapid In-situ Detection of LegiONella”. This project has received funding from the European Union's Horizon 2020 research and innovation programme under grant agreement no. 644669.

I'd like to thank all the people who contributed to this work:

Agnese Antognoli, Erica Cretaio, Roberto Pierobon, Agnese Sonato, Alessandro Surpi, Gianluca Ruffato, Gabriele Zacco and Filippo Romanato.

7. Side activities

During my PhD work, developed in Veneto Nanotech Laboratories, I've been involved in other activities further than those described in this Thesis and the results of these side activities produced the following publications (01/2013-01/2016):

Peer Reviewed Journal:

- D. Silvestri, A. Sonato, G. Ruffato, A. Meneghello, A. Antognoli, E. Cretaio, M. Dettin, A. Zamuner, E. Casarin, G. Zacco, F. Romanato, M. Morpurgo. “Peptide nucleic acid label-free biosensor for *Mycobacterium tuberculosis* DNA detection via azimuthally-controlled grating-coupling SPR” **Analytical Methods**, 2015, 7, 4173-4180.
- F. Todescato, A. Antognoli, A. Meneghello, E. Cretaio, R. Signorini, R. Bozio. “Sensitive detection of Ochratoxin A in food and drinks using metal-enhanced fluorescence.” **Biosensors and Bioelectronics** 2014, 57, 125–132.
- Susic, A. Meneghello, A. Antognoli, E. Cretaio, B. Gatto: “Development of a multiplex Sandwich Aptamer Microarray (SAM) for the detection of VEGF165 and thrombin.” **Sensors** 2013, 13(10), 13425-13438.

Abstract in International Conference Proceeding:

- 13-19/09/2015 International Conference: 18th International Symposium on Health-Related Water Microbiology: WaterMicro2015, Lisbon, Portugal.
POSTER: “Sewage monitoring for pathogenic microorganisms detection by using a low density microarray” Verani M., Cretaio E., Cadonna M., Meneghello A., Carducci A.
- 26-28/11/2014 International Conference: “NanotechItaly 2014”, Venezia, Italy.

POSTER: “Detection of Wine Contamination Using a Surface Plasmon Resonance Sensor Based on Azimuthal Angle Modulation” A. Antognoli, E. Pasqualotto, A. Meneghello, E. Cretaio, V. Brunaccioli, D. Beniz, L. Gasparotto, R. Moratti, S. Ferrante, N. Venco, A. De Toni.

POSTER: “Development of RT-PCR Methods for Quality Control of Fresh-Cut Products” A. Meneghello, A. Antognoli, E. Cretaio, B. Stivanello, F. Pinton, L. Sgardolo.

- 27-29/11/2013 International Conference: “NanotechItaly 2013”, Venezia, Italy.

POSTER: “Study and preparation of scaffolds through replication method using bioactive glass 70S30C” V. Vascotto, M. Gjika, M. Fantin, S. Costacurta, E. Cretaio, A. Meneghello, A. Antognoli, P. Scopece, G. Brusatin.

- 08-13/09/2013 International Conference “EUROMAT2013 European Congress and Exhibition on Advanced Materials and Processes.” Sevilla, Spain.

ORAL: “PECVD-plasma polymerisation of COOH- groups for biological applications” M. Colasuonno, A. Meneghello, A. Antognoli, A. Patelli, E. Cretaio, R. Pierobon, R. Olivotto.

During my PhD I’ve attended the following conferences and courses:

Conferences:

- International Conference: “NanotechItaly 2015”, Bologna, Italy (2015)
- International Conference: “NanotechItaly 2014”, Venezia, Italy (2014)
- International Conference: “Advances in Biodetection & Biosensors”, co located event with Advances in Microarray Technology, Single Cell Analysis Europe and Lab-on-a-Chip. Berlin, Germany. (2014)

- International Conference: “NanotechItaly 2013”, Venezia, Italy (2013)

Courses:

- 14/10/2015 Workshop: “Biacore User Day”, Bologna, GE.
- 26-27/02/2015 “First Scientific Retreat of the Department of Biology”, Università degli Studi di Padova, Centro Interdipartimentale Vallisneri, Padova.
- 02/12/2014 Training course for Real Time PCR “Eco-Illumina”, Ortoromi, Borgoricco, Padova.
- 27-31/10/2014 “Genetics and Molecular Biology of Development Models in Genetic Disease” Università degli Studi di Padova, Centro Interdipartimentale Vallisneri, Padova.
- 13/05/2014 “Sanificazione Aziende Alimentari: criticità del processo, problematiche legate al biofilm e controllo delle operazioni, Confindustria Venezia.
- 02-04/04/2014 PhD Spring School on Computational Biology, Università degli Studi di Padova, Centro Interdipartimentale Vallisneri, Padova.
- 31/03/2014 – 01/04/2014 “PROTEINE 2014”, Università degli Studi di Padova.
- 02-05/09/2013 “Next Generation Sequencing: from sample preparation to data analysis” Università degli Studi di Padova, Centro Interdipartimentale Vallisneri, Padova.

8. Bibliography

1. Thévenot, D. R., Toth, K., Durst, R. a. & Wilson, G. S. Electrochemical biosensors: Recommended definitions and classification. *Biosens. Bioelectron.* 16, 121–131 (2001).
2. Gonçalves, A. *et al.* Trends in Protein-Based Biosensor Assemblies for Drug Screening and Pharmaceutical Kinetic Studies. *Molecules* 19, 12461–12485 (2014).
3. Mungroo, N. & Neethirajan, S. Biosensors for the Detection of Antibiotics in Poultry Industry—A Review. *Biosensors* 4, 472–493 (2014).
4. Narayanaswamy, R. & Wolfbeis, O. S. *Optical sensors: industrial, environmental and diagnostic applications*. 1, (Springer Science & Business Media, 2004).
5. Patel, P. ., Mishra, V. & Mandloi, a. S. Optical Biosensors: Fundamentals & Trends. *J. Eng. Res. Stud.* I, 15–34 (2010).
6. Fan, X. *et al.* Sensitive optical biosensors for unlabeled targets: A review. *Anal. Chim. Acta* 620, 8–26 (2008).
7. Homola, J. Surface plasmon resonance sensors for detection of chemical and biological species. *Chem. Rev.* 108, 462–493 (2008).
8. Maier, S. a. *Plasmonics: Fundamentals and applications*. *Plasmonics: Fundamentals and Applications* (2007). doi:10.1007/0-387-37825-1
9. Šípová, H. & Homola, J. Surface plasmon resonance sensing of nucleic acids: A review. *Anal. Chim. Acta* 773, 9–23 (2013).
10. Turner, A. P. F. Biosensors: sense and sensibility. *Chem. Soc. Rev.* 42, 3184–96 (2013).
11. Raether, H. *Surface Plasmons on Smooth and Rough Surfaces and on Gratings*. Springer 111, (1988).
12. Benson, O. Assembly of hybrid photonic architectures from nanophotonic constituents. *Nature* 480, 193–199 (2011).
13. Homola, J. & Piliarik, M. Surface plasmon resonance (SPR) sensors. *Surf. plasmon Reson. based sensors* 45–67 (2006). doi:10.1007/5346

14. Barnes, W. L., Dereux, A. & Ebbesen, T. W. Surface plasmon subwavelength optics. *Nature* 424, 824–30 (2003).
15. Kretschmann, E. & Raether, H. Radiative decay of non-radiative surface plasmons excited by light. *Z. Naturforsch.* 23, 2135–2136 (1968).
16. Rich, R. L. & Myszka, D. G. Higher-throughput, label-free, real-time molecular interaction analysis. *Anal. Biochem.* 361, 1–6 (2007).
17. Homola, J., Yee, S. S. & Gauglitz, G. Surface plasmon resonance sensors: review. *Sensors Actuators B Chem.* 54, 3–15 (1999).
18. Ruffato, G. *et al.* Implementation and testing of a compact and high-resolution sensing device based on grating-coupled surface plasmon resonance with polarization modulation. *Sensors Actuators B Chem.* 185, 179–187 (2013).
19. Sonato, A. *et al.* Enhanced sensitivity azimuthally controlled grating-coupled surface plasmon resonance applied to the calibration of thiol-poly(ethylene oxide) grafting. *Sensors Actuators B Chem.* 181, 559–566 (2013).
20. Sonato, A. *et al.* Quantitative control of poly(ethylene oxide) surface antifouling and biodetection through azimuthally enhanced grating coupled-surface plasmon resonance sensing. *Appl. Surf. Sci.* 286, 22–30 (2013).
21. Romanato, F., Lee, K. H., Kang, H. K., Ruffato, G. & Wong, C. C. Sensitivity enhancement in grating coupled surface plasmon resonance by azimuthal control. *Opt. Express* 17, 12145–12154 (2009).
22. Ruffato, G. & Romanato, F. Grating-coupled surface plasmon resonance in conical mounting with polarization modulation. *Opt. Lett.* 37, 2718–20 (2012).
23. Pasqualotto, E. *et al.* Plasmonic platforms for innovative surface plasmon resonance configuration with sensing applications. *Microelectron. Eng.* 111, 48–353 (2013).
24. Ruffato, G. *et al.* Novel compact architecture for high-resolution sensing with plasmonic gratings in conical mounting. *Proc. SPIE Vol. 8722 87220U-1 8722, 87220U* (2013).
25. Meneghello, A. *et al.* Label-Free Efficient and Accurate Detection of Cystic Fibrosis Causing Mutations Using an Azimuthally Rotated GC-SPR Platform. *Anal. Chem.* 86, 11773–11781 (2014).

26. Miller, M. B. *Molecular Microbiology*. (American Society of Microbiology, 2011). doi:10.1128/9781555816834
27. Yoo, S. M., Choi, J. H., Lee, S. Y. & Yoo, N. C. Applications of DNA microarray in disease diagnostics. *J. Microbiol. Biotechnol.* 19, 635–646 (2009).
28. Mikhailovich, V., Gryadunov, D., Kolchinsky, A., Makarov, A. a. & Zasedatelev, A. DNA microarrays in the clinic: Infectious diseases. *BioEssays* 30, 673–682 (2008).
29. Cretich, M., Pirri, G., Damin, F., Solinas, I. & Chiari, M. A new polymeric coating for protein microarrays. *Anal. Biochem.* 332, 67–74 (2004).
30. Martin, Y. & Vermette, P. Low-fouling amine-terminated poly(ethylene glycol) thin layers and effect of immobilization conditions on their mechanical and physicochemical properties. *Macromolecules* 39, 8083–8091 (2006).
31. Murphy, E. F., Lu, J. R., Brewer, J., Russell, J. & Penfold, J. The reduced adsorption of proteins at the phosphoryl choline incorporated polymer-water interface. *Langmuir* 15, 1313–1322 (1999).
32. Heuberger, M., Drobek, T. & Spencer, N. D. Interaction forces and morphology of a protein-resistant poly(ethylene glycol) layer. *Biophys. J.* 88, 495–504 (2005).
33. Arakawa, T. & Timasheff, S. N. Mechanism of poly(ethylene glycol) interaction with proteins. *Biochemistry* 24, 6756–6762 (1985).
34. Uchida, K., Otsuka, H., Kaneko, M., Kataoka, K. & Nagasaki, Y. A Reactive Poly(ethylene glycol) Layer To Achieve Specific Surface Plasmon Resonance Sensing with a High S/N Ratio: The Substantial Role of a Short Underbrushed PEG Layer in Minimizing Nonspecific Adsorption. *Anal. Chem.* 77, 1075–1080 (2005).
35. Du, H., Chandaroy, P. & Hui, S. W. Grafted poly-(ethylene glycol) on lipid surfaces inhibits protein adsorption and cell adhesion. *Biochim. Biophys. Acta* 1326, 236–248 (1997).
36. Harder, P., Grunze, M., Dahint, R., Whitesides, G. M. & Laibinis, P. E. Molecular Conformation in Oligo(ethylene glycol)-Terminated Self-Assembled Monolayers on Gold and Silver Surfaces Determines Their Ability To Resist Protein Adsorption. *J. Phys. Chem. B* 102, 426–436 (1998).
37. Lowe, S., O'Brien-Simpson, N. M. & Connal, L. A. Antibiofouling polymer interfaces: poly(ethylene glycol) and other promising candidates. *Polym. Chem.* 6, 198–212 (2015).

38. Lu, H. B., Campbell, C. T. & Castner, D. G. Attachment of functionalized poly(ethylene glycol) films to gold surfaces. *Langmuir* 16, 1711–1718 (2000).
39. Love, J. C., Estroff, L. a., Kriebel, J. K., Nuzzo, R. G. & Whitesides, G. M. *Self-assembled monolayers of thiolates on metals as a form of nanotechnology*. *Chemical Reviews* 105, (2005).
40. Christopher Love, J. *et al.* Formation and structure of self-assembled monolayers of alkanethiolates on palladium. *J. Am. Chem. Soc.* 125, 2597–2609 (2003).
41. Ulman, A. *et al.* Self-assembled monolayers of rigid thiols. *J. Biotechnol.* 74, 175–188 (2000).
42. Ulman, A. Formation and Structure of Self-Assembled Monolayers. *Chem Rev* 96, 1533–1554 (1996).
43. Sano, S., Kato, K. & Ikada, Y. Introduction of functional groups onto the surface of polyethylene for protein immobilization. *Biomaterials* 14, 817–822 (1993).
44. Nguyen, V. H. & Nguyen, B. H. Quantum dynamics of plasmons in nanomaterials. *Adv. Nat. Sci. Nanosci. Nanotechnol.* 3, 035009 (2012).
45. Romanato, F., Lee, K. H., Ruffato, G. & Wong, C. C. The role of polarization on surface plasmon polariton excitation on metallic gratings in the conical mounting. *Appl. Phys. Lett.* 96, 111103 (2010).
46. Rommens, J. *et al.* Identification of the cystic fibrosis gene: chromosome walking and jumping. *Science (80-.)*. 245, 1059–1065 (1989).
47. Riordan, J. R. *et al.* Identification of the cystic fibrosis gene: cloning and characterization of complementary DNA. *Science* 245, 1066–73 (1989).
48. Andersen, D. H. Cystic Fibrosis of the Pancreas and Its Relation to Celiac Disease. *Am. J. Dis. Child.* 56, 344 (1938).
49. Kerem, B. *et al.* Identification of the cystic fibrosis gene: genetic analysis. *Science (80-.)*. 245, 1073–80 (1989).
50. MacDonald, K. D., McKenzie, K. R. & Zeitlin, P. L. Cystic fibrosis transmembrane regulator protein mutations: ‘class’ opportunity for novel drug innovation. *Paediatr. Drugs* 9, 1–10 (2007).
51. *The Metabolic and Molecular Bases of Inherited Disease* (Scriver, C. R., Beaudet, A. L., Sly, W. S., Valle, D., Childs, B., Kinzler, K. W., and Vogelstein, B., eds., 8th ed., McGraw-Hill, New-York,

- 2001, 7012 p., \$550.00). *Biochem.* 67, 611–612 (2002).
52. Rendine, S. *et al.* Genetic history of cystic fibrosis mutations in Italy. I. Regional distribution. *Ann. Hum. Genet.* 61, 411–24 (1997).
 53. Picci, L. *et al.* A 10-year large-scale cystic fibrosis carrier screening in the Italian population. *J. Cyst. Fibros.* 9, 29–35 (2010).
 54. O’Sullivan, B. P. & Freedman, S. D. Cystic fibrosis. *Lancet* 373, 1891–904 (2009).
 55. Castaldo, G. *et al.* Molecular epidemiology of cystic fibrosis mutations and haplotypes in southern Italy evaluated with an improved semiautomated robotic procedure. *J. Med. Genet.* 33, 475–9 (1996).
 56. Castaldo, G. *et al.* Detection of five rare cystic fibrosis mutations peculiar to southern Italy: Implications in screening for the disease and phenotype characterization for patients with homozygote mutations. *Clin. Chem.* 45, 957–962 (1999).
 57. Chehab, F. F. & Wall, J. Detection of multiple cystic fibrosis mutations by reverse dot blot hybridization: a technology for carrier screening. *Hum. Genet.* 89, 163–168 (1992).
 58. Cuppens, H., Marynen, P., De Boeck, C. & Cassiman, J.-J. Detection of 98.5% of the mutations in 200 Belgian cystic fibrosis alleles by reverse dot-blot and sequencing of the complete coding region and exon/intron junctions of the CFTR gene. *Genomics* 18, 693–697 (1993).
 59. Bradley, L. A., Johnson, D. A., Chaparro, C. A., Robertson, N. H. & Ferrie, R. M. A multiplex ARMS test for 10 cystic fibrosis (CF) mutations: evaluation in a prenatal CF screening program. *Genet Test* 2, 337–341 (1998).
 60. Ferrie, R. M. *et al.* Development, multiplexing, and application of ARMS tests for common mutations in the CFTR gene. *Am. J. Hum. Genet.* 51, 251–262 (1992).
 61. Brinson, E. C. *et al.* Introduction to PCR/OLA/SCS, a multiplex DNA test, and its application to cystic fibrosis. *Genet. Test.* 1, 61–68 (1997).
 62. Rommens, J. *et al.* Rapid nonradioactive detection of the major cystic fibrosis mutation. *Am. J. Hum. Genet.* 46, 395–396 (1990).
 63. Grade, K., Grunewald, I., Graupner, I., Behrens, F. & Coutelle, C. Identification of three novel mutations in the CFTR gene using temperature-optimized non-radioactive conditions for SSCP

- analysis. *Hum. Genet.* 94, 154–8 (1994).
64. Orita, M., Iwahana, H., Kanazawa, H., Hayashi, K. & Sekiya, T. Detection of polymorphisms of human DNA by gel electrophoresis as single-strand conformation polymorphisms. *Proc. Natl. Acad. Sci. U. S. A.* 86, 2766–70 (1989).
 65. Ferec, C. *et al.* Detection of over 98% cystic fibrosis mutations in a Celtic population. *Nat. Genet.* 1, 188–191 (1992).
 66. Nasef, H., Beni, V. & O’Sullivan, C. K. Methylene blue as an electrochemical indicator for DF508 cystic fibrosis mutation detection. *Anal. Bioanal. Chem.* 396, 1423–1432 (2010).
 67. Salvado, C. S., Trounson, A. O. & Cram, D. S. Towards preimplantation diagnosis of cystic fibrosis using microarrays. *Reprod. Biomed. Online* 8, 107–14 (2004).
 68. Schrijver, I., Oitmaa, E., Metspalu, A. & Gardner, P. Genotyping microarray for the detection of more than 200 CFTR mutations in ethnically diverse populations. *J. Mol. Diagn.* 7, 375–387 (2005).
 69. Eaker, S., Johnson, M., Jenkins, J., Bauer, M. & Little, S. Detection of CFTR mutations using ARMS and low-density microarrays. *Biosens. Bioelectron.* 21, 933–939 (2005).
 70. Galvin, P., Clarke, L. a, Harvey, S. & Amaral, M. D. Microarray analysis in cystic fibrosis. *J. Cyst. Fibros.* 3 Suppl 2, 29–33 (2004).
 71. Ubertelli, V., Josse, C., Bauland, F. & Valat, C. Fast development of CE IVD molecular diagnostic kits: Highly specific microarray kit for 49 cystic fibrosis mutations. *IRBM* 28, 224–229 (2007).
 72. Murphy, D. & Redmond, G. Optical detection and discrimination of cystic fibrosis-related genetic mutations using oligonucleotide-nanoparticle conjugates. *Anal. Bioanal. Chem.* 381, 1122–9 (2005).
 73. Bassil, N. *et al.* One hundred spots parallel monitoring of DNA interactions by SPR imaging of polymer-functionalized surfaces applied to the detection of cystic fibrosis mutations. *Sensors Actuators, B Chem.* 94, 313–323 (2003).
 74. Feriotto, G., Lucci, M., Bianchi, N., Mischiati, C. & Gambari, R. Detection of the deltaF508 (F508del) mutation of the cystic fibrosis gene by surface plasmon resonance and biosensor technology. *Hum. Mutat.* 13, 390–400 (1999).

75. Feriotto, G. *et al.* Biosensor technology for real-time detection of the cystic fibrosis W1282X mutation in CFTR. *Hum. Mutat.* 18, 70–81 (2001).
76. Hottin, J. *et al.* in *Biophotonics: Photonic Solutions For Better Health Care* 6991, Q9910–Q9910 (2008).
77. Mannelli, I. *et al.* Surface plasmon resonance imaging (SPRI) system and real-time monitoring of DNA biochip for human genetic mutation diagnosis of DNA amplified samples. *Sensors Actuators, B Chem.* 119, 583–591 (2006).
78. Corradini, R., Feriotto, G., Sforza, S., Marchelli, R. & Gambari, R. Enhanced recognition of cystic fibrosis W1282X DNA point mutation by chiral peptide nucleic acid probes by a surface plasmon resonance biosensor. *J. Mol. Recognit.* 17, 76–84 (2004).
79. Feriotto, G. *et al.* Peptide nucleic acids and biosensor technology for real-time detection of the cystic fibrosis W1282X mutation by surface plasmon resonance. *Lab. Invest.* 81, 1415–27 (2001).
80. Li, Y., Wark, A. W., Lee, H. J. & Corn, R. M. Single-nucleotide polymorphism genotyping by nanoparticle-enhanced surface plasmon resonance imaging measurements of surface ligation reactions. *Anal. Chem.* 78, 3158–3164 (2006).
81. Nilsson, P., Persson, B., Larsson, A., Uhlén, M. & Nygren, P. A. Detection of mutations in PCR products from clinical samples by surface plasmon resonance. *J. Mol. Recognit.* 10, 7–17 (1997).
82. Sonato, A. *et al.* Enhanced sensitivity azimuthally controlled grating-coupled surface plasmon resonance applied to the calibration of thiol-poly(ethylene oxide) grafting. *Sensors Actuators, B Chem.* 181, 559–566 (2013).
83. Broude, N. E. Stem-loop oligonucleotides: A robust tool for molecular biology and biotechnology. *Trends Biotechnol.* 20, 249–256 (2002).
84. Buzdin, A. A. & Lukyanov, S. A. *Nucleic Acids Hybridization Modern Applications. Nucleic Acids Hybridization: Modern Applications* (2007). doi:10.1007/978-1-4020-6040-3
85. Zielenski, J. *et al.* Genomic DNA sequence of the cystic fibrosis transmembrane conductance regulator (CFTR) gene. *Genomics* 10, 214–228 (1991).
86. Tyagi, S. & Kramer, F. R. Molecular beacons: probes that fluoresce upon hybridization. *Nat. Biotechnol.* 14, 303–308 (1996).

87. Marras, S. E., Russell Kramer, F. & Tyagi, S. in *Single Nucleotide Polymorphisms SE - 8* (ed. Kwok, P.-Y.) 212, 111–128 (Springer New York, 2003).
88. Piatek, A. S. *et al.* Molecular beacon sequence analysis for detecting drug resistance in *Mycobacterium tuberculosis*. *Nat Biotechnol* 16, 359–363 (1998).
89. Letowski, J., Brousseau, R. & Masson, L. Designing better probes: effect of probe size, mismatch position and number on hybridization in DNA oligonucleotide microarrays. *J. Microbiol. Methods* 57, 269–78 (2004).
90. Syvänen, a C. Accessing genetic variation: genotyping single nucleotide polymorphisms. *Nat. Rev. Genet.* 2, 930–42 (2001).
91. Bolton, E. T. & McCarthy, B. J. A GENERAL METHOD FOR THE ISOLATION OF RNA COMPLEMENTARY TO DNA. *Proc. Natl. Acad. Sci. U. S. A.* 48, 1390–1397 (1962).
92. Sousa, D. *et al.* Community-acquired pneumonia in immunocompromised older patients: Incidence, causative organisms and outcome. *Clin. Microbiol. Infect.* 19, 187–192 (2013).
93. Lazcka, O., Campo, F. J. Del & Muñoz, F. X. Pathogen detection: A perspective of traditional methods and biosensors. *Biosens. Bioelectron.* 22, 1205–1217 (2007).
94. Park, S., Min, J. & Kim, Y.-K. Chemiluminescent enzyme-linked immunosorbent assay on a strip to detect *Escherichia coli* O157:H7. *Int. J. Environ. Anal. Chem.* 92, 655–664 (2012).
95. Yang, L. & Bashir, R. Electrical/electrochemical impedance for rapid detection of foodborne pathogenic bacteria. *Biotechnol. Adv.* 26, 135–150 (2008).
96. Skottrup, P. D., Nicolaisen, M. & Justesen, A. F. Towards on-site pathogen detection using antibody-based sensors. *Biosens. Bioelectron.* 24, 339–348 (2008).
97. Fritz, J. Cantilever biosensors. *Analyst* 133, 855–863 (2008).
98. Mujika, M. *et al.* Magnetoresistive immunosensor for the detection of *Escherichia coli* O157:H7 including a microfluidic network. *Biosens. Bioelectron.* 24, 1253–1258 (2009).
99. Abadian, P. N., Kelley, C. P. & Goluch, E. D. Cellular analysis and detection using surface plasmon resonance techniques. *Analytical Chemistry* 86, 2799–2812 (2014).
100. Taylor, A. D., Yu, Q., Chen, S., Homola, J. & Jiang, S. Comparison of *E. coli* O157:H7 preparation methods used for detection with surface plasmon resonance sensor. *Sensors Actuators B Chem.*

- 107, 202–208 (2005).
101. Wang, Y., Ye, Z., Si, C. & Ying, Y. Monitoring of Escherichia coli O157:H7 in food samples using lectin based surface plasmon resonance biosensor. *Food Chem.* 136, 1303–8 (2013).
102. Subramanian, A., Irudayaraj, J. & Ryan, T. A mixed self-assembled monolayer-based surface plasmon immunosensor for detection of E. coli O157:H7. *Biosens. Bioelectron.* 21, 998–1006 (2006).
103. Subramanian, A., Irudayaraj, J. & Ryan, T. Mono and dithiol surfaces on surface plasmon resonance biosensors for detection of Staphylococcus aureus. *Sensors Actuators, B Chem.* 114, 192–198 (2006).
104. Tawil, N., Sacher, E., Mandeville, R. & Meunier, M. Surface plasmon resonance detection of E. coli and methicillin-resistant S. aureus using bacteriophages. *Biosens. Bioelectron.* 37, 24–29 (2012).
105. Jyoung, J.-Y., Hong, S., Lee, W. & Choi, J.-W. Immunosensor for the detection of Vibrio cholerae O1 using surface plasmon resonance. *Biosens. Bioelectron.* 21, 2315–9 (2006).
106. Engleberg, N. C. in (ed. Schaechter, M. B. T.-E. of M. (Third E.) 170–181 (Academic Press, 2009). doi:<http://dx.doi.org/10.1016/B978-012373944-5.00194-2>
107. McDade, J. E. Legionella and the Prevention of Legionellosis. *Emerg. Infect. Dis.* 14, 1006 (2008).
108. Benson, R. F. & Fields, B. S. Classification of the genus Legionella. *Semin Respir Infect* 13, 90–99 (1998).
109. Joseph, C. a & Ricketts, K. D. Legionnaires disease in Europe 2007-2008. *Euro Surveill.* 15, 19493 (2010).
110. Beauté, J., Zucs, P. & de Jong, B. Legionnaires disease in Europe, 2009-2010. *Euro Surveill.* 18, 20417 (2013).
111. Tikhomirov, E. WHO programme for the control of hospital infections. *Chemioterapia* 6, 148–51 (1987).
112. Tesh, M. J. & Miller, R. D. Amino acid requirements for Legionella pneumophila growth. *J. Clin. Microbiol.* 13, 865–9 (1981).
113. Piao, Z., Sze, C. C., Barysheva, O., Iida, K. I. & Yoshida, S. I. Temperature-regulated formation of

mycelial mat-like biofilms by *Legionella pneumophila*. *Appl. Environ. Microbiol.* 72, 1613–1622 (2006).